

Rare Earth Pincer Complexes: Synthesis, Reaction Chemistry, and Catalysis

Mikko M. Hänninen, Matthew T. Zamora, and Paul G. Hayes

Abstract The research field surrounding rare earth pincer complexes has reached a stage where a comprehensive review about the reactivity and catalytic behavior of these species is justified. In this contribution, we begin with a brief introduction on common strategies for the preparation of rare earth pincer complexes, continuing with a section devoted to the versatile reactivity observed for this class of compound. Thereafter, several types of compounds are discussed, including extremely reactive hydrides, cationic species, and intriguing scandium imido complexes. Finally, the last portion of this chapter sums up the hitherto reported catalytic studies, including discussions on ring-opening polymerization of cyclic esters, polymerization of olefins and hydroamination reactions, as well as several examples of more infrequently encountered catalytic processes.

Keywords Catalysis · Lanthanides · Pincer ligands · Rare earth metals · Reactivity

Contents

1	Introduction	94
2	Preparation of Rare Earth Complexes Supported by Pincer Ligands	95
2.1	Common Synthetic Routes to Rare Earth Pincer Complexes	95
2.2	Reactions of Metal Complexes That Produce Pincer Complexes	98
3	Reactivity and Chemical Transformations Induced by Rare Earth Pincer Complexes ...	102
3.1	Stoichiometric Bond Activation Reactions	103
3.2	Alkane Elimination and Alkyl Migration	116
3.3	Ligand Metathesis Reactions	123
4	Catalytic Properties of Rare Earth Pincer Complexes	130
4.1	Ring-Opening Polymerization of Cyclic Esters	130

M.M. Hänninen, M.T. Zamora, and P.G. Hayes (✉)
Department of Chemistry and Biochemistry, University of Lethbridge, 4401 University Dr W,
Lethbridge, AB, Canada, T1K 3M4
e-mail: p.hayes@uleth.ca

4.2	Polymerization of Dienes	151
4.3	Other Polymerization Reactions	163
4.4	Hydroamination Reactions	166
4.5	Other Catalytic Reactions	171
5	Conclusion	173
	References	174

1 Introduction

Although multifunctional pincer ligands have been widely exploited in organometallic transition metal chemistry for almost 40 years [1–7], rare earth pincer complexes have not received nearly as much attention. This paucity may be due to the general synthetic challenges associated with, and the high intrinsic reactivity of, the rare earth elements. However, the evolution of sophisticated experimental techniques and increasing availability of novel starting materials, particularly over the past decade, have paved the way for the preparation of numerous rare earth analogues of transition metal pincer counterparts.

The ubiquitous bis(cyclopentadienyl) moiety dominated early organometallic rare earth chemistry, as other types of ancillary ligands had difficulty protecting the voraciously reactive metals [8]. Given the extreme electropositive nature of the rare earth metals, the most sought-after ancillary properties typically include the ability to preclude Lewis base (e.g., THF) coordination and prevent dimerization/oligomerization, ligand redistribution, and “ate” complex formation. As such, the most prominent rare earth scaffolds generally feature electron-rich donors and substantial steric bulk. Furthermore, the charge of the ligand is of critical importance when considering intended applications as most rare earth metals exist almost exclusively in the +3 oxidation state. Given the electronic and steric variability of pincer ligands, it should be of little surprise that many such frameworks fulfill all of the preceding conditions and have thus become very popular.

The chemistry of pincer ligands with transition metals has been comprehensively surveyed in both the current and previous editions of this book; hence, readers interested in such work are directed to those sources. This contribution, which is the first to specifically address the synthesis, reactivity, and catalytic behavior of rare earth pincer complexes, has been prompted by the recent maturation of this field, such that a thorough review is now warranted. This chapter focuses primarily upon the reactivity and catalytic applications of well-defined and characterized rare earth complexes supported by pincer ancillaries. Hence, scientific contributions that merely describe the synthesis and/or solid-state structures of such species, while noteworthy and significant in their own right, are generally beyond the scope of this review. Furthermore, the extent of this chapter is limited to the definition that pincer ligands must be capable of binding to a metal center (usually in a meridional fashion) via exactly three main group donors. Finally, upon coordination to a metal, a five-membered or larger metallacycle must be formed

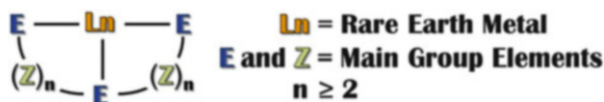


Fig. 1 General definition of a rare earth pincer complex

(Fig. 1). Though not bona fide organometallic, compounds without a metal–carbon bond have been included when they otherwise meet pincer complex criteria and are deemed to be sufficiently important.

2 Preparation of Rare Earth Complexes Supported by Pincer Ligands

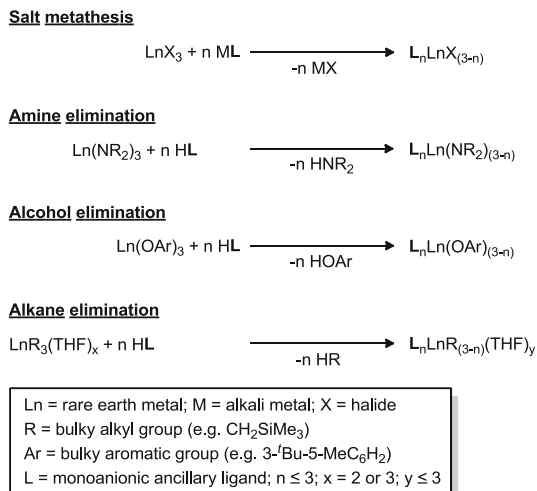
Although the emphasis of this chapter is not on the preparation of rare earth metal complexes [2–5], it is worthwhile to briefly address typical metal attachment strategies. Hence, we begin by presenting, in chronological order, the most frequently encountered syntheses, procedures, and starting materials. The latter part of this section introduces the reader to various novel and often unexpected routes to pincer-supported rare earth metal complexes.

2.1 Common Synthetic Routes to Rare Earth Pincer Complexes

Synthetic methods for metal attachment are well known for rare earth and other metals with both pincer and non-pincer ligands. Such chemistry, corresponding reaction mechanisms, and various examples can be found in most inorganic and organometallic chemistry textbooks and, hence, will not be discussed at length. However, because of the overwhelming importance of such methodologies, the four most prevalent approaches for coordinating pincer ligands to rare earth metals are presented in Scheme 1. The advantages and disadvantages of each process are briefly addressed below.

2.1.1 Salt Metathesis

In 1988, Fryzuk synthesized one of the first rare earth pincer complexes by the straightforward salt metathesis reaction of anhydrous YCl_3 with 2 equiv. of $\text{LiN}(\text{SiMe}_2\text{CH}_2\text{PMe}_2)_2$ to generate the seven-coordinate monomeric complex $\text{YCl}[\text{N}(\text{SiMe}_2\text{CH}_2\text{PMe}_2)_2]_2$ [9]. This approach can also be employed with heavier halides, which are often desirable because of the lower reduction potential of the



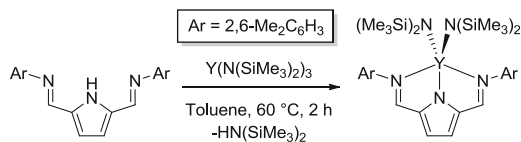
Scheme 1 The four most commonly encountered rare earth metal (Ln) attachment strategies

corresponding metal complexes, as demonstrated by Evans et al. wherein SmI₃ was utilized to prepare chiral samarium complexes [10]. In addition, rare earth tris(borohydrides) Ln(BH₄)₃(THF)₃ can be utilized as a metal source in salt metathesis reactions because the BH₄⁻ anion usually behaves as a pseudohalide with rare earth metals, although it occasionally takes part in redox reactions (vide infra) [11].

This synthetic methodology has proven exceedingly popular for metal complexes in general and is frequently used, though several other routes to rare earth pincer complexes are also typically employed. The most distinct advantage of this practice is the versatility of the resulting halide complexes. These species can be further reacted with virtually any amide, alkoxide, or alkyl salt to produce a wide range of novel compounds.

2.1.2 Amine Elimination

More than a decade after Fryzuk's first rare earth pincer complex was published, Mashima et al. prepared a series of yttrium pincer complexes, LY(N(SiMe₃)₂)₂ (L = 2,5-bis-[N-(2,6-Me₂C₆H₃)iminomethyl]pyrrolyl), by an amine elimination reaction between a bis(iminomethyl)pyrrolyl ligand and the homoleptic tris(amido) complex Y[N(SiMe₃)₂]₃ (Scheme 2) [12]. Conveniently, this procedure does not require initial conversion of the ligand into a metal salt. Furthermore, the extruded amine often exhibits high vapor pressure and is thus simple to remove from the reaction mixture. One potentially detractive aspect of this strategy, however, is the fact that the resultant product often bears one or more sterically demanding amido groups.



Scheme 2 Preparation of a bis(amido) yttrium complex by amine elimination

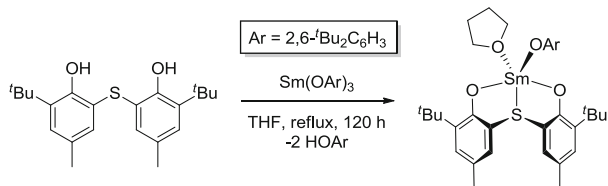
2.1.3 Alcohol Elimination

Another interesting, but not broadly utilized, synthetic pathway was introduced by Arnold and co-workers when they made mono- and dinuclear Sm(III) aryloxide complexes $[\text{LSm}(\text{OAr})(\text{THF})]$ and $[\text{LSm}(\text{OAr})_2]$ ($\text{L} = 1,1'\text{-S}(2\text{-O-3-}^t\text{Bu-5-MeC}_6\text{H}_2)$) bearing sulfur-bridged biphenolate ligands via an alcohol elimination protocol (Scheme 3) [13]. With proper aryl substituents, homoleptic rare earth tris(aryloxides) were produced as hydrocarbon-soluble crystalline solids. Such alkoxide ligands are desirable ancillaries in certain catalytic reactions, such as the ring-opening polymerization of cyclic ethers. However, alcohol elimination requires the use of ligands with a relatively acidic proton, and the by-product alcohol is fairly reactive and often difficult to remove (high boiling point and solubility).

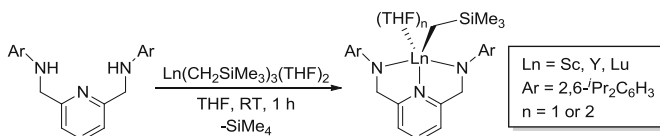
2.1.4 Alkane Elimination

Highly reactive ($\text{LnR}_3(\text{THF})_n$, $\text{R} = \text{CH}_2\text{Ph}$, CH_2SiMe_3 , $\text{CH}(\text{SiMe}_3)_2$, $\text{CH}_2\text{SiMe}_2\text{Ph}$, etc.) complexes of the rare earth metals, which feature sterically demanding alkyl groups, can be prepared from their trihalide precursors, and while these complexes have been known for many years, it was not until the beginning of the twenty-first century that alkane elimination became a common synthetic strategy for the preparation of organometallic pincer species. In 2003, Anwender et al. reacted $\text{Ln}(\text{CH}_2\text{SiMe}_3)_3(\text{THF})_2$ ($\text{Ln} = \text{Sc}$, Y , Lu) trialkyl complexes with tridentate diamide ligands to produce the corresponding monoalkyl complexes $\text{LLn}(\text{CH}_2\text{SiMe}_3)(\text{THF})_n$ ($\text{Ln} = \text{Sc}$, $n = 1$; $\text{Ln} = \text{Y}$, Lu , $n = 2$; $\text{L} = 2,6\text{-bis-}[N\text{-}(2,6\text{-}^t\text{Pr}_2\text{C}_6\text{H}_3)\text{aminomethyl}]pyridine$) (Scheme 4) [14].

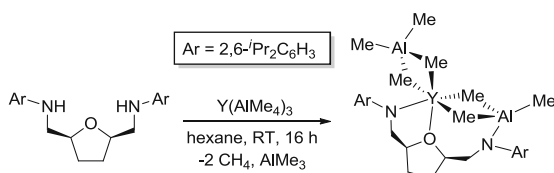
Since Anwender's pioneering work, this technique has become increasingly popular, and many of the rare earth pincer complexes reported herein have been generated in this manner. Notably, the synthesis and isolation of the requisite trialkyl precursors is difficult, as most of these compounds are prone to decomposition at ambient temperature. Nonetheless, during the past decade, numerous new homoleptic compounds containing Ln-C σ -bonds that range in thermal stability have been reported; this area has recently been thoroughly reviewed [15]. In addition to the relative ease with which many alkane elimination reactions proceed, the released alkane is also inert and often sufficiently volatile to permit facile separation from the metal complex. However, the bulky alkyl group sometimes shuts down subsequent reaction chemistry, and it can be difficult to convert such moieties into other functionalities. A tactful balance is therefore required.



Scheme 3 An example of alcohol elimination for the synthesis of rare earth pincer complexes



Scheme 4 Synthesis of monoalkyl rare earth pincer complexes by an alkane elimination protocol

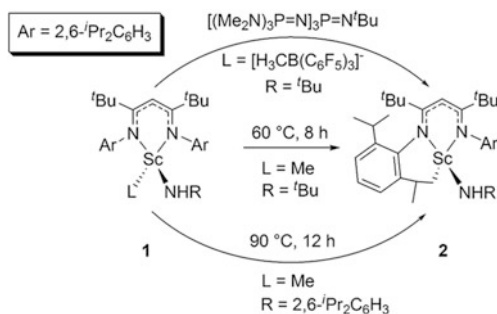


Scheme 5 An example of $\text{Ln}(\text{AlMe}_4)_3$ as a starting material for the synthesis of rare earth pincer complexes

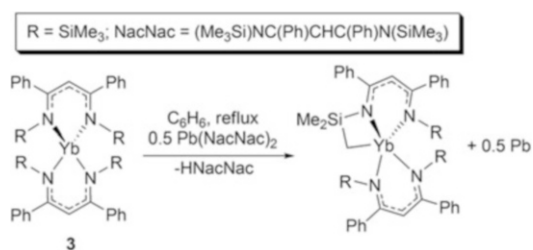
In 2006, Anwander et al. described the use of $\text{Ln}(\text{AlMe}_4)_3$ in the preparation of postlanthanidocene complexes [16]. Similar to rare earth trialkyl compounds, homoleptic tetraalkylaluminate species can be used with pincer ligands in distinct metal attachment reactions to promote alkane elimination and complex formation. These reactions typically lead to heterodinuclear complexes, such as $\text{LY}(\text{AlMe}_4)(\text{AlMe}_3)$ ($\text{L} = \text{cis-2,5-bis}[N,N-((2,6\text{-}^t\text{Pr}_2\text{C}_6\text{H}_3)\text{amino})\text{methyl}] \text{tetrahydrofuran}$) (Scheme 5) with methane and trimethylaluminum eliminated as by-products.

2.2 Reactions of Metal Complexes That Produce Pincer Complexes

Although well-defined synthetic routes are normally utilized for generating metal complexes, occasionally unprecedented reactions can afford unique or unusual products that would be difficult or even impossible to prepare by conventional procedures. The following section is intended to showcase atypical reactions wherein transient rare earth complexes bearing non-pincer ligands can be transformed into species supported by a pincer ancillary.



Scheme 6 Cyclometalation of β -diketiminato supported scandium complexes that leads to pincer-type complexes

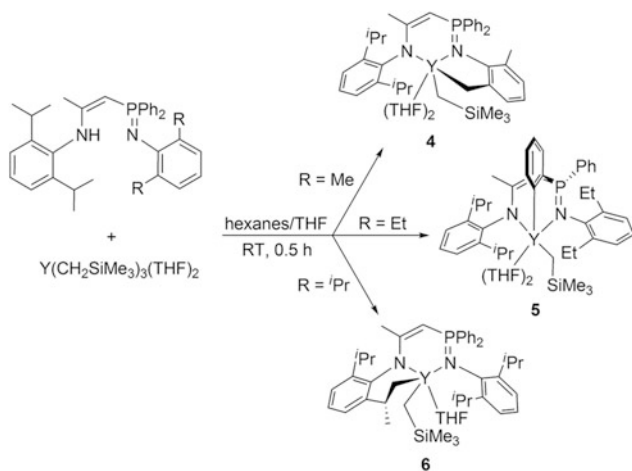


Scheme 7 Oxidative cyclometalation of a homoleptic Yb(II) complex

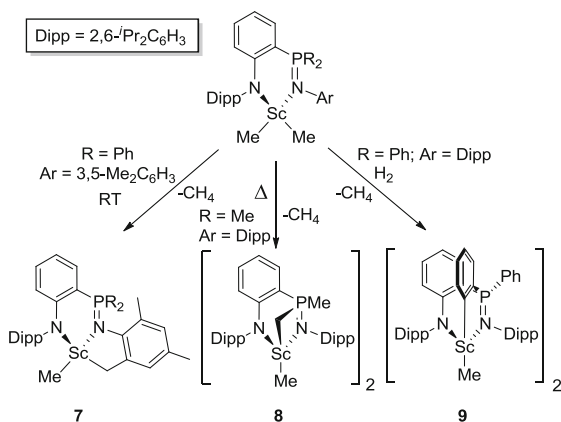
β -Diketiminato (NacNac) ligands are particularly popular auxiliaries that can form complexes with metals spanning the periodic table [17, 18]. Hence, numerous rare earth β -diketiminates have been prepared, some of which exhibit interesting reactivity patterns that produce pincer-type complexes relevant to this review. Most of these reactions begin with a C–H bond activation event, one of the most important and studied reactions in organometallic chemistry [19, 20].

Piers et al. were among the first to prepare rare earth metal complexes bearing β -diketiminato and related ligands, and it was quickly discovered that such species are prone to pincer-forming cyclometalation pathways [21]. In one particularly intriguing example, cyclometalated **2**, prepared by thermolysis of amido-methyl complex $\text{LSc}(\text{CH}_3)\text{NHAr}$ ($\text{L} = (\text{Ar})\text{NC}(\text{tBu})\text{CHC}(\text{tBu})\text{N}(\text{Ar})$, $\text{Ar} = 2,6\text{-}^i\text{Pr}_2\text{C}_6\text{H}_3$; $\text{R} = \text{tBu}$, or $2,6\text{-}^i\text{Pr}_2\text{C}_6\text{H}_3$), **1**, at temperatures between 60°C and 90°C (Scheme 6) [22, 23], was found to react with 4-*N,N*-dimethylaminopyridine (DMAP) to afford a remarkable imido complex $\text{LSc}=\text{NAr} \cdot \text{DMAP}$ [23]. Cyclometalated complex **2** is also formed upon reaction of complex **1** with a bulky phosphazene base $[(\text{Me}_2\text{N})_3\text{P}=\text{N}]_3\text{P}=\text{N}^t\text{Bu}$ [24]. Similar C–H bond activation occurs in the homoleptic Yb(II) NacNac complex $\text{Yb}(\text{L})_2$ ($\text{L} = (\text{Me}_3\text{Si})\text{NC}(\text{Ph})\text{CHC}(\text{Ph})\text{N}(\text{SiMe}_3)$), **3**, when it is heated, or if it is in the presence of either the analogous Pb(II)NacNac species PbL_2 or $\text{Pb}(\text{N}(\text{SiMe}_3)_2)_2$ (Scheme 7) [25].

Closely related phosphinimine-amido complexes studied by both Cui and co-workers [26] and Piers et al. [27] also revealed prevalent C–H bond activation



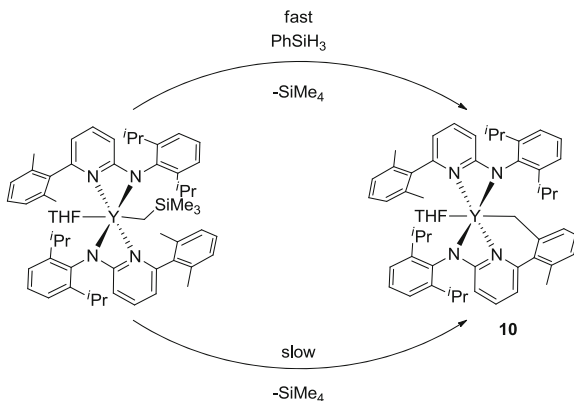
Scheme 8 Cyclometalation of phosphininimine-amido supported yttrium complexes



Scheme 9 Synthesis of scandium pincer complexes via ligand cyclometalation

chemistry. In both of these studies, cyclometalation occurred at multiple ligand sites, depending on the substituents and/or conditions of the specific reaction. In Cui's work, methyl, ethyl, and *isopropyl* substituents on the phenyl ring bound to the phosphininimine nitrogen triggered different cyclometalation behaviors upon complexation. Notably, when substituted with methyls, metalation of one of these groups occurred, affording the monoalkyl species **4**. However, the presence of ethyl or *isopropyl* substituents resulted in the activation of other moieties (i.e., *P*-phenyl, **5**, and *N*-2,6-*i*-Pr₂C₆H₃ (Dipp), **6**, groups, respectively) (Scheme 8).

Ligand substitution also played a key role in cyclometalation reported by Piers and co-workers (Scheme 9) [27]. For example, at ambient temperature, the activation of the *N*-mesityl group produced cyclometalated L^1ScMe ($L^1 = 1-(NDipp)-2-$

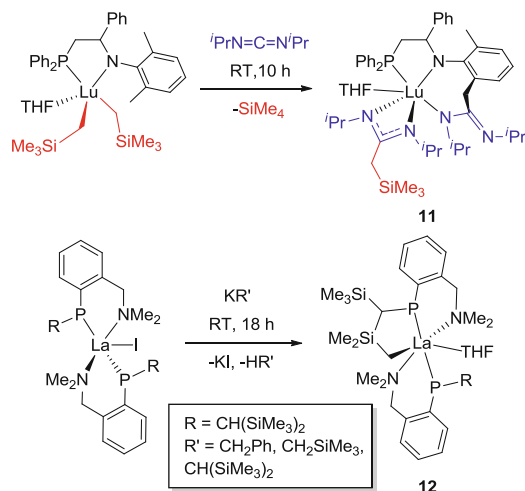


Scheme 10 Synthesis of complex **10**

(PR₂=NAr)C₆H₄; Dipp = 2,6-*i*-Pr₂C₆H₃; R = Ph; Ar = 2,4-Me₂-6-CH₂C₆H₂), **7**. Conversely, complexes bearing the more sterically demanding 2,6-*i*-Pr₂C₆H₃-substituted ligands required heating or the addition of dihydrogen before cyclometalation was observed. With these complexes, metalation occurred at the P-R (R = Me or Ph) group instead of the phosphinimine *N*-aryl moiety. Cyclometalation of PMe groups was rapid at 65°C to give L²ScMe (L² = 1-(NDipp)-2-(PRR' = NDipp)C₆H₄; R = Me; R' = CH₂), **8**, whereas the analogous phenyl-substituted species, **9**, only cyclometalated when dihydrogen was added. The latter reaction presumably proceeds through a putative scandium hydride intermediate.

Substantial rates of C–H activation were also observed for the yttrium complex L₂YCH₂SiMe₃ (L = 2,6-(*i*-Pr₂C₆H₃)-[6-(2,6-dimethylphenyl)pyridin-2-yl]amine) which readily cyclometalated to give complex **10** (Scheme 10). Notably, the rate of cyclometalation was approximately 500 times greater upon the addition of 1 equiv. of PhSiH₃ [28]. Trifonov, Giambastiani, and co-workers observed similar pincer forming cyclometalation reactivity when related bidentate amidopyridinate ligands were reacted with trialkyl yttrium species. Interestingly, these complexes were active in ethylene polymerization; hence, a more detailed discussion is presented in Sect. 4 [29].

Cyclometalation reactions affording pincer complexes have also been reported for PN ligated lutetium and lanthanum complexes. Specifically, Cui et al. recently reported the metalated complex LLu(NCN)(THF) (L = 2-Me-6-CH₂-*i*-PrNC=N^{*i*}-Pr-C₆H₃-NCH(Ph)CH₂P(Ph)₂; NCN = *i*-PrNC(CH₂SiMe₃)N^{*i*}-Pr), **11**, which was postulated to have formed by an initial C–H activation of an NAr methyl, followed by the reaction with *N,N'*-diisopropylcarbodiimide (Scheme 11, top) [30]. Meanwhile, the bis(aminophosphide) lanthanum iodide complex [(CH(SiMe₃)₂)(C₆H₄-2-CH₂NMe₂)P]₂LnI was converted to the cyclometalated complex **12**, upon reaction with organopotassium salts (Scheme 11, bottom) [31]. Presumably, the expected



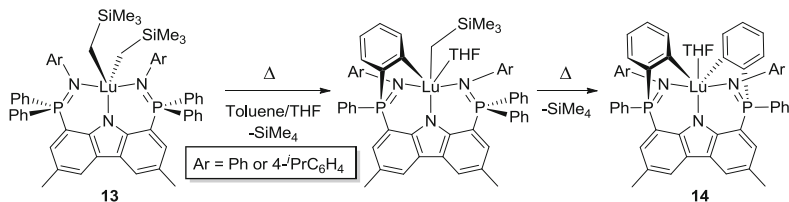
Scheme 11 Pincer complexes generated by C–H activation reactions in rare earth complexes supported by PN-donor ligands

organometallic intermediate formed but decomposed at a rate greater than its formation (i.e., $k_{\text{decomposition}} > k_{\text{formation}}$).

Cyclometalation of rare earth complexes is a prevalent decomposition pathway; hence, those species that bear bidentate scaffolds can give rise to unusual pincer-type complexes. These compounds tend to be particularly intriguing when they are formed in the presence of other reagents, such as carbodiimides, as they provide interesting options for creative ligand design. However, cyclometalation is customarily considered detrimental since it is typically undesirable and the resulting complexes are generally less reactive and/or less useful in targeted chemical transformations.

3 Reactivity and Chemical Transformations Induced by Rare Earth Pincer Complexes

The general reactivity of a metal complex is exceedingly important if one wishes to address the stability of the complex or survey potential applications. Since rare earth pincer chemistry is still quite new compared to the wealth of information on transition metal variants, the reaction chemistry of such complexes remains of special interest. In the following paragraphs, we review a wide variety of stoichiometric reactions reported to take place with rare earth pincer complexes. Judiciously selected examples were collected to compile this section, which is divided into three different subsections: stoichiometric bond activation reactions (3.1), alkane elimination and alkyl migration (3.2), and ligand metathesis reactions (3.3).



Scheme 12 Intramolecular decomposition of **13** to doubly cyclometalated complex **14**

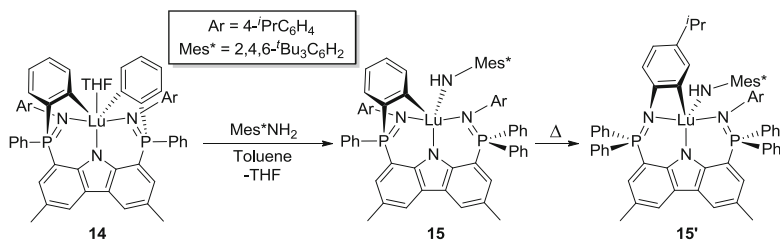
3.1 Stoichiometric Bond Activation Reactions

3.1.1 C–H Bond Activation

The making and breaking of bonds are obviously central to synthetic chemistry; hence, the ability of a rare earth pincer complex to activate various types of bonds is of great importance and of vital significance for catalytic applications. The intrinsic reactivity of rare earth complexes can sometimes promote facile reaction at sp^2 and sp^3 C–H groups that are often considered to be quite inert. The intramolecular activation of C–H bonds generally leads to cyclometalated species that can be relevant to various catalytic transformations [32, 33]. These complexes also serve as excellent platforms from which unique bonding and reactivity patterns can be studied [20].

Ligand architecture has proven to be a determining factor as to where specific cyclometalated species reside on the reactivity spectrum, ranging from completely inert to transient intermediates that cannot be isolated. For example, when using a sterically demanding bis(phosphinimine) pincer ligand, Hayes et al. prepared lutetium dialkyl complexes $\text{LLu}(\text{CH}_2\text{SiMe}_3)_2$ ($\text{L} = 1,8\text{-}(\text{Ph}_2\text{P}=\text{NAr})_2\text{-}3,6\text{-dimethylcarbazolide}$; $\text{Ar} = \text{Ph}, 4\text{-}^i\text{PrPh}$), **13**, which undergo a rapid two-stage metalation of the phosphine phenyl groups at temperatures above 0°C , to ultimately produce the doubly cyclometalated compound $\text{LLu}(\text{THF})$ ($\text{L} = 1,8\text{-}(\text{Ph}(\text{C}_6\text{H}_4)\text{P}=\text{NAr})_2\text{-}3,6\text{-dimethylcarbazolide}$), **14** (Scheme 12) [34].

Later on, the reactivity of complex **14** was probed, and it was found that methyl- or isopropyl-substituted anilines induce metallacycle ring opening of both metalated phenyl groups to generate the bis(anilide) products $\text{LLu}(\text{NHAr})_2$ ($\text{Ar} = 2,4,6\text{-Me}_3\text{C}_6\text{H}_2, 2,4,6\text{-}^i\text{Pr}_3\text{C}_6\text{H}_2$). Notably, monoanilide products were not observed in these reactions, regardless of what experimental conditions and quantity of aniline were utilized. Conversely, when the more bulky $2,4,6\text{-}^t\text{Bu}_3\text{C}_6\text{H}_2\text{NH}_2$ was employed, metallacycle ring opening was limited to only one of the *ortho*-metalated *P*-phenyl groups, leading to exclusive formation of the monoanilide complex $\text{LLu}(\text{NHMe}^*)$ ($\text{L} = 1\text{-}(\text{Ph}_2\text{P}=\text{NAr})\text{-}8\text{-}(\text{Ph}(\text{C}_6\text{H}_4)\text{P}=\text{NAr})\text{-}3,6\text{-dimethylcarbazolide}$; $\text{Ar} = \text{Ph}, 4\text{-}^i\text{PrPh}$; $\text{Me}^* = 2,4,6\text{-}^t\text{Bu}_3\text{C}_6\text{H}_2$), **15** (Scheme 13). Intriguingly, this species undergoes an unusual rearrangement to afford the *N*-aryl metalated isomer **15'**. Deuterium labeling and kinetic studies were conducted, establishing that this transformation does not involve an imido intermediate [35].

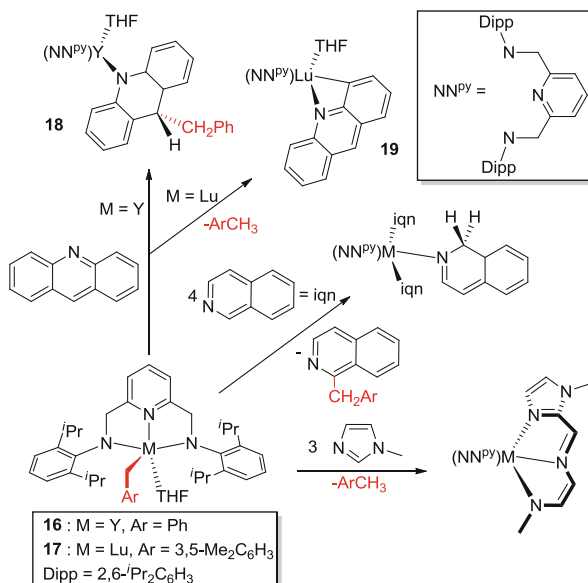


Scheme 13 Metallacycle ring-opening reaction of **14** with 1 equiv. of 2,4,6-*t*-Bu₃C₆H₂NH₂

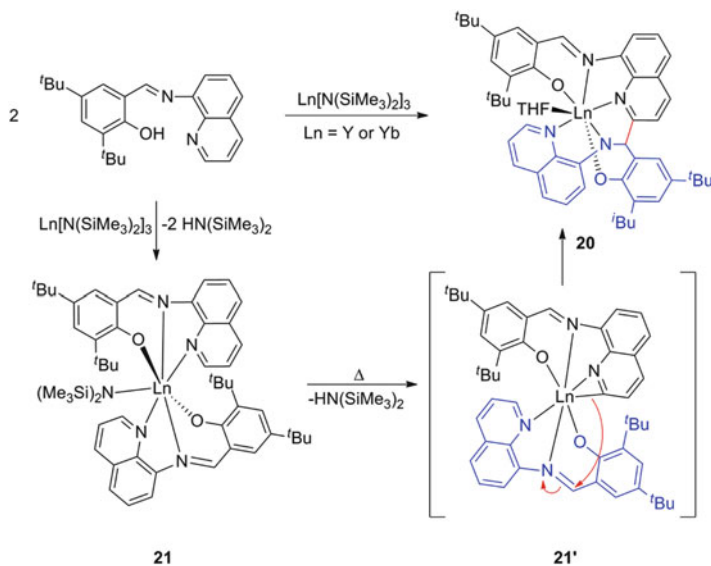
As previously mentioned, cyclometalated rare earth complexes can be reactive species that are observed or postulated to be reaction intermediates. Hence, cyclometalated molecules can lead to unanticipated reactivity. Diaconescu and co-workers studied monoalkyl yttrium and lutetium complexes supported by a pyridine diamide scaffold 2,6-(CH₂N(2,6-*i*-Pr₂C₆H₃)₂)NC₅H₃ (**L**) [36]. Depending on the substrate, these complexes reacted with aromatic *N*-heterocycles via a diverse series of C–H activation, C–C coupling, or heterocycle dearomatization reactions. Mechanistic studies revealed that these reactions proceed through cyclometalated intermediates. Although both lutetium and yttrium complexes generally behaved in a similar fashion, considerable differences in reaction rates were observed. Interestingly, the reaction between LYCH₂Ar(THF) (Ar = Ph), **16**, and acridine afforded the alkyl migrated product LY(R)(THF) (R = 9-CH₂Ph-9-*H*-acridine), **18**, in which the benzyl group was transferred to the 9-position of acridine. However, the same reaction with lutetium complex **17** formed the stable cyclometalated compound **19** (Scheme 14).

As demonstrated by Shen et al., cyclometalation during metal attachment can also lead to new and unexpected ligand frameworks [37]. The amine elimination reaction between Ln(N(SiMe₃)₂)₃ (Ln = Y or Yb) and a salicylaldimine ligand (HL = 3,5-*t*-Bu₂-2-(OH)-C₆H₂CH=N-8-C₉H₆N) gave complex **20**, which was supported by a trianionic NOO-type ligand (Scheme 15). Complex **20** was hypothesized to have formed from the bis(ligand) species L₂LnN(SiMe₃)₂, **21**, which presumably undergoes cyclometalation of a ligand quinoline ring, **21'**, followed by subsequent nucleophilic attack by the metalated carbon on the imine group of the remaining monoanionic ligand. Complex **21** was independently prepared by slow addition of a toluene solution of HL onto Ln(N(SiMe₃)₂)₃ at -50°C. Heating **21** in THF at 40°C also produced complex **20**, thereby further substantiating the proposed mechanism.

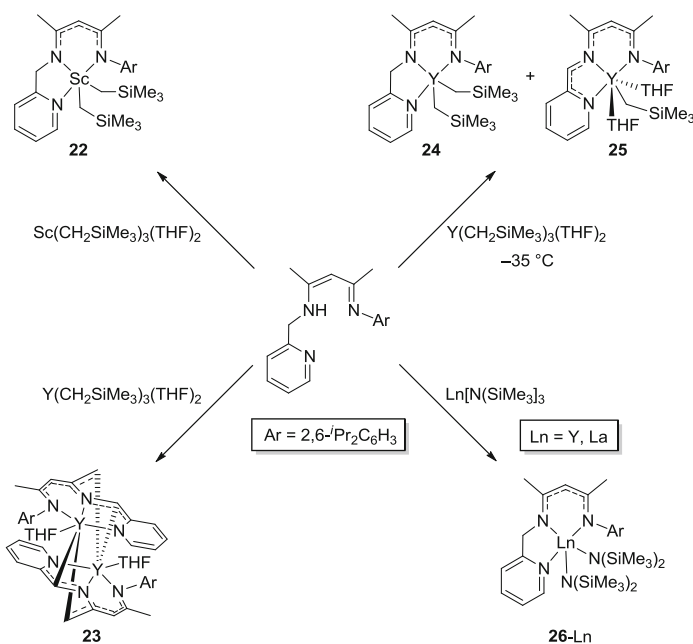
Although C–H bond activation usually leads to well-defined cyclometalated products, in certain occasions, it can create a rigid framework that prevents intramolecular metallacycle formation. In a recent report, Chen et al. prepared scandium, yttrium, and lanthanum complexes of a β-diketiminato-derived pincer ligand that bears a pendant pyridyl donor (Scheme 16) [38]. When Sc(CH₂SiMe₃)₃(THF)₂ was allowed to react with the proteo ligand at ambient temperature, the expected dialkyl complex LSc(CH₂SiMe₃)₂ (L = CH₃C(NDippN)CHC(CH₃)-(NCH₂CNC₅H₄)), **22**, formed, but when the larger metal yttrium was utilized, an



Scheme 14 Examples of C–H activation, C–C coupling, and heterocycle dearomatization



Scheme 15 Conversion of a monoanionic ligand into a macrocyclic trianionic framework via a putative cyclometalated intermediate



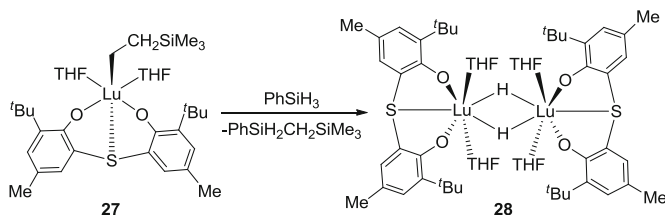
Scheme 16 Rare earth complexes supported by monoanionic, dianionic, and trianionic forms of a β -diketiminato-based pincer ligand

unusual dinuclear complex, **23**, which features two trianionic intermolecularly cyclometalated ligands, prevailed. When the temperature was lowered to -35°C , the reaction generated a mixture of yttrium complexes supported by either mono- or dianionic versions of the β -diketiminato ancillary, **24** and **25**, respectively. However, when $\text{Ln}[\text{N}(\text{SiMe}_3)_2]_2$ ($\text{Ln} = \text{Y}, \text{La}$) was used as the metal source, even the ambient temperature reaction gave the desired bis(amide) complexes $\text{LLn}(\text{N}(\text{SiMe}_3)_2)_2$, **26-Ln**.

3.1.2 Hydride Complexes: Formation and Reactivity

Metal hydrides are another type of influential complex prevalent in organometallic transition metal chemistry and homogenous catalysis [39, 40]. By comparison, non-Cp rare earth hydride complexes are relatively scarce [8, 41], and thus, the reports of molecules bearing pincer-type ligands are even less common. Nonetheless, in recent years, numerous novel polyhydride species have been reported [42], and perhaps unsurprisingly, many demonstrate unique reactivity and, hence, potential for catalysis [43, 44].

The activation of Si–H bonds by oxidative addition of silanes is a well-established synthetic strategy for preparing transition metal hydride species.



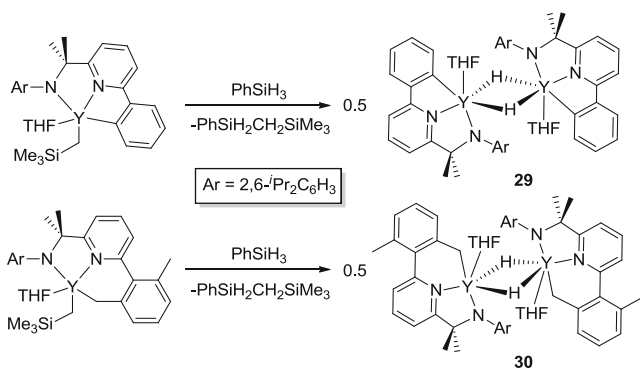
Scheme 17 Preparation of rare earth pincer supported hydride complexes **28**-Ln

However, since the majority of rare earth metals exist predominantly in the +3 oxidation state, they do not readily participate in redox reactions with silanes. Regardless, rare earth alkyl complexes typically react with silanes by σ -bond metathesis pathways to conveniently afford hydride species. In addition, hydrogenolysis reactions between rare earth alkyl complexes and H₂ also serve as a viable route to distinct polyhydride complexes [43].

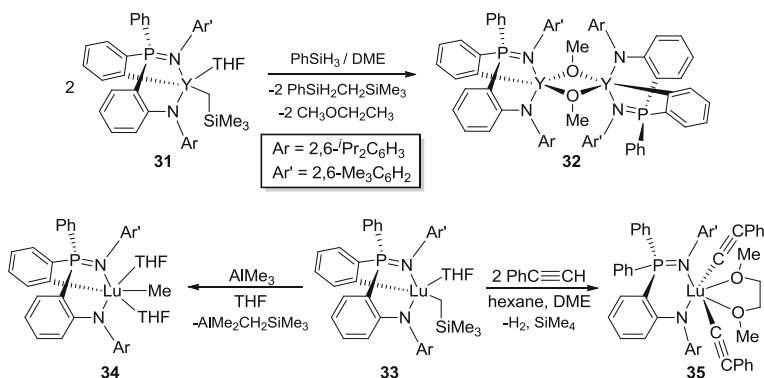
Early examples of rare earth hydrides supported by pincer-type ligands were reported by Okuda and co-workers in 2007 [45]. The lutetium complex $\text{LLu}(\text{CH}_2\text{SiMe}_3)(\text{THF})_2$ (L = 2,2'-thiobis(6-*tert*-butyl-4-methylphenolate)), **27**, reacted with PhSiH₃ to form dimeric hydride-bridged $[\text{LLu}(\mu\text{-H})(\text{THF})_2]_2$, **28** (Scheme 17). Bis(phenolate) ligated **28** readily reacted with phenyl acetylene (PhC \equiv CH) or benzophenone (Ph₂CO) at ambient temperature to form the corresponding insertion products. In addition, preliminary catalytic studies showed that in the presence of ^{*i*}PrOH complex, **27** exhibited modest activity as a catalyst for the ring-opening polymerization of L-lactide. Shortly thereafter, Sc, Y, and Ho derivatives of **27** were synthesized and their reactivity toward phenyl silane was studied. Unfortunately, the holmium complex **28**-Ho was the only isolable hydride species [46].

In late 2009, Giambastiani and Trifonov and Cui et al. reported similar cyclometalated rare earth complexes supported by amidopyridinate and anilido-phosphinimine ligands, respectively. They studied the utility of such compounds as precursors to rare earth hydrides [47, 48]. Although reactions with H₂ were not successful, the groups of Giambastiani and Trifonov isolated and characterized well-behaved dinuclear hydride-bridged yttrium complexes **29** and **30** via the reaction between the metalated monoalkyl complexes and phenylsilane (Scheme 18). Notably, the Y-C_{aryl} metallacycle appears inert, as it remained intact in all reported reactions. Unfortunately, preliminary investigations indicated these compounds were only modestly active catalysts for the polymerization of ethylene.

Cui and co-workers also attempted to prepare yttrium hydride species by the reaction of $\text{LY}(\text{CH}_2\text{SiMe}_3)(\text{THF})$ (L = (2,6-^{*i*}Pr₂C₆H₃)NC₆H₄PPhC₆H₄N(2,4,6-C₆H₂Me₃), **31**, with phenyl silane [48]. In this case, the isolated methoxido-bridged dinuclear product, $[\text{LY}(\mu\text{-OMe})]_2$, **32**, is the result of unpredicted C–O bond activation of dimethoxyethane (DME) (Scheme 19). It was proposed that the reaction mechanism proceeds via a transient terminal hydride intermediate, although the authors were unable to isolate such a species. However, in situ studies



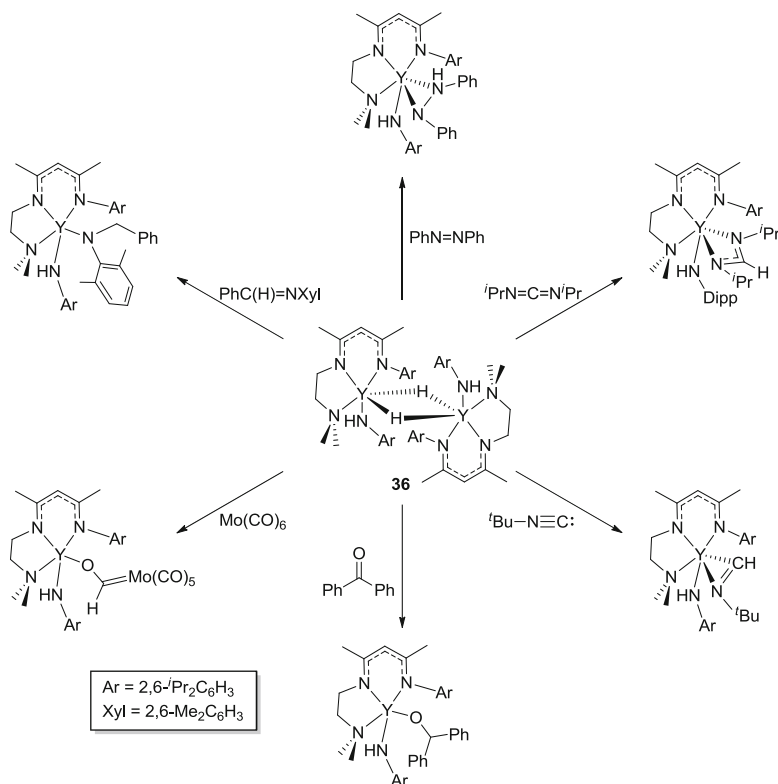
Scheme 18 Formation of yttrium dihydride complexes stabilized by a cyclometalated amidopyridinate ligand



Scheme 19 Reaction of Y and Lu anido-phosphinimine complexes with PhSiH_3 , $\text{PhC}\equiv\text{CPh}$, and AlMe_3

with isoprene afforded a new compound identified as the η^3 -pentenyl yttrium complex $\text{LY}(\eta^3\text{-CH}_2\text{C}(\text{CH}_3)\text{CHCH}_3)(\text{THF})$. The solid-state structure of the pentenyl fragment suggested that an yttrium hydride species reacted with one molecule of isoprene via 1,4-addition. The lutetium analogue, **33**, of complex **31** reacted with AlMe_3 to produce the corresponding lutetium methyl complex **34**, again with the metalated $\text{Lu-C}_{\text{aryl}}$ linkage intact. Conversely, the addition of phenylacetylene cleaved the metallacycle bond and gave the bis(alkynyl) lutetium complex $\text{LLu}(\text{C}\equiv\text{CPh})_2(\text{DME})$, **35** (Scheme 19).

Shortly after the work of Gambastiani, Trifonov, and Cui, Chen et al. reported the synthesis and structure of dinuclear yttrium anido hydride complexes **36** which exhibit a rich reaction chemistry with various unsaturated substrates (Scheme 20) [49]. Specifically, dinuclear species **36** reacts readily with a versatile selection of small molecules to give the expected Y-H addition products in good yields. Notably, no reaction was observed with the robust $\text{Y-N}_{\text{anido}}$ bond.

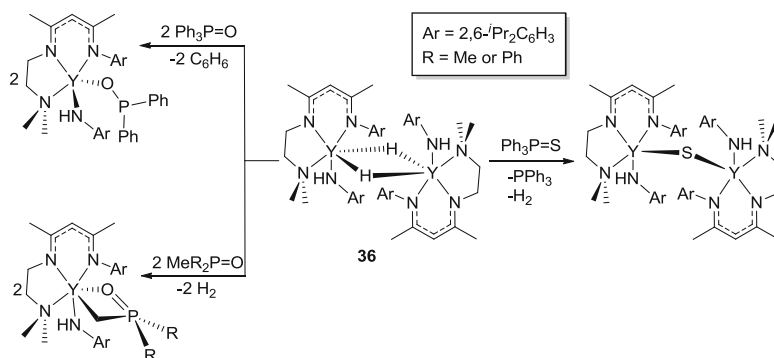


Scheme 20 Reactivity of hydride-bridged dinuclear yttrium anido complexes **36** toward unsaturated substrates

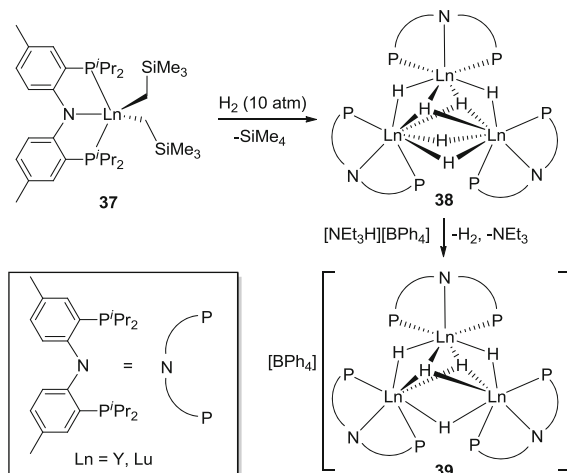
More recently, Chen et al. extended the scope of dihydride **36** to reactions with phosphine oxides and sulfides [50]. Depending on the substrate, diverse reactivity patterns including C–P, C–H, or P–S bond cleavage was observed (Scheme 21). Furthermore, the reaction of **36** with $\text{Ph}_3\text{P}=\text{O}$ gave the first example of a rare earth diorganophosphinoyl complex via C–P bond cleavage.

Molecular rare earth polyhydride complexes having hydride-to-metal ratios larger than 1 have shown interesting and even unprecedented reactivity [43, 44]. Since the polyhydrides generally form as robust, polynuclear clusters, bulky ancillaries are often used to restrict the nuclearity and stabilize the resultant compounds.

Hou and co-workers demonstrated that hydrogenolysis of dialkyl yttrium and lutetium complexes **37**, which bear the rigid bis(phosphinophenyl)amido ligand, with H_2 produced structurally novel trinuclear hexahydrides **38** (Scheme 22). These complexes, upon the addition of $[\text{NEt}_3\text{H}][\text{BPh}_4]$ at ambient temperature, can be converted into the cationic pentahydrides **39** in high yields [51]. In addition, if the original hydrogenolysis reaction is conducted in the presence of 0.5 equiv. of $[\text{NEt}_3\text{H}][\text{BPh}_4]$, dinuclear trihydride complexes prevail.



Scheme 21 Reaction of **36** with phosphine oxides and sulfides

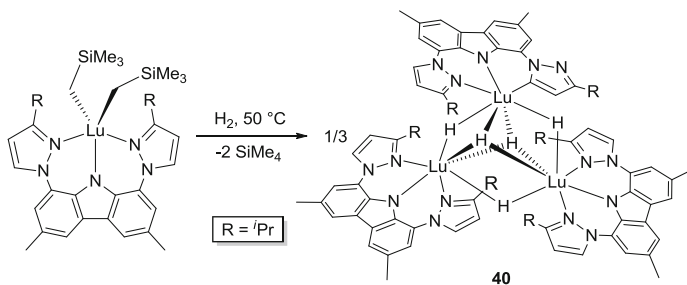


Scheme 22 Synthesis of hexahydride **38** and cationic **39**

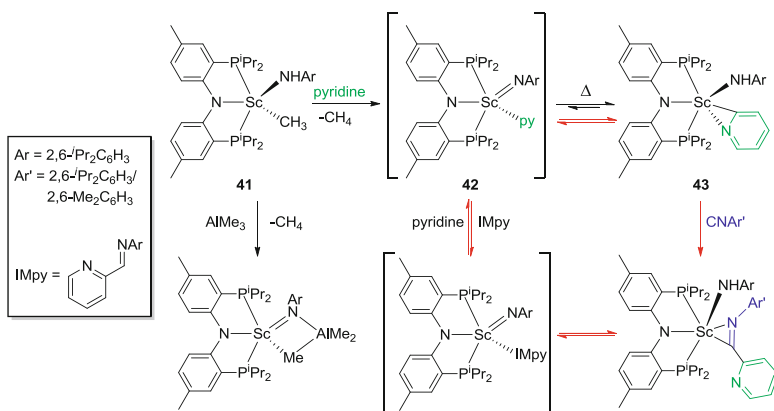
A related neutral pentahydride species **40**, prepared by the hydrogenolysis of a bis(pyrazolyl)carbazole lutetium complex (Scheme 23), was recently reported by our group [52]. Unlike complex **38**, the putative hexahydride complex was transformed into the pentahydride variant upon C–H bond activation of one of the pyrazole donors.

3.1.3 Metal Complexes with Multiply Bonded Ligands

Despite the wide range of applications found for countless transition metal and actinide complexes that bear terminal multiply bonded ligands [53–55], rare earth counterparts of this type of complex are scarce. In fact, only three structurally characterized complexes containing terminal, *unsupported* (monodentate) multiply



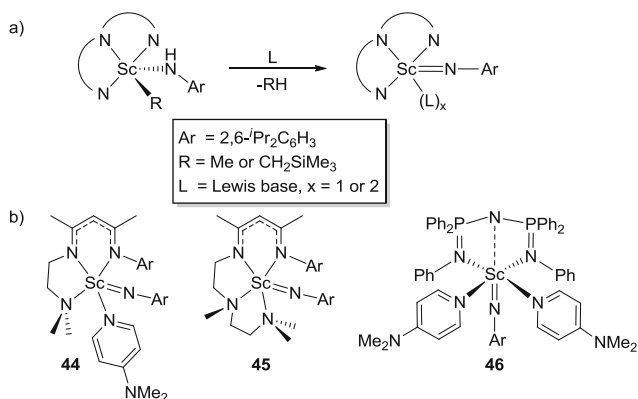
Scheme 23 Hydrogenolysis of a bis(pyrazolyl)carbazole lutetium dialkyl complex



Scheme 24 Formation and reactivity of terminal scandium imido **41** and synthetic cycle for C–H activation and functionalization of pyridines (marked with red arrows)

bound main group element fragments have been reported to date [56, 57]. Notably, all of these examples are scandium(III) imido species supported by pincer-type or closely related ligands. In addition, Piers and colleagues isolated and spectroscopically characterized a scandium NacNac complex that exhibited reactivity which could be attributed to a terminal imido functionality [23]. Furthermore, elegant mechanistic studies have been reported that demonstrate the presence of Sc=NR-containing species in solution (*vide infra*).

Initial evidence for the formation of a terminal scandium imido group was delivered by Mindiola et al. in 2008. Alkane elimination from the alkyl amido complex $\text{LSc}(\text{Me})(\text{NHAr})$ ($\text{L} = \text{N}[2\text{-}^i\text{Pr}_2\text{-4-Me-C}_6\text{H}_3]_2$, $\text{Ar} = 2,6\text{-}^i\text{Pr}_2\text{C}_6\text{H}_3$), **41**, purportedly afforded the transient imido intermediate $\text{LSc}=\text{NAr}(\text{py})$, **42**. The observation of intermolecular C–H activation of pyridine and benzene, as well as the isolation of an AlMe_3 trapped derivative, provided a strong argument for the presence of a Sc=NR species in the reaction mixture (Scheme 24) [58]. Later on, Mindiola reported that a scandium pyridyl-anilide compound $\text{LSc}(\text{NHAr})\text{-}(\eta^2\text{-NC}_5\text{H}_4)$, **43**, and an alleged pyridine adduct of an imido complex **42** were related

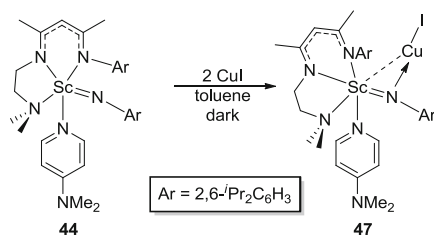
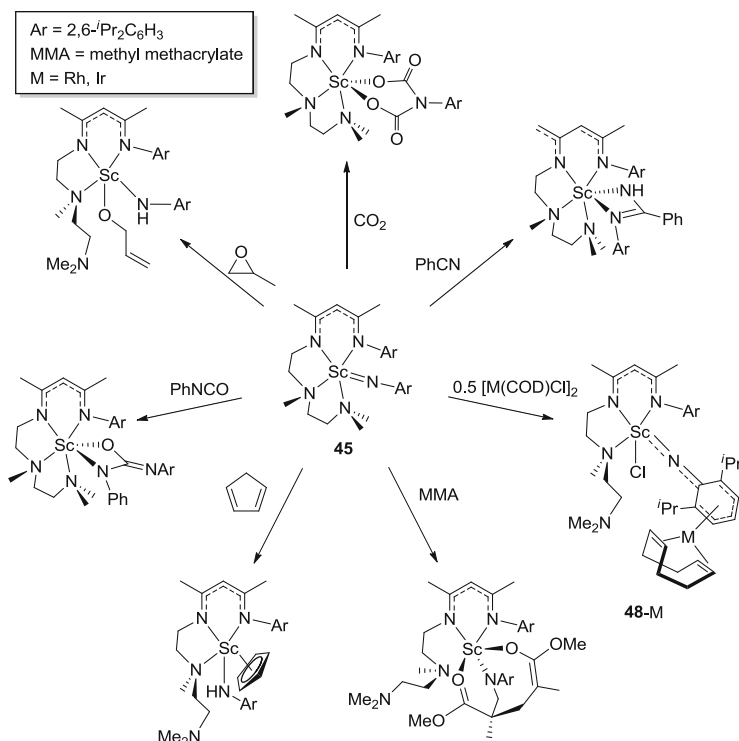


Scheme 25 (a) General route for the synthesis of LSc=NR complexes. (b) Schematic presentation of structurally characterized rare earth terminal imido complexes

by an interesting tautomeric equilibrium. As a result, his group capitalized on this process in order to facilitate the stoichiometric and catalytic functionalization of pyridines with isonitriles, establishing an atom economical route to mono- and bis(imino)-substituted pyridines (Scheme 24) [33].

In 2010, a seminal contribution by Chen et al. reported the first structurally characterized rare earth species bearing a terminal imido group LSc=NAr(DMAP) (L = MeC(NDipp)CHC(Me)(NCH₂CH₂NMe₂)); DMAP = 4-dimethylamino-pyridine; Dipp = 2,6-*i*-Pr₂C₆H₃), **44**. The scandium complex was prepared via methane elimination from the alkyl-amido precursor upon the introduction of the strongly coordinating base DMAP (Scheme 25) [59]. Shortly after, Chen and co-workers utilized a modified ligand framework with a pendant dimethylamino group that promoted alkane elimination in a similar fashion to DMAP, except it produced an imido complex (LSc=NDipp (L = MeC(Dipp)NH)CHC(Me)(NCH₂CH₂N(Me)CH₂CH₂NMe₂)), **45**) devoid of coordinated external base [60]. The third example of a structurally characterized terminal rare earth imido complex was reported 3 years later, when Cui et al. synthesized the first hexacoordinate Sc=NR species, LSc=NDipp(DMAP)₂ (L = N(Ph₂P=NPh)₂), **46** [57].

Exploratory experiments of the scandium imido complex **44** with CuI and [M(COD)Cl]₂ (M = Rh, Ir) revealed intriguing chemistry at the imido group [61]. More specifically, the nucleophilic nitrogen coordinated to the Cu(I) cation of CuI to form the imido-bridged heterodinuclear complex LSc=NDipp(CuI)(DMAP) (L = MeC(NDipp)CHC(Me)(NCH₂CH₂NMe₂)), **47** (Scheme 26). Although reaction of **44** with [M(COD)Cl]₂ (M = Rh, Ir) released one molecule of DMAP which hampered the purification of the metal-containing products, the addition of **45** to [M(COD)Cl]₂ proceeded cleanly to one product after 1 h at ambient temperature. An X-ray diffraction study indicated that the electrophilic Sc center had abstracted a chloride anion from [M(COD)Cl]₂ and the resultant [M(COD)]⁺ fragment coordinated to the aryl ring of the imido ligand, ultimately affording the unusual scandium–rhodium/iridium mixed metal species LSc=N(ηⁿ-Dipp)M(COD) (M = Rh, n = 4; Ir,

**Scheme 26** Reactivity of complex **44** with CuI**Scheme 27** Reactivity of imido **45** with various unsaturated substrates and transition metal complexes

$n = 3-5$; COD = 1,5-cyclooctadiene), **48-M** (Scheme 27). In addition to the remarkable structural features of the preceding complexes, **48-Ir** exhibited promising performance as an alkyne hydroboration catalyst.

After the first reports implicating the accessibility of rare earth imido species, the field flourished, confirming the expected versatility of this kind of complex. For example, Chen et al. demonstrated that elemental selenium reacted readily with Sc=NR fragments. Depending on the ancillary ligand, selenolation of one of the sp^2 aromatic or sp^3 NMe₂ carbons in DMAP was observed. Instead of the relatively

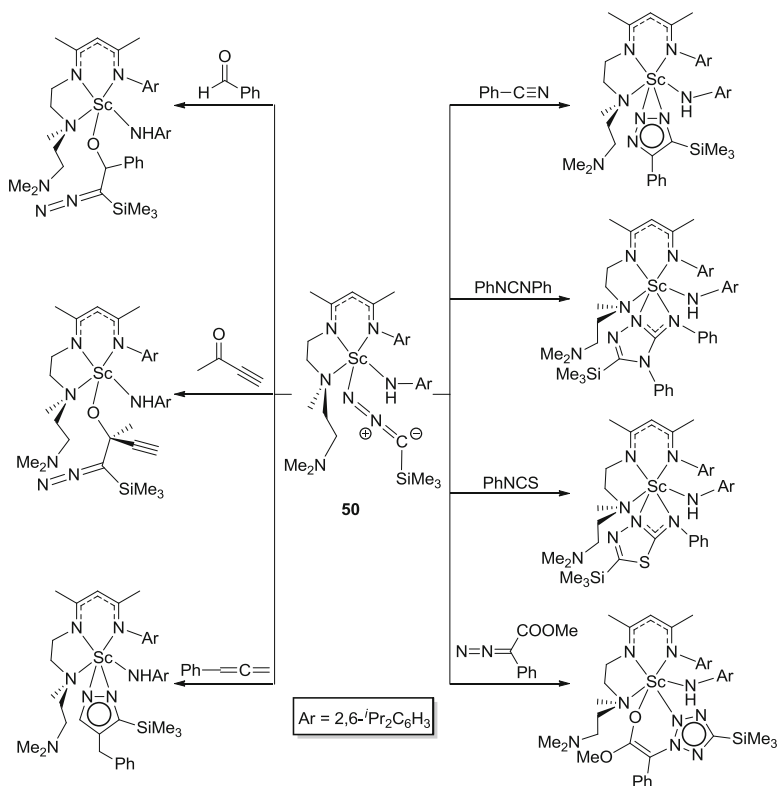
common activation of a coordinated DMAP C–H bond, the selenations were proposed to proceed through an unusual Sc–N–Se ring, formed upon [2 + 1] cycloaddition of a Se atom to the Sc=N double bond [60]. In the follow-up paper, Chen et al. surveyed the cycloaddition chemistry of complex **45** with a wide selection of unsaturated substrates (Scheme 27) [62]. The imido functionality readily reacted with CO₂, benzonitrile (PhCN), methyl methacrylate (MMA), and phenyl isocyanate (PhNCO) through [2 + 2] or [2 + 4] cycloadditions, highlighting the nucleophilicity of the nitrogen atom but also the notable Lewis acidity of the Sc(III) center. The cycloadditions were often followed by subsequent reaction chemistry, such as Michael additions or isomerizations. Furthermore, imido complex **45** undergoes hydrogen transfer with cyclopentadiene and propylene oxide, again demonstrating the proton acceptor and ring-opening capability of the complex.

In addition to C–H bond activations, complex **45** also reversibly activated the Si–H bond of phenylsilane to give the corresponding scandium anilido hydride complex $\text{LSc(H)[N(Dipp)(SiH}_2\text{Ph)]}$ (L = MeC(NDipp)CHC(Me)-(NCH₂CH₂NMe₂)), **49**, which undergoes a rapid σ -bond metathesis process between the Sc–H and Si–H bonds of phenylsilane (demonstrated by deuterium-labeling experiments) [63]. The terminal hydrido complex **49** was not isolable per se, but upon trapping with diphenylcarbodiimide, a stable scandium anilido amidinate, $\text{LSc[N(Dipp)(SiH}_2\text{Ph)](PhNCHNPh)}$, was identified and structurally characterized. Furthermore, preliminary catalytic experiments showed that a 5 mol% loading of imido complex **45** selectively catalyzed the conversion of *N*-benzylidenepropan-1-amine to the corresponding monoaminosilane in 2 h at 50°C.

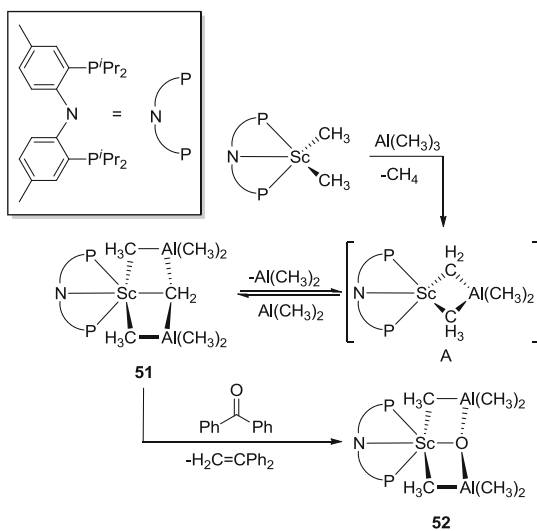
Recently, Chen and co-workers utilized **45** to prepare the first scandium nitrilimine derivative $\text{LSc(NHDipp)(NNCSiMe}_3)$ (L = MeC(NDipp)CHC(Me)-(NCH₂CH₂NMe₂)), **50** [64]. The thermal stability of this novel complex allowed for an in-depth analysis of its reactivity with a selection of unsaturated substrates, including aldehydes, ketones, nitriles, and allenes (Scheme 28). This work, which was complemented by sophisticated computational experiments, established the versatility of the nitrilimine species, as the reactivity of complex **50** is related to either diazoalkenes or organic nitrilimines, depending upon the given substrate.

To date, imido species are the only type of structurally characterized rare earth complex to feature terminal, multiply bonded, unsupported ligands. However, several other examples that have bridging and/or functionalities wherein the nature of the bonding is more ambiguous have also been reported [56]. For example, Mindiola et al. utilized Tebbe's strategy of trapping group 4 alkylidene species to prepare scandium complex $\text{LSc}(\mu_3\text{-CH}_2)(\mu_2\text{-CH}_3)_2[\text{Al}(\text{CH}_3)_2]_2$ (L = N[2-*P*^{Pr}₂-4-Me-C₆H₃]₂), **51**, which contains a methyldiene ligand supported by two coordinated AlMe₃ groups [65]. Notably, the methyldiene ligand can be protonated with an excess of H₂NAr (Ar = 2,6-*i*Pr₂C₆H₃) to form the alkyl complex $\text{LSc}(\text{CH}_3)(\text{NHAr})$ or transferred to benzophenone to afford H₂C=CPh₂ and the scandium oxide complex $\text{LSc}(\mu_3\text{-O})(\mu_2\text{-CH}_3)_2[\text{Al}(\text{CH}_3)_2]_2$, **52** (Scheme 29).

Thus far heavier rare earth analogues of scandium imido species remain unknown, likely because of the enhanced reactivity of larger metals. For example, Cui et al. were able to synthesize yttrium and lutetium analogues of the scandium



Scheme 28 Reactivity of **50** with unsaturated substrates



Scheme 29 Synthesis and reactivity of an AlMe_3 stabilized scandium methylidene complex

alkyl amido precursor to complex **46**; however, even in the presence of DMAP, only bis(anilido) and unidentified ligand redistribution products were generated [57]. Nonetheless, the rich reaction chemistry observed for scandium complexes bearing terminal imido moieties is sure to amplify future endeavors to prepare heavier rare earth congeners of these exceptional molecules.

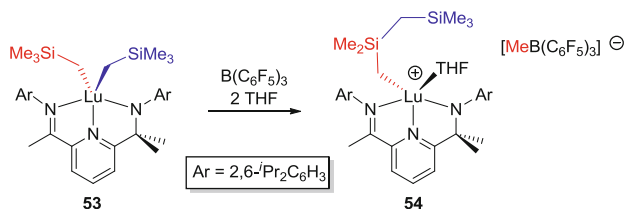
3.2 Alkane Elimination and Alkyl Migration

Alkane elimination is a widely used method to coordinate pincer ligands to rare earth metals, and it is also frequently exploited when studying subsequent reactivity of such complexes. For example, imido and various amido functionalities are often prepared by alkane elimination (*vide supra*), as are cationic rare earth pincer compounds. Frequently, unanticipated alkyl migration reactions are observed and are responsible for the formation of many unusual complexes.

3.2.1 Cationic Rare Earth Complexes

Cationic rare earth complexes are commonly used in catalytic applications, such as olefin polymerization (see Sects. 4.2 and 4.3). These species tend to be extremely reactive and, thus, are often generated and used *in situ*. However, a handful of well-defined cationic rare earth pincer complexes have been reported, the details of which are summarized below.

In 2003, Gordon et al. isolated the first example of a cationic rare earth pincer complex, [2-(2,6-*i*-Pr₂C₆H₃N=CMe)-6-(2,6-*i*-Pr₂C₆H₃NCMe₂)NC₅H₃Lu-(CH₂SiMe₂CH₂SiMe₃)(THF)][MeB(C₆F₅)₃], **54**. This anilido-pyridine-imine-supported species was prepared by the reaction of B(C₆F₅)₃ with LLu(CH₂SiMe₃)₂, **53**, wherein abstraction of a Si–Me group promoted migration of a CH₂SiMe₃ moiety to give rise to the CH₂SiMe₂CH₂SiMe₃ group in cationic complex **54** (Scheme 30) [66]. Presumably the steric bulk of this system prevented the Lewis acidic borane from abstracting the entire trimethylsilylmethyl group.



Scheme 30 Synthesis of cationic lutetium complex **54**

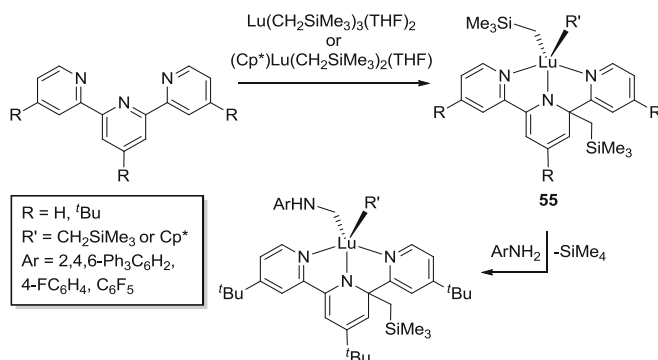
Cationic complexes with larger rare earth metals were reported by Berg et al. [67]. Dialkyl complexes $LLn(CH_2SiMe_3)_2$ ($Ln = Y, Yb, Er$; $L = 1,8$ -bis(4',4'-dimethyloxazolin-2'-yl)-3,6-di-*tert*butylcarbazole) were prepared either by straightforward alkane elimination or by the addition of the deprotonated ligand to $LnCl_3(THF)_n$ ($n = 3$ or 3.5), followed by reaction with 2 equiv. of $LiCH_2SiMe_3$. These dialkyl species were activated with $[Ph_3C][B(C_6F_5)_4]$ and tested for their ability to polymerize olefins. Aside from trace quantities of polymer produced solely by the trityl activator, no polymerization was observed. Nonetheless, multinuclear NMR spectroscopy confirmed that one of the alkyl groups of $LLn(CH_2SiMe_3)_2$ was indeed abstracted by $[Ph_3C]^+$ to generate the anticipated alkyl cation $[LLn(CH_2SiMe_3)_2][B(C_6F_5)_4]$. This compound is thermally stable in solution for more than a week, but all efforts to isolate it resulted in decomposition.

In 2009, Cui and co-workers examined the ability of the $LiCl$ adduct of $[Ph_3C][B(C_6F_5)_4]$ to abstract an alkyl group from the lutetium analogue of anilido-phosphinimine complex **33** (see Sect. 3.1.2) [48]. The authors hypothesized that the putative complex $[LLu(DME)][B(C_6F_5)_4]$ ($L = (2,6\text{-}^i\text{Pr}_2C_6H_3)NC_6H_4\text{-}PPhC_6H_4N(2,4,6\text{-}C_6H_2Me_3)$) formed upon alkyl abstraction by $[Ph_3C][B(C_6F_5)_4]$, and this ion pair was rapidly converted into the corresponding chloride complex $LLuCl(DME)$ via metathesis with $LiCl$. This proposed mechanism was corroborated by the identification of $[Li(DME)_3][B(C_6F_5)_4]$ as a reaction by-product.

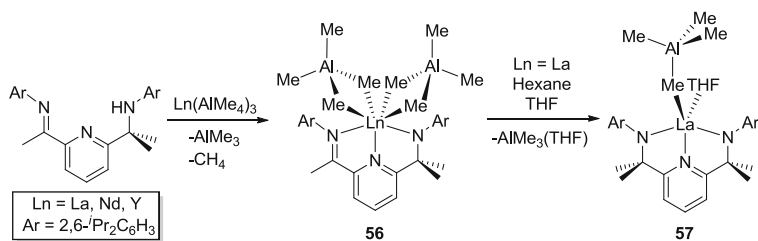
Although protonation is another well-known methodology utilized to create cationic metal species, this approach has rarely been reported for rare earth pincer complexes. Izod et al. protonated a cyclometalated lanthanum phosphide complex $[(Me_3Si)_2CH](C_6H_4\text{-}2\text{-}CH_2NMe_2)PLa(THF)[P(C_6H_4\text{-}2\text{-}CH_2NMe_2)\{CH(SiMe_3)\text{-}(SiMe_2CH_2)\}]$ [31], **12** (see Sect. 2.2), with $[Et_3NH][BPh_4]$, generating the unusual alkyl cation $[(THF)_4LaP(C_6H_4\text{-}2\text{-}CH_2NMe_2)\{CH(SiMe_3)(SiMe_2CH_2)\}][BPh_4]$. Rather surprisingly, protonation occurred at the lanthanum–phosphorus bond, instead of the expected La–C bond. [68]. More recently, Hou and co-workers used $[NEt_3H][BPh_4]$ to prepare examples of cationic bi- and trinuclear polyhydrides (see Sect. 3.1.2) [51], while Hayes et al. treated dialkyl $LLu(CH_2SiMe_3)_2$ ($L = 2,5\text{-}((4\text{-}^i\text{Pr}C_6H_4)N=PPh_2)_2NC_4H_2$) with the oxonium acid $([H(OEt_2)_2][B(C_6F_5)_4])$ to synthesize the cationic complex $[LLu(CH_2SiMe_3)(OEt_2)_2][B(C_6F_5)_4]$ [69].

3.2.2 Alkyl Migration

Reactive rare earth alkyl complexes can trigger diverse alkyl migration reactions which often result in functionalization of pincer ancillary ligands. For example, in 2006, Kiplinger et al. reported the 1,3-migration of a CH_2SiMe_3 group from lutetium to the *ortho* position of the central ring of a terpyridine ligand (Scheme 31) [70], resulting in loss of aromaticity and transformation of the neutral terpyridine pincer into an anionic ligand. A similar migration was also observed when the dialkyl lutetium complex $(Cp^*)Lu(CH_2SiMe_3)_2(THF)$ was used. The potential for this monoanionic tridentate NNN' ligand system to support multiply bonded rare earth species was examined a few years later when the alkyl amido and bis(amido)



Scheme 31 Preparation of the alkyl migrated lutetium complex **55**

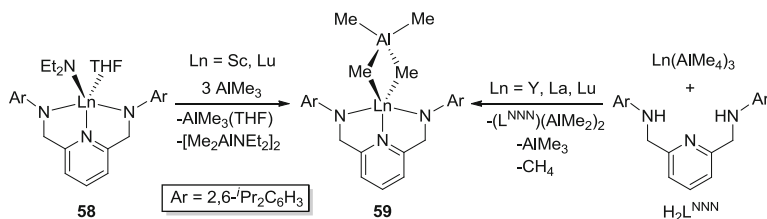


Scheme 32 Formation and reactivity of heterotrimetallic imino–amido complexes **56**

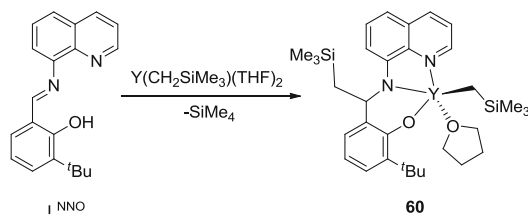
derivatives of complex **55** were prepared by alkane elimination reactions with different anilines. Unfortunately, thermolysis of the amido complexes did not result in the formation of the corresponding lutetium imido species, regardless of the nature of the anilide ligand [71].

Anwander and colleagues exploited $\text{Ln}(\text{AlMe}_4)_3$ as a novel metal precursor for the synthesis of heterotrimetallic imino–amido complexes $\text{LLn}(\eta^2\text{-AlMe}_4)_2$ ($\text{Ln} = \text{La}, \text{Nd}, \text{Y}$; $\text{L} = 2\text{-}(2,6\text{-}^i\text{Pr}_2\text{C}_6\text{H}_3)\text{NCMe}_2\text{-6-(2,6-}^i\text{Pr}_2\text{C}_6\text{H}_3)\text{N}=\text{C}(\text{Me})\text{NC}_5\text{H}_3$), **56** (Scheme 32) [72]. Intriguingly, relatively modest yields prompted closer inspection of the reaction mixture, ultimately revealing the presence of two additional methyl aluminum complexes with alkylation of the remaining imino carbon atom transforming the original monoanionic ancillary into a dianionic bis(amido)pyridine ligand. Further experiments suggested that the alkylation occurred via an exceedingly reactive $[\text{Ln}\text{-Me}]$ moiety, instead of AlMe_3 released during the reaction. Efforts to convert the heteroleptic complex into an organoaluminum-free methyl derivate only yielded the partially cleaved compound $\text{LLa}(\eta^1\text{-AlMe}_4)(\text{THF})$ ($\text{L} = 2,6\text{-}\{2,6\text{-}^i\text{Pr}_2\text{C}_6\text{H}_3\}\text{NCMe}_2\}_2\text{NC}_5\text{H}_3$), **57** (Scheme 32). The formation of complex **57** is speculated to originate from a rapid process initiated by donor-induced loss of one tetramethylaluminate ligand to give a reactive $[\text{Ln}\text{-Me}]$ species which then undergoes methyl migration from the metal center to the imino carbon of the supporting ligand.

Heterodinuclear Ln/Al complexes of dianionic NNN and NON donor ligands have typically been synthesized from $\text{Ln}(\text{AlMe}_4)_3$ metal sources [14, 72]. Rare



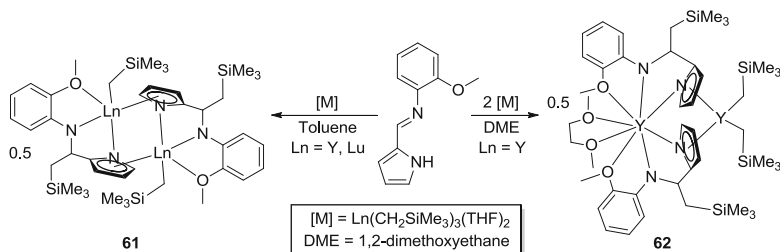
Scheme 33 Two different synthetic routes for the preparation of heterodinuclear **59**



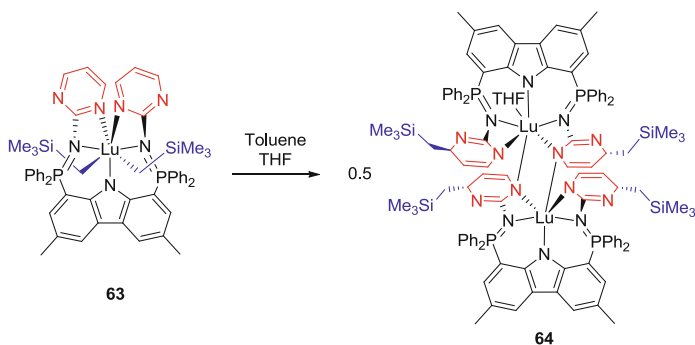
Scheme 34 Formation of yttrium complex **60**

earth metal tetramethylaluminate complexes bearing another $[\text{NNN}]^{2-}$ -type bis(amido)pyridine pincer were obtained by trimethylaluminum promoted lanthanide-amide alkylation. Reaction of $\text{L}^{\text{NNN}}\text{Ln}(\text{NEt}_2)(\text{THF})$ ($\text{Ln} = \text{Sc}, \text{Lu}$; $\text{L}^{\text{NNN}} = 2,6\text{-}\{(2,6\text{-}i\text{Pr}_2\text{C}_6\text{H}_3)\text{NCH}_2\}_2\text{NC}_5\text{H}_3$), **58**, with trimethylaluminum afforded complexes ($\text{L}^{\text{NNN}}\text{Ln}(\eta^2\text{-AlMe}_4)$) ($\text{Ln} = \text{Sc}, \text{Lu}$), **59** of scandium and lutetium. The corresponding yttrium and lanthanum analogues, **59-Y** and **59-La**, respectively, were prepared similarly to **56-Ln** via reaction of $\text{Ln}(\text{AlMe}_4)_3$ with the proteo ligand; however, these compounds were contaminated with $(\text{L}^{\text{NNN}})(\text{AlMe}_2)_2$ (Scheme 33) [73]. The solution state behavior of these complexes was studied by NMR spectroscopy which indicated dissociative (Sc) or associative (Lu) methyl group exchange of the AlMe_4 ligand depending on the size of the rare earth metal. Notably, in the presence of trimethylaluminum, the yttrium species **59-Y** underwent metalation of an isopropyl methyl group, whereas the isopropyl methine carbon was metalated when THF was added to **59-Lu**. Although these complexes exhibit complicated chemistry, they serve to shed insight into possible deactivation mechanisms for olefin polymerization catalysts that require an excess of organoaluminum co-catalyst.

Yttrium dihalide complexes of quinolone-imine-phenoxide NNO donor ligands L^{NNO} were prepared by the reaction of the deprotonated ligand with anhydrous YCl_3 . However, attempts to prepare the corresponding dimethyl derivative $\text{L}^{\text{NNO}}\text{YMe}_2$ ($\text{L}^{\text{NNO}} = 2\text{-}i\text{Bu-6-(quinolin-8-yliminomethyl)phenoxide}$) by the addition of the Grignard reagent MeMgBr gave the magnesium complex $[\text{Mg}_2\text{BrCl}(\text{L}^{\text{NNO}(\text{Me})\text{O}})(\text{THF})_2]$ ($\text{L}^{\text{NNO}(\text{Me})\text{O}} = 2\text{-}i\text{Bu-6-[1-(quinolin-8-ylamido)ethyl]phenoxide}$) as the only isolable product. Alternatively, reaction of HL^{NNO} with $\text{Y}(\text{CH}_2\text{SiMe}_3)_3(\text{THF})_2$ afforded $[\text{Y}(\text{CH}_2\text{SiMe}_3)(\text{L}^{\text{NN}(\text{CH}_2\text{SiMe}_3)\text{O}})(\text{THF})]$ ($\text{L}^{\text{NN}(\text{CH}_2\text{SiMe}_3)\text{O}} = 2\text{-}i\text{Bu-6-[1-(quinolin-8-$



Scheme 35 Synthesis of alkyl migrated Y and Lu complexes **61** and **62**

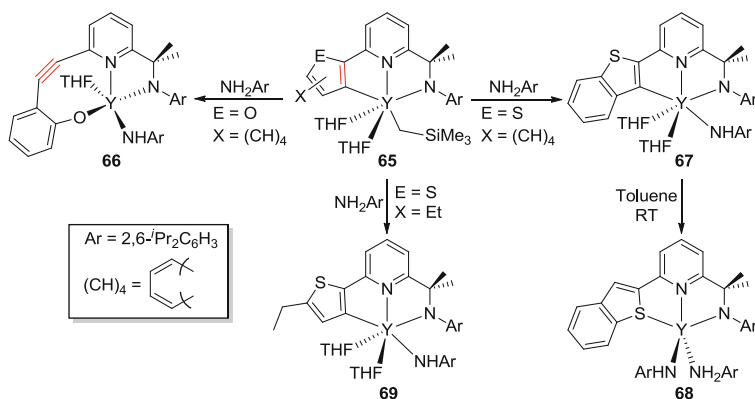


Scheme 36 Lutetium dialkyl **63** and its alkyl migration chemistry

ylamido)-2-trimethylsilylanylethyl]phenoxide), **60**, the result of alkyl migration (Scheme 34) [74].

Similar alkyl shifts were reported in reactions involving the iminopyrrolyl ligand (2-(2- $\text{CH}_3\text{OC}_6\text{H}_3\text{N}=\text{CH}$) $\text{C}_4\text{H}_3\text{NH}$) and $\text{Ln}(\text{CH}_2\text{SiMe}_3)_3(\text{THF})_2$ ($\text{Ln} = \text{Y}, \text{Lu}$) (Scheme 35) [75]. Dinuclear monoalkyl, **61**, or dialkyl, **62**, species were formed depending upon which solvent (toluene or 1,2-dimethoxyethane) was used. Both complexes **61** and **62** feature amide donors formed upon nucleophilic attack by CH_2SiMe_3 groups on one or more imine carbons. Notably, benzophenone inserted into the $\text{Lu}-\text{CH}_2\text{SiMe}_3$ bond of **61**-Lu to afford the corresponding alkoxide species [(2-(2- $\text{MeOC}_6\text{H}_3\text{NC}(\text{H})\text{CH}_2\text{SiMe}_3$) $\text{C}_4\text{H}_3\text{N}$) $\text{LuOCPh}_2\text{CH}_2\text{SiMe}_3$]₂.

Recently, Hayes et al. reported a pyrimidine-substituted bis(phosphinimine) carbazole ligand which reacted with $\text{Lu}(\text{CH}_2\text{SiMe}_3)_3(\text{THF})_2$ to produce the thermally sensitive dialkyl lutetium complex 1,8-($\text{N}_2\text{C}_4\text{H}_3\text{N}=\text{PPh}_2$)₂-3,6-dimethylcarbazole **63** (Scheme 36) [76]. Despite the fact that complex **63** was not prone to intramolecular C–H bond activation like Lu complexes supported by previous incarnations of the carbazole-based pincer [34], it undergoes double alkyl migration in which both of the alkyl groups bound to the lutetium center migrate to the ligand pyrimidine rings. The resultant product was an asymmetric dinuclear complex, **64**, wherein the now trianionic ligand was κ^5 coordinated to lutetium through five nitrogen atoms. The alkyl migration process was also studied with other rare



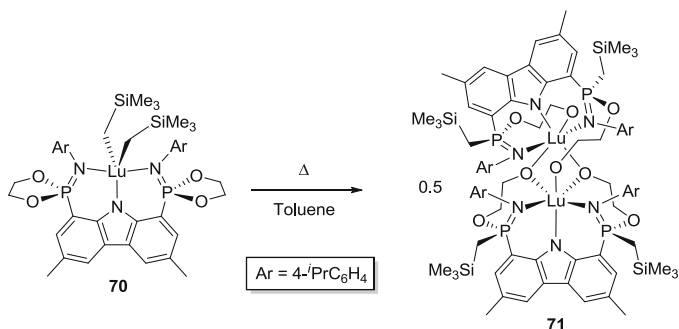
Scheme 37 Reaction of **65** with $(2,6\text{-}i\text{-Pr}_2\text{C}_6\text{H}_3)\text{NH}_2$

earth elements, but only intractable mixtures were obtained when scandium and yttrium derivatives of **63** decomposed.

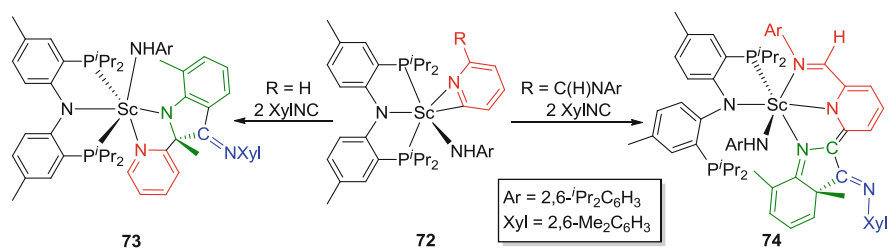
Trifonov and Giambastiani et al. studied amine-triggered alkane elimination from $\text{LLn}(\text{CH}_2\text{SiMe}_3)(\text{THF})_2$ ($\text{L} = 2\text{-}(2,6\text{-}i\text{-Pr}_2\text{C}_6\text{H}_3)\text{NCMe}_2\text{-6-R-NC}_5\text{H}_3$; $\text{R} = \text{benzofuran, benzothiophene, 2-ethylthiophene}$), **65** [29] in an effort to synthesize yttrium imido complexes [77]. Although reactions with equimolar quantities of 2,6-diisopropylaniline were proposed to proceed through a putative imido intermediate, only the resultant anilido or bis(anilido) products were observed (Scheme 37). The nature of the 6-R group bound to the pyridine donor greatly influenced the course of the reaction, as well as the stability of the resultant complex. In the case of the benzofuran derivative, the furan ring opened, leading to an unusual amido–yne–phenolate species, **66**. Meanwhile, no ring opening took place in the benzothiophene analogue, perhaps because of the difference between forming an Y–O vs. an Y–S bond. In toluene solution, Y–C bond protonolysis of $\text{LLn}(\text{NHAr})_2$ ($\text{L} = 2\text{-}(2,6\text{-}i\text{-Pr}_2\text{C}_6\text{H}_3)\text{NCMe}_2\text{-6-C}_7\text{H}_4\text{S-NC}_5\text{H}_3$; $\text{Ar} = 2,6\text{-}i\text{-Pr}_2\text{C}_6\text{H}_3$), **67** gave bis(amido) **68**, which was supported by a monoanionic NNS pincer ligand. Conversely, anilido complex **69** proved to be relatively inert, with no evidence for ligand rearrangement at 100°C .

An example of the propensity for rare earth metals to form strong Ln–O bonds was recently demonstrated by the decomposition of an organolutetium complex bearing a bis(phosphinimine)carbazole ligand with flanking dioxaphospholane groups [78]. More specifically, dialkyl complex $\text{LLu}(\text{CH}_2\text{SiMe}_3)_2$ ($\text{L} = 1,8\text{-}[4\text{-}i\text{-PrC}_6\text{H}_4\text{N}=\text{P}(\text{O}_2\text{C}_2\text{H}_4)_2]\text{-3,6-dimethylcarbazole}$) **70** was found to undergo a cascading inter- and intramolecular ring-opening insertion reaction into Lu–C bonds, resulting in the formation of asymmetric bimetallic tetraalkoxide complex **71** (Scheme 38).

Mindiola et al. observed unique reactivity when $2,6\text{-Me}_2\text{C}_6\text{H}_3\text{NC}$ (XylNC) reacted with the coordinated pyridine/iminoacyl ligands in scandium complex **72** [58], resulting in the formation of novel indoline species (Scheme 39) [79]. Initially, complex **72** reacted with 1 equiv. of XylNC to afford an isolable iminoacyl complex



Scheme 38 Dioxaphospholane ring-opening reaction of **70**



Scheme 39 Reaction of **72** with 2,6-Me₂C₆H₃NC. *Red* represents the initially coordinated pyridine, while *green* and *blue* denote the first and second inserted isocyanide molecules, respectively

which subsequently reacted with a second equivalent of XylNC to give either **73** or **74** depending on the substituents on the pyridine ligand. With the naked η^2 -pyridine, a bidentate 2-indoline-pyridine ligand is formed by [3,5] migration of one of the methyl groups of a xylyl ring to the β -carbon of the former iminoacyl functionality, **73**. However, when the pyridine ligand is substituted with an imine group at the *ortho* position, an intermediate prior to methyl migration can be isolated. In this case, the imine nitrogen binds tightly to scandium, which interestingly prevents the relocation of the methyl group and leaves the tridentate 2-imino-6-indole-pyridine ligand intact, **74**.

The alkane elimination and alkyl migration reactions of rare earth pincer complexes presented above generally produce highly reactive complexes and/or low-coordinate intermediates that trigger further, and even more, peculiar reactivity. Although many such reactions are not targeted, they tend to produce unprecedented ligand transformations and exceptional compounds, which, in some

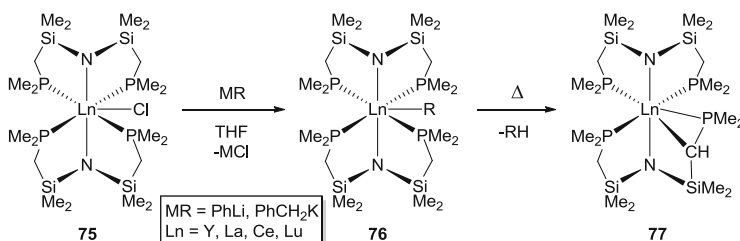
instances, reveal completely new types of reactivity not previously seen in those systems.

3.3 Ligand Metathesis Reactions

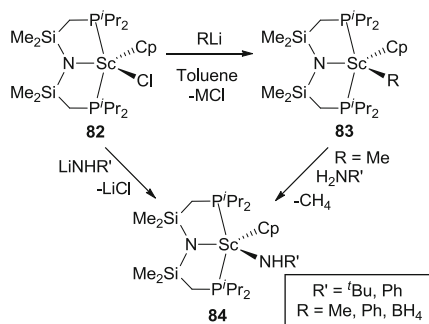
In coordination and organometallic chemistry, distinct ligand metathesis or exchange reactions commonly constitute the first attempts to scope chemical reactivity and potential catalytic properties of a metal complex. Thus, it is not surprising that these types of reactions are among the most studied in the field of rare earth pincer complexes. The pioneering work of Fryzuk et al. in this area on early rare earth pincer species has laid a solid foundation for many of the forthcoming studies in group 3 and lanthanide chemistry. The results from these initial reports are interwoven with more recent contributions from other authors and summarized below. This section then concludes with a discussion on related ligand exchange involving phosphorus-containing reagents.

3.3.1 Alkylation by Organoalkali Compounds

The salt metathesis chemistry of transition metal complexes is very well known and understood. In the late 1980s and early 1990s, Fryzuk et al. extended this reactivity to rare earth pincer species in a series of publications that reported numerous novel molecules prepared by alkylation with discrete organoalkali compounds. For example, the species $[\text{N}(\text{SiMe}_2\text{CH}_2\text{PMe}_2)_2]\text{LnCl}$ ($\text{Ln} = \text{Y}, \text{La}, \text{Ce}, \text{Lu}$), **75**, reacted readily with PhLi or PhCH_2K to form the corresponding alkyl complexes **76**. While the Y and Lu analogues were isolated as stable compounds, cyclometalation of the ligand took place when $\text{Ln} = \text{La}$ and Ce, producing 1 equiv. of hydrocarbon along with concomitant elimination of metalate **77** (Scheme 40) [9, 80, 81]. A series of comprehensive kinetic studies provided evidence for a four-centered σ -bond metathesis transition state, with prior η^2 to η^1 -benzyl reorganization. In addition, the reaction rate increased proportionately with increasing ionic radius of the rare earth metal (i.e., from Lu, to Y, to La), thus suggesting that the proposed seven-



Scheme 40 Alkylation and subsequent cyclometalation of $\text{LnCl}[\text{N}(\text{SiMe}_2\text{CH}_2\text{PMe}_2)_2]$



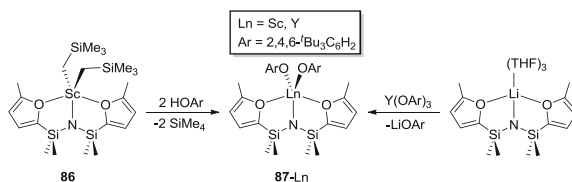
Scheme 41 Reactivity of scandium cyclopentadienyl halide complex **82**

coordinate transition state was more accessible for larger metal ions. Although most of the kinetic and reactivity studies have been performed on complexes supported by PNP ligands bearing methyl substituents at phosphorus, phenyl- and isopropyl-substituted species have also been prepared [82].

Fryzuk and co-workers also studied the salt metathesis chemistry of $[\text{N}(\text{SiMe}_2\text{CH}_2\text{PMe}_2)_2\text{YCl}]$ with allyl Grignard reagents producing dimeric $[[\text{N}(\text{SiMe}_2\text{CH}_2\text{PMe}_2)_2\text{Y}(\text{C}_3\text{H}_5)(\mu\text{-Cl})_2]$, **78**, and the corresponding bis(allyl) compound $[\text{N}(\text{SiMe}_2\text{CH}_2\text{PMe}_2)_2\text{Y}(\text{C}_3\text{H}_5)_2]$, **79**. Preliminary catalytic studies indicated that complex **79** was an active catalyst for the polymerization of ethylene, whereas neither **75-Y** nor **78** exhibited any catalytic activity [83].

Several years later, Fryzuk et al. extended the aforementioned salt metathesis chemistry to the smallest rare earth metal scandium [84]. Scandium readily formed the monomeric, dihalide complex $[\text{N}(\text{SiMe}_2\text{CH}_2\text{P}^i\text{Pr}_2)_2]\text{ScCl}_2(\text{THF})$, **80**, instead of the bis(ligand) derivatives observed for heavier congeners (vide supra). Reaction with a range of organolithium compounds invariably generated the expected dialkyl species $[\text{N}(\text{SiMe}_2\text{CH}_2\text{P}^i\text{Pr}_2)_2]\text{ScR}_2(\text{THF})$, **81** (R = Me, Et, CH_2SiMe_3), although some tendency for the incorporation of LiCl via the formation of “ate” complexes was observed. All reactions with small molecules (H_2 , CH_3I , CO, CO_2 , nitriles, isocyanides, silanes) caused decomposition. A computational study suggested that the frontier molecular orbitals of the scandium species are not well suited for strong σ donors, such as CO, hence hindering the reactivity of the complexes. The addition of an excess of ethylene gas to **81** produced polyethylene, but the catalytically active species could not be identified.

Reaction of the PNP scandium complex $[\text{N}(\text{SiMe}_2\text{CH}_2\text{P}^i\text{Pr}_2)_2]\text{ScCl}_2(\text{THF})$ with $\text{NaCp}(\text{DME})$ generated the robust alkylscandium species $[\text{N}(\text{SiMe}_2\text{CH}_2\text{P}^i\text{Pr}_2)_2]\text{-Sc}(\eta^5\text{-C}_5\text{H}_5)\text{Cl}$ **82** [85]. The remaining chloride ligand in **82** could be readily exchanged for alkyl, aryl, borohydride, or amido groups by straightforward reaction with the requisite lithium reagents (Scheme 41). The addition of primary amines to $[\text{N}(\text{SiMe}_2\text{CH}_2\text{P}^i\text{Pr}_2)_2]\text{Sc}(\eta^5\text{-C}_5\text{H}_5)\text{Me}$, **83-Me**, yielded the same amido complexes, **84**, that were acquired by direct salt metathesis between complex **82** and LiNHR' (R' = 'Bu, Ph). A ^{11}B NMR spectroscopic study of the borohydride derivate



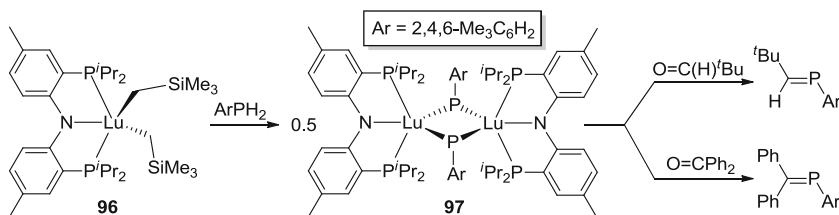
Scheme 42 Synthesis of bis(alkoxide) complexes **87-Ln**

$[N(\text{SiMe}_2\text{CH}_2\text{P}^i\text{Pr}_2)_2]\text{Sc}(\eta^5\text{-C}_5\text{H}_5)\text{BH}_4$, **83-BH₄**, in the presence of excess PMe_3 indicated an equilibrium reaction between a putative hydride complex $[N(\text{SiMe}_2\text{CH}_2\text{P}^i\text{Pr}_2)_2]\text{Sc}(\eta^5\text{-C}_5\text{H}_5)(\text{H})$, **85**, and the initial borohydride species. Further kinetic experiments suggested that it was unlikely that the scandium hydride species could be isolated since the equilibrium favored the borohydride complex even in the presence of a 100-fold excess of PMe_3 at 68°C .

In 2010, Coles and Cloke reported a series of scandium and yttrium complexes supported by a furyl-substituted disilazide framework. Scandium dialkyl $\text{LSc}(\text{CH}_2\text{-SiMe}_3)_2$ ($\text{L} = 1,3\text{-bis}(2\text{-methylfuryl})\text{-}1,1',3,3'\text{-tetramethyldisilazide}$), **86**, was prepared by alkane elimination upon the reaction of HL and $\text{Sc}(\text{CH}_2\text{SiMe}_3)_3(\text{THF})_2$ or by the combination of $\text{LLi}(\text{THF})_3$ and $\text{ScCl}_3(\text{THF})_2$, followed by the addition of 2 equiv. of $\text{LiCH}_2\text{SiMe}_3$ [86]. Subsequent reaction of complex **86** with 2 equiv. of $2,6\text{-}^t\text{Bu}_2\text{C}_6\text{H}_2\text{OH}$ produced bis(alkoxide) **87-Sc** (Scheme 42). In contrast, reaction of $\text{Y}(\text{CH}_2\text{SiMe}_3)_3(\text{THF})_2$ with the proteo ligand proceeded to an undesired yttrium species ($(\eta^1\text{-L})\text{Y}(\text{CH}_2\text{SiMe}_3)_2(\text{THF})_2$) wherein L was bound to the metal center by an η^1 bonding mode. Likewise, efforts to generate a κ^3 -pincer-supported dialkyl complex by the reaction of a stoichiometric quantity of $\text{LLi}(\text{THF})_3$ and $\text{YCl}_3(\text{THF})_3$ were also fraught with failure. However, salt metathesis between $\text{YCl}_3(\text{THF})_3$ and 2 equiv. of $\text{LLi}(\text{THF})_3$ formed dimeric $[(\eta^2\text{-L})_2\text{Y}(\mu\text{-Cl})]_2$, from which the benzyl derivative $(\eta^2\text{-L})(\eta^3\text{-L})\text{Y}(\text{CH}_2\text{Ph})$, **88**, was produced upon the addition of PhCH_2K . It was also discovered that the bis(alkoxide) complex $\text{LY}(\text{OAr})_2$ ($\text{Ar} = 2,6\text{-}^t\text{Bu}_2\text{C}_6\text{H}_3$), **87-Y**, could be prepared by the reaction of $\text{LLi}(\text{THF})_3$ and $\text{Y}(\text{OAr})_3$, but this pathway necessitated harsh reaction conditions and extended reaction times to reach complete conversion.

The organometallic complexes **86** and **88** were briefly examined for their ability to catalyze ethylene polymerization and intramolecular hydroamination, respectively. Unfortunately, even upon in situ activation with Lewis or Brønsted acid co-catalysts, complex **86** proved to be a poor olefin polymerization catalyst. Although complex **88** did react with 2,2-dimethyl-1-aminopent-4-ene, it did not release the cyclized product [86].

Mononuclear complexes of the larger ionic radii, heavier rare earth metals that bear a single ancillary ligand are often challenging to prepare. However, Fryzuk and co-workers found success with their so-called NPN diamidophosphine pincer (Scheme 43) [87]. The dilithiated salt of this ligand reacts readily with the THF adducts of yttrium, samarium, holmium, ytterbium, and lutetium trichloride to give the desired halide complexes $\text{LLn}(\text{Cl})(\text{THF})$ ($\text{Ln} = \text{Y}, \text{Sm}, \text{Ho}, \text{Yb}, \text{Lu}$; $\text{L} = \text{PhP}$



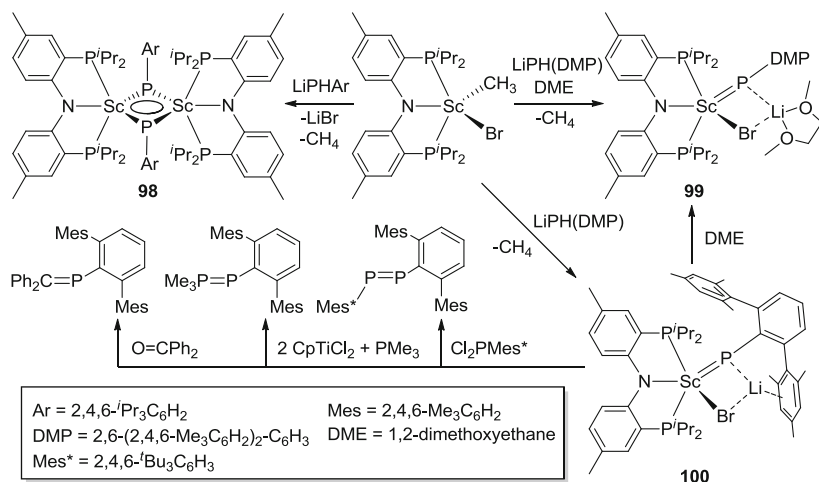
Scheme 45 Preparation and phospho-Wittig reactivity of complex **97**

3.3.2 Reactions with Phosphorus-Containing Molecules

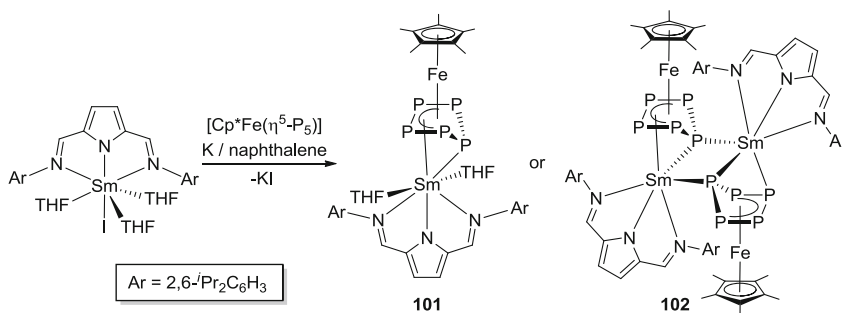
Phosphines are one of the most well-known donors in coordination chemistry, and transition metal complexes with phosphorus-containing ligands are used as catalysts in a wide array of industrial processes [91]. Since rare earth elements can be considered as hard ions and phosphorus as soft, phosphorus-containing moieties are not generally considered to be good ligands for these metals. Regardless, rare earth complexes with phosphorus-based donor ligands have gained increasing attention over the past two decades [92, 93]. Although still scarce, a handful of studies on such compounds have been reported – the results from this work are presented below.

Similar to first row main group elements, attempts have been made to prepare rare earth species featuring terminal multiply bonded ligands of heavier *p*-block elements. The first rare earth phosphinidene was reported in 2008 by Kiplinger and co-workers. An alkane elimination between the primary phosphine MesPH_2 ($\text{Mes} = 2,4,6\text{-Me}_3\text{C}_6\text{H}_2$) and $(\text{PNP})\text{Lu}(\text{CH}_2\text{SiMe}_3)_2$ ($\text{PNP} = \text{N}(2\text{-P}^i\text{Pr}_2\text{-4-Me-C}_6\text{H}_4)_2$), **96**, produced dinuclear phosphinidene-bridged **97** (Scheme 45) [94]. Complex **97** readily reacts as a phospho-Wittig-type reagent with aldehydes and ketones to afford phosphoalkenes (Scheme 45). Unfortunately, all attempts to generate and stabilize a terminal phosphinidene complex via the introduction of different Lewis bases (e.g., PMe_3 , tetramethylethylenediamine, DMAP, or bipyridines) resulted in decomposition. Nonetheless, it is important to note that kinetic stabilization using sterically demanding 2,4,6-tri-*tert*-butylphenylphosphine triggered the formation of phosphaindole, which has been interpreted as being indicative of the presence of transient phosphinidene species in certain transition metal systems.

In 2010, Mindiola and co-workers reported the synthesis of the related bridging phosphinidene scandium complex $[\text{LSc}(\mu\text{-PAR})]_2$ ($\text{L} = \text{N}(2\text{-P}^i\text{Pr}_2\text{-4-MeC}_6\text{H}_3)_2$; $\text{Ar} = 2,4,6\text{-}^t\text{Pr}_3\text{C}_6\text{H}_2$), **98**. When more bulky phosphines were used, two remarkable mononuclear complexes, $\text{LSc}[\mu\text{-P}(\text{DMP})](\mu\text{-Br})\text{Li}$ ($\text{DMP} = 2,6\text{-}(2,4,6\text{-Me}_3\text{C}_6\text{H}_2)_2\text{C}_6\text{H}_3$), **99**, and $\text{LSc}[\mu_2\text{-P}(\text{DMP})](\mu\text{-Br})\text{Li}(\text{DME})$, **100**, that contained Lewis acid-supported phosphinidenes (Scheme 46) were prepared [95]. In a similar fashion to complex **97**, the mononuclear “ate” complex **100** exhibited well-behaved phospho-Wittig chemistry with ketones and dichlorophosphines. Intriguingly, complex **100** also seems to participate in a phosphinidene extrusion process that can be utilized to form the known phosphinidene complex $\text{Cp}_2\text{Zr}=\text{P}(\text{DMP})\text{PMe}_3$.



Scheme 46 Synthesis and reactivity of scandium phosphinidene complexes **98–100**

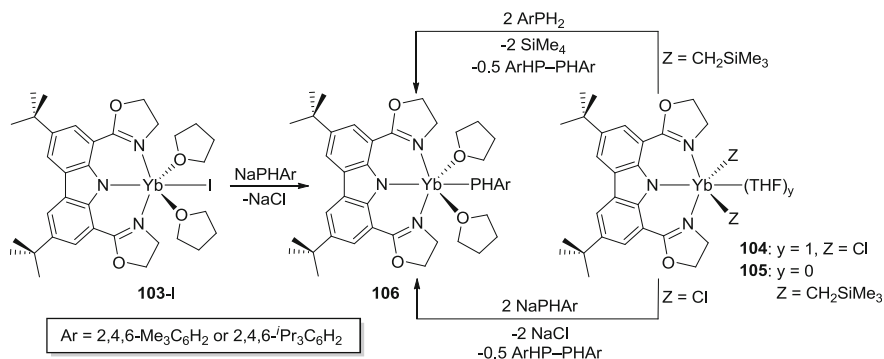


Scheme 47 Synthesis of polyphosphide complexes **101** and **102**

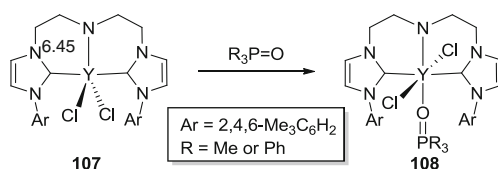
Unfortunately, decomposition products present in the reaction mixture prevented the separation of this species.

A particularly unusual example of rare earth phosphorus chemistry was recently reported by Roesky et al. wherein mixed metal polyphosphide complexes **101** and **102** were synthesized by the reduction of pentaphosphaferrocene [Cp*Fe(η⁵-P₅)] in the presence of LSmI(THF)₃ (L = (2,5-(2,6-ⁱPr₂C₆H₃)N=CH)₂NC₄H₂) (Scheme 47) [96]. Monomeric **101** was obtained by recrystallization from a THF/toluene mixture, whereas dimeric **102** was isolated by recrystallization from toluene/pentane. The reduction led to a [Cp*FeP₅]²⁻ subunit, and the authors proposed that the phosphorous ligand could be considered a cyclo-P₅³⁻ polyphosphide anion.

Berg et al. have also prepared divalent lanthanide complexes that contain phosphorus-based ligands [97]. Specifically, monohalide complexes LYbX(THF)₂ (L = 1,8-bis(4,4-dimethyloxazolin-2-yl)-3,6-di-*tert*-butylcarbazole; X = I, **103-I**, Cl, **103-Cl**) were prepared by the reaction of YbX₂ and NaL or by Na/Hg reduction



Scheme 48 Synthesis of phosphide complex **106** through salt metathesis or alkane elimination routes



Scheme 49 Reactivity of dicarbene complex **107** with phosphine oxides

of the Yb(III) species $\text{LYbCl}_2(\text{THF})$, **104**. Notably, divalent silylamide, alkyl, and phosphide complexes could be prepared from complex **103-I**. Also noteworthy is the fact that the addition of $\text{LiCH}_2\text{SiMe}_3$ to $\text{LYbX}(\text{THF})_2$ afforded the oxidized product $\text{LYb}(\text{CH}_2\text{SiMe}_3)_2$, **105**. Equally intriguing redox chemistry was observed upon the reaction of **104** and **105** with ArPH_2 and NaPHR , respectively (Scheme 48).

In addition to phosphine and phosphide reagents, phosphine oxides can also be used as suitable ligands for stabilizing rare earth pincer complexes. Arnold and colleagues employed the lithium chloride adduct of a tridentate amido-bridged di-*N*-heterocyclic carbene ligand, **L** ($\text{L} = \text{N}\{\text{CH}_2\text{CH}_2[1\text{-C}(\text{NCHCHNAr})]\}_2$, $\text{Ar} = 2,4,6\text{-Me}_3\text{C}_6\text{H}_2$), in order to prepare the yttrium amidodicarbene pincer complex $\text{LYClN}(\text{SiMe}_3)_2$, by transamination. In addition, dihalide species YCl_2 , **107**, were prepared by salt metathesis between anhydrous YCl_3 and LLi . Although the addition of phosphine oxides to $\text{LYClN}(\text{SiMe}_3)_2$ resulted in decomposition, discrete, albeit somewhat thermally sensitive (when $\text{R} = \text{Ph}$), complexes $\text{LYCl}_2(\text{O}=\text{PR}_3)$ ($\text{R} = \text{Me, Ph}$), **108**, were isolated when the same phosphine oxides were reacted with **107** (Scheme 49) [98].

4 Catalytic Properties of Rare Earth Pincer Complexes

As with other metals across the periodic table, the ultimate goal when preparing new rare earth pincer complexes is often the utilization of such species as catalysts in specific chemical transformations. Despite the fact that the number of reactions catalyzed by rare earth pincer complexes is somewhat limited when compared to transition metal analogues, rare earth pincer complexes have exhibited exceptional catalytic activity in polymerization reactions, especially in the ring-opening polymerization (ROP) of cyclic esters and the polymerization of dienes such as isoprene and butadiene. This section discusses these two research domains in separate segments and concludes with a review of reactions that are less prominent, but still noteworthy, in rare earth pincer complex catalysis (e.g., hydroamination).

4.1 Ring-Opening Polymerization of Cyclic Esters

The field of polymerization catalysis is a broad area with rich history [99]. At the turn of the twentieth century, chemists pioneered foundational work in this area, establishing the first synthetic-based polymers, such as Bakelite and rayon. The exhaustion of natural latex, wool, silk, and other resources during World War II sparked developments in alkene polymerization for the preparation of nylon, acrylic, neoprene, polyethylene, and other polymers. Subsequently, the development of high-polymer technology culminated with significant discoveries from Nobel laureates Karl Ziegler and Giulio Natta (1963) [100]. Meanwhile, the development of ring-opening processes of *cyclic* monomers garnered attention in the late 1970s and reached a climax with the popularity of ring-opening metathesis polymerization (ROMP), which ultimately led to Nobel Prizes for Richard Schrock, Robert Grubbs, and Yves Chauvin (2005) [101]. As a result of the modern renaissance in polymer technologies, contemporary studies have been initiated to develop single-site (homogeneous) catalysts for the polymerization of *heterocyclic* monomers. Though many of these studies primarily involve transition metal catalysts, the polymerization of cyclic esters, especially lactide [102], a cyclic diester monomer, is frequently initiated by rare earth complexes [103, 104].

4.1.1 Polymerization of Lactide

Lactide (LA), which is a cyclic dimer of lactic acid, can be transformed into a biodegradable polymer, polylactide (PLA), via ring-opening polymerization. Lactide is one of, if not the most studied, monomers in the ROP of cyclic esters, and many rare earth metal complexes have been investigated for their ability to mediate this process [103].

High molecular weight PLA can be prepared via a coordination–insertion mechanism using metal catalysts that bear suitable initiating groups. Other mechanisms, such as cationic or anionic, are also viable, but these pathways often lead to low molecular weight polymers or problems in molecular weight distribution, respectively. The control of molecular weight distribution (polydispersity) is of special interest as it has major consequences on the physical properties of the resulting polymer. The measure of this property, known as the polydispersity index (PDI), is calculated by dividing the weight averaged molecular weight (M_w) by the number averaged quantity (M_n). Values close to unity represent polymer chains possessing uniform length, and higher values describe materials containing a wider range of molecular masses in the polymer.

Another important feature of the lactide precursor is the two stereogenic centers in the molecule's backbone. Hence, three different stereoisomers are possible: (*S,S*)-lactide (L-LA), (*R,R*)-lactide (D-LA), and (*R,S*)-lactide (*meso*-LA); a racemic mixture of the first two is known as *rac*-LA. The presence of chiral carbons in the monomer leads to the possibility of different tacticities of the resultant polymer. While many polymer microstructures are possible, isotactic (adjacent chiral centers possess the same configuration (*R* or *S*)), heterotactic (two adjacent stereogenic centers have the same configuration that are different from neighboring pairs (–RRSSRRSS–)), syndiotactic (alternating configurations (–RSRSRSRS–)), and atactic (no stereoregularity) are the most common.

In the transformation of lactide to PLA, the nature of the initiating group on the metal catalyst plays a key role in its activity, and alkoxides have generally proven to be the most effective. In addition to the role of the initiating group, steric factors of the ancillary ligands can have a major impact on the stereocontrol of the catalyst (via an enantiomorphic site-control mechanism). However, despite the prevalence of metal alkoxides as initiators in the ROP of lactide, the use of amides is more widespread in the area of rare earth pincer catalysis, and distinct alkyl complexes have also shown modest activity. Presumably, synthetic challenges and limited availability of the heteroleptic alkoxide species have limited their use. For example, these complexes can be prone to facile ligand redistribution, whereas a range of Ln(NR₂)₃ starting materials are well known. Furthermore, amine elimination strategies can be employed to easily attach a variety of ancillary ligands, whereas alcohol elimination routes from Ln(OR)₃ sources are infrequently encountered (see Sect. 2.1).

One of the first examples of rare earth pincer complexes initiating the ROP of LA was reported by Cui et al. when they prepared a dinuclear dialkyl yttrium complex [L₂Y(THF)][Y(CH₂SiMe₃)₂] (L = 2-[(*N*-2-diphenylphosphinophenyl)iminomethyl]pyrrole), **109**, which was shown to be as efficient an initiator as previously reported (non-pincer) monoalkyl counterparts. The resultant PLA had lower molecular weights and broad molecular weight distributions since both alkyl groups supposedly participated in polymerization [105].

Cui and co-workers continued the exploration of yttrium pincer catalysts bearing modified β-diimines and anilido-imine ancillaries. In these studies, dialkyl LY(CH₂SiMe₃)₂, **110** and **111**, and diamido species LY(NH-2,6-^{*i*}Pr₂C₆H₃)₂, **112**

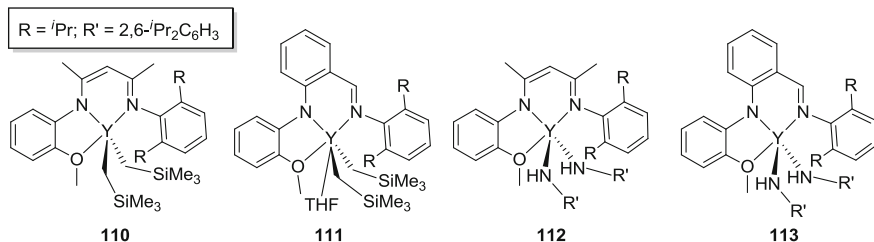


Chart 1 Dialkyl and diamido complexes **110–113** supported by NNO pincer ligands

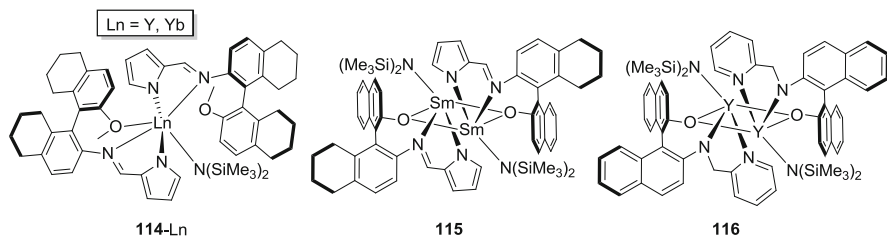


Chart 2 Rare earth amido **114-Ln**, **115**, and **116** complexes active in the ROP of LA

and **113** (**110** and **112**: $L = 2\text{-OMe-C}_6\text{H}_4\text{NCMeCHCMeNH-2,6-}^i\text{Pr}_2\text{C}_6\text{H}_4$; **111** and **113**: $L = 2\text{-OMeC}_6\text{H}_4\text{-NC}_6\text{H}_4\text{-CH=N-2,6-}^i\text{Pr}_2\text{C}_6\text{H}_3$) (Chart 1), were prepared and utilized in LA polymerization studies. All complexes exhibited high activity and gave high molecular weight PLA, although PDIs were somewhat broad in certain occasions (1.31–1.72). Despite the similarities in ligand framework, **110** and **112** behave as double-site catalysts, whereas **111** and **113** produced PLA with features that indicated the involvement of a single-site active species. For the dialkyl complexes **110** and **111**, this behavior was attributed to the unique arrangement of alkyl groups since the ancillary ligand adopted *mer*-coordination or *fac*-coordination, respectively. In the cases of **112** and **113**, the amido ligands were positioned similarly around the metal; hence, the difference in polymerization behavior was most likely electronic in origin. Moreover, the solvent used in these transformations had a notable effect on the molecular weight of the obtained polymer. In nonpolar solvents such as toluene or benzene, the polymerization was less controlled, producing higher than expected molecular weights and large PDIs. This behavior may be due to poor solubility of the monomer, which in turn might introduce heterogeneous features to the polymerization process [106, 107].

In 2008, Zi and colleagues used chiral ancillaries to prepare monoamido complexes $\text{L}_2\text{LnN}(\text{SiMe}_3)_2$ ($\text{Ln} = \text{Y}$ or Yb ; $L = (S)\text{-5,5',6,6',7,7',8,8'}$ -octahydro-2-(pyrrol-2-ylmethyleneamino)-2'-methoxy-1,1'-binaphthyl), **114-Ln** (Chart 2). Both species were active in the ROP of *rac*-LA under mild conditions. The yttrium complex **114-Y** produced isotactic-rich PLA with complete conversion of 500 equiv. of lactide to polymer in just over 1 h in THF solvent. By comparison, the ytterbium counterpart **114-Yb** reached 88% conversion under identical

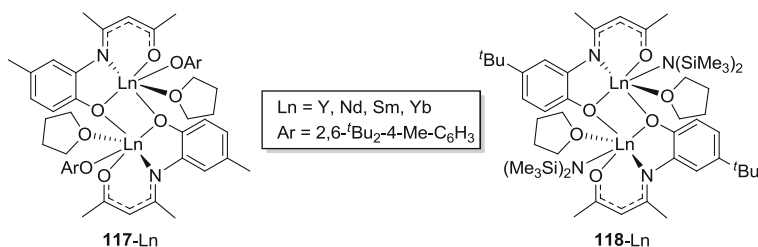


Chart 3 Dinuclear aryloxide **117-Ln** and amido **118-Ln** rare earth complexes

conditions. Interestingly, the relative activities were reversed when toluene was used as the solvent [108].

Shortly thereafter, Zi et al. synthesized the dinuclear samarium species, [LSmN(SiMe₃)₂]₂ (L = (*S*)-5,5',6,6',7,7',8,8'-octahydro-2-(pyrrol-2-ylmethyleneamino)-2'-hydroxy-1,1'-binaphthyl), **115**, and the closely related [LYN(SiMe₃)₂]₂ (L = (*S*)-2-(pyridin-2-ylmethylamino)-2'-hydroxy-1,1'-binaphthyl), **116** (Chart 2), and studied the performance of these complexes in the ROP of LA. The characteristics of the generated PLA were similar to polymers formed with **114-Ln**. The effect of ionic radius was again visible in reactions performed in toluene as the samarium species **115** was found to be more active. However, the difference in activities was minor when THF was used as a solvent, which is most likely because the effects of competitive coordination between the solvent and monomer (LA) are more pronounced with the smaller yttrium center [109].

Also in 2008, Yan, Cheng, and co-workers demonstrated that dinuclear aryloxide-bridged complexes [LLn(OAr)(THF)]₂ (Ln = Y, Nd, Sm, Yb; 4-(2-hydroxy-5-methylphenyl)imino-2-pentanone) **117-Ln** (Chart 3) were active in *L*-LA polymerization, although higher temperatures (70°C) and longer reaction times (4 h) were required to obtain close to complete conversion. The ionic radius of the metal was observed to have significant influence on the activity of the complexes, with **117-Nd** and **117-Sm** being the most active. All prepared PLA samples possessed high molecular weights, but the PDIs of the polymers were relatively large, suggesting that polymerization was not well controlled. These results indicate that initiation may be slow relative to propagation. This behavior seems consistent with **117-Ln** persisting as a dimer in solution, hindering monomer coordination [110].

Two years later, Yao and colleagues prepared monoamido analogues [LLnN(SiMe₃)₂(THF)]₂ (Ln = Y, Nd, Sm, Yb; L = 4-(2-hydroxy-5-*tert*-butyl-phenyl)imino-2-pentanone), **118-Ln** (Chart 3), which were capable of initiating the ROP of lactide, although with lower activities than the corresponding lanthanide aryloxide species **117-Ln**. The poor catalytic activity of **117-Ln** is most likely a consequence of the more electrophilic silylamide ligand, compared to the aryloxide in **118-Ln**, hampering nucleophilic attack at the carbonyl carbon of the coordinated lactide monomer [111].

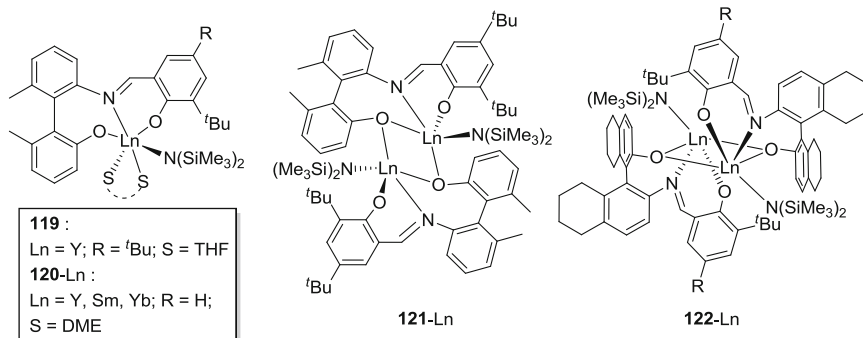


Chart 4 Mono- and dinuclear rare earth complexes with chiral biaryl ligands

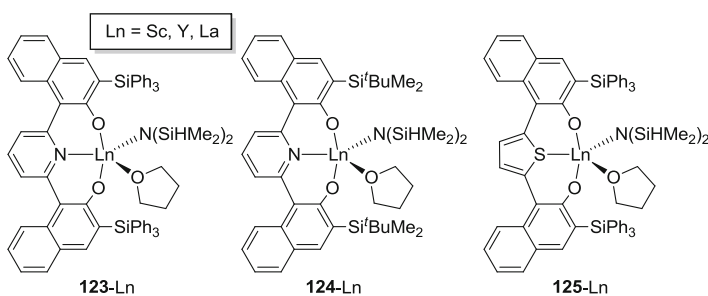


Chart 5 Mononuclear rare earth amido complexes supported by bis(naphtholate) ancillary ligands

Very recently, Zi et al. expanded their family of complexes bearing binaphthyl-derived ligands to include a series of monoamido species $\text{LYN}(\text{SiMe}_3)_2(\text{THF})_2$, **119** ($\text{R} = \text{tBu}$), $\text{LLnN}(\text{SiMe}_3)_2(\text{DME})$, **120-Ln**, $[\text{LLnN}(\text{SiMe}_3)_2]_2$, **121-Ln**, and **122-Ln**, ($\text{Ln} = \text{Y, Sm, Yb}$; $\text{L} = (S)$ -2-amino-2'-hydroxy-6,6'-dimethyl-1,1'-biphenyl or differently substituted (S) -5,5',6,6',7,7',8,8'-octahydro-2-amino-2'-hydroxy-1,1'-binaphthyl) (Chart 4) [112]. All complexes promoted the ROP of *rac*-LA, but the mononuclear species were more active, converting 500 equiv. of lactide to PLA within 4 h at ambient temperature. In agreement with previous studies, metal cations with larger ionic radii were most active, and toluene was shown to be a better solvent than the more strongly coordinating THF (vide supra). The resulting PLA was isotactic rich with P_m values up to 0.74. In general, the activities of **119**–**122-Ln** were similar to that of complex **109**, and the polymer features were similar to the ones produced using catalysts **114-Ln** [105, 108].

Kirillov, Carpentier, and co-workers have prepared an impressive series of complexes of the form $\text{LLnN}(\text{SiHMe}_2)_2(\text{THF})$ ($\text{Ln} = \text{Sc, Y, La}$; $\text{L} = \text{silyl } ortho\text{-substituted } 2,6\text{-bis(naphtholate)pyridine}$ or $2,5\text{-bis(naphtholate)thiophene}$; see Chart 5), **123**–**125-Ln**, for the ROP of lactide, that feature $\text{N}(\text{SiHMe}_2)_2$ initiating groups. Compounds **123**–**125-Ln** were shown to be active initiators of *rac*-LA,

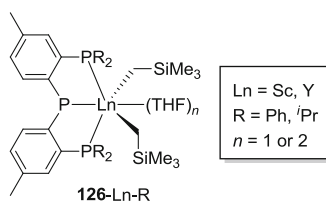


Chart 6 Dialkyl Sc and Y PNP complexes **126-Ln**

producing low PDI PLA with molecular weights similar to the predicted values. Conversion of 100–500 equiv. of *rac*-LA into PLA was achieved at ambient temperature in less than 12 h. Furthermore, immortal polymerization behavior was attained when isopropanol was added as a chain transfer agent. Interestingly, when reactions were performed in THF, ROP produced heterotactic-rich PLA with P_r values up to 0.93, whereas in toluene, all stereocontrol was lost with only atactic polymers formed. The ionic radius of the metal, as well as the identity of the donor atom in the ancillary backbone, appeared to affect the tacticity of the polymer, implying that the rigidity of the ancillary framework plays a role in stereocontrol. For example, with complexes **124-Ln**, the scandium derivative produced PLA with $P_r = 0.93$, whereas the use of the corresponding lanthanum compound resulted in atactic polymers. Notably, the trend was not uniform as it was inverted with complexes **123-Ln**, limiting definitive conclusions regarding the factors affecting stereochemistry. In addition to polymerization of LA, complexes **123-Ln** and **124-Ln** were also active in the ROP of *rac*- β -butyrolactone (BBL) (vide infra) [113].

Mononuclear PPP dialkyl complexes $\text{LLn}(\text{CH}_2\text{SiMe}_3)_2(\text{THF})_n$ ($\text{Ln} = \text{Y}, \text{Sc}$; $\text{L} = (4\text{-methyl-6-PR}_2\text{-C}_6\text{H}_3)_2\text{P}$, $\text{R} = \text{Ph}, ^i\text{Pr}$) **126-Ln-R** were studied by Peters and Pellecchia for the ROP of *L*-LA (Chart 6) [114]. Yttrium derivatives were shown to be particularly active producing PLA almost quantitatively in 15 min at ambient temperature with a monomer to initiator ratio ($[\text{LA}]_0/[\text{I}]_0$) of 200. The phenyl-substituted **126-Y-Ph** was more active than **126-ⁱPr**, perhaps because the weakly donating phenyl groups increased the metal's Lewis acidity. High molecular weight polymers were produced in 3 h at ambient temperature with 99% conversion when a $[\text{LA}]_0/[\text{I}]_0$ ratio of 1,000 was used. Unfortunately, the observed molecular weights were lower than theoretical values, accompanied by large PDIs. Mass spectrometric analysis of oligomers prepared with a $[\text{LA}]_0/[\text{I}]_0$ value of 20 revealed primarily linear oligomer formation, although cyclic species were also detected, confirming competitive transesterification during polymerization. More detailed kinetic analysis of the polymerization reactions indicated a single-site nature of the catalysts, which is consistent with “controlled-living” characteristics. A slight preference for heterotactic polymer formation (P_r values of 0.60–0.64) was observed when **126-Ln-R** was used to polymerize *rac*-LA. Analysis of solvent dependence determined that solvent effects were comparable with previous studies, i.e., higher catalytic activities were observed in toluene compared to THF. Solvent-free LA polymerization with **126-Y-R** as initiators reached satisfactory conversions in a controlled fashion. It is important to note, however, that measured molecular weights

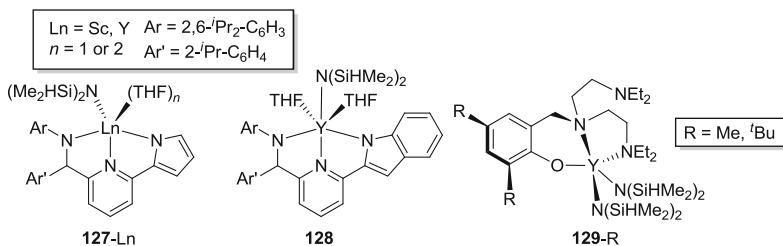


Chart 7 Monoamido, **127-Ln** and **128**, and diamido, **129-R**, rare earth complexes

suggested that both alkyl groups were active initiating groups in the absence of solvent.

Following these studies, the ROP of L-LA by **126-Ln-R** in the presence of isopropanol was investigated [115]. The addition of 2 equiv. of isopropanol to the reaction mixture of **126-Ln-R** and L-LA resulted in catalyst activity virtually identical to those conducted in the absence of alcohol, and the molecular weights of the formed PLA were in excellent agreement with theoretical values. An alcohol/initiator ratio of 5:1 resulted in reduced molecular weights and narrowed PDIs, confirming that excess isopropanol acts as an efficient chain-transfer agent. Furthermore, living polymerization was suggested owing to the rapid “growing chain to isopropanol” exchange.

Lamberti, Pellecchia, and co-workers investigated the scandium and yttrium complexes $\text{LLnN}(\text{SiHMe}_2)_2(\text{THF})_n$ ($\text{Ln} = \text{Sc, Y}$; $\text{L} = N\text{-}((6\text{-}(1H\text{-pyrrol-2-yl)pyridin-2-yl})(2\text{-isopropylphenyl)methyl)-2,6\text{-diisopropylaniline}$, **127-Ln**, and $N\text{-}((6\text{-}(1H\text{-indol-2-yl)pyridin-2-yl})(2\text{-isopropylphenyl)methyl)-2,6\text{-diisopropylaniline}$, **128**; $n = 1$ or 2) as initiators for the ROP of *rac*-LA (Chart 7) [116]. The yttrium species were again found to be highly active, converting 200 equiv. of monomer to PLA within minutes at ambient temperature. The polymerization rate also exhibited significant solvent dependence following the order $\text{CH}_2\text{Cl}_2 > \text{toluene} > \text{THF}$. Complex **127-Y** was found to be slightly more active than **128**, most likely originating from the steric protection and/or higher electron donating character offered by the indole group. Notably, **127-Y** was able to convert 1,050 equiv. of LA to PLA in 6 min at 20°C with a remarkable turnover frequency (TOF) of $1 \times 10^4 \text{ mol}_{\text{LA}} \text{ mol}_{\text{Y}}^{-1} \text{ h}^{-1}$. The scandium derivative **127-Sc** displayed lower activity (vide infra), as observed in previous similar studies. The PDI values of the prepared PLA were relatively high, perhaps because of transesterification reactions.

In situ polymerization was studied at 130°C , with all complexes found to be active under these conditions, producing PLA with conversions up to 87% in 10 min. The molecular weights and PDIs were similar to those observed in solution state reactions, indicating well-controlled polymerization even in the absence of a solvent. All of the catalysts bestowed good to moderate heterotacticity on the polymer, with **127-Y** producing the best P_r values of up to 0.84 in THF. Polymerization experiments in the presence of isopropanol were also investigated in order to study the role of an alkoxide initiating group. In studies involving 1 equiv. of

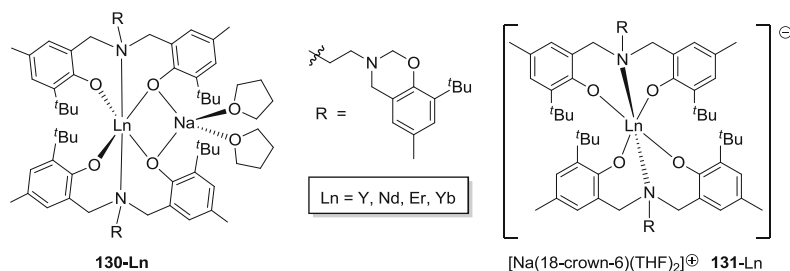


Chart 8 Heterodinuclear rare earth complexes **130-Ln** and **131-Ln**

isopropanol, complex **127-Y** polymerized 1,200 equiv. of LA in 2 min at 20°C with a remarkable TOF of $3.5 \times 10^4 \text{ mol}_{\text{LA}} \text{ mol}_{\text{Y}}^{-1} \text{ h}^{-1}$. The addition of 5 equiv. of isopropanol resulted in immortal polymerization behavior, producing narrow PDI PLA with molecular weights proportional to the amount of added isopropanol. In addition, no silylamido end groups were observed, confirming that the isopropoxide ligand is the true initiating group.

Diamido yttrium complexes $\text{LY}(\text{N}(\text{SiHMe}_2)_2)_2$ ($\text{L} = 2,4\text{-dialkyl-6-bis-}(2\text{-}(\text{diethylamino})\text{ethyl})\text{aminomethylphenol}$, $\text{R} = \text{Me}, \text{tBu}$) **129-R** (Chart 7) bearing unique pincer ligands were prepared by Arnold and co-workers [117]. Compounds **129-Me** and **129-tBu** are active catalysts for the ROP of *rac*-LA, turning up to 1,000 equiv. of monomer into narrow PDI PLA within 30 min. Both complexes gave better conversion and more narrow PDI than $\text{Y}[\text{N}(\text{SiMe}_3)_2]_3$, demonstrating the influence imparted by the ancillary ligands. Notably, extended reaction times increased PDI values, suggesting competitive transesterification. No stereocontrol was observed during the polymerization of *rac*-LA, and the use of L-LA as the monomer resulted in atactic polymer growth, signifying epimerization processes during polymerization.

The heterodinuclear ate complexes $\text{L}_2\text{LnNa}(\text{THF})_2$ ($\text{Ln} = \text{Y, Nd, Er, Yb}$; $\text{L} = 6,6'\text{-}(2\text{-}(8\text{-tert-butyl-6-methyl-2H-benzo}[e][1,3]\text{oxazin-3}(4H)\text{-yl})\text{ethylazanediyl})\text{-bis(methylene)bis}(2\text{-tert-butyl-4-methylphenolato})$) **130-Ln** and their corresponding ion pairs $[\text{L}_2\text{Ln}][(\text{18-crown-6})\text{Na}(\text{THF})_2]$ ($\text{Ln} = \text{Y, Yb}$) **131-Ln** (Chart 8) were prepared by Shen et al. [118]. The complexes were shown to be highly active in the polymerization of $\epsilon\text{-CL}$ (vide infra). In addition, the neodymium derivative **130-Nd** was shown to be a moderately active catalyst for the polymerization of L-LA at ambient temperature, resulting in virtually complete consumption of 100 equiv. of monomer in just over 6 h. Intriguingly, the corresponding yttrium complex **130-Y** did not exhibit any activity at 20°C, and only a mere 3% conversion was achieved after 24 h at 50°C.

Very recently, Ward and co-workers prepared an extensive series of dialkyl $\text{LY}(\text{CH}_2\text{SiMe}_2\text{Ph})_2$, **132–134**, and diamido complexes $\text{LLn}(\text{N}(\text{SiMe}_3)_2)_2$, **135–137-Ln** ($\text{Ln} = \text{Y, La, Pr, Nd, Sm}$; $\text{L} = \text{bis}(\text{oxazolinyphenyl})\text{amide}$) (Chart 9) [119]. Upon reaction with $[\text{Ph}_3\text{C}][\text{B}(\text{C}_6\text{F}_5)_4]$, the generated cationic yttrium, lanthanum, and samarium derivatives were utilized to polymerize *rac*-LA, while complexes of other metals were used as catalysts for hydroamination (vide infra).

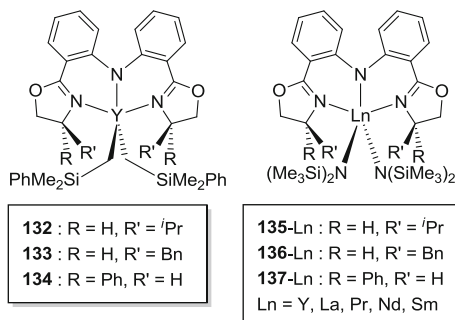


Chart 9 Ward's dialkyl and diamido complexes **132–134** and **135–137-Ln**

All compounds studied were found to be suitable initiators, with **132** being the most active, converting 100 equiv. of *rac*-LA into PLA in less than 2 min. Higher than predicted molecular weights and relatively broad molecular weight distributions indicated only moderate control, and notably, the alkyl species exhibited slightly higher activity than the corresponding amido complexes. The PLA obtained was shown to be heterotactic rich with P_r values of 0.66–0.81.

Despite the plethora of catalytic information provided above, comparing the performance of distinct rare earth metal complexes as initiators in the ROP of lactide is not straightforward. Polymerization experiments are often conducted under different conditions (temperature, reaction time, solvent, etc.) with variable monomer-to-initiator ratios. Nevertheless, a collection of data from representative runs has been tabulated in Table 1 (mononuclear initiators) and Table 2 (dinuclear initiators). For specific information regarding each distinct catalyst, the reader is directed to the corresponding reference. The disparate nature of experimental variables notwithstanding, certain conclusions can be drawn:

1. Pincer ligands can be used to effectively stabilize rare earth metal complexes to produce well-behaving, efficient initiators for the ROP of lactide.
2. Following the general trend inherent to rare earth complexes, larger ionic radii bring about more reactive species and thus more active ROP catalysts. On the other hand, there is often a trade-off between activity and control, wherein prior to optimization studies, the most active catalysts typically afford lower-quality polymers.
3. The solvent used in polymerization reactions has a major affect on the performance of the initiator. For example, coordinating solvents, such as THF, tend to hamper the activity of smaller metals, presumably by competitive coordination with the monomer. Conversely, poor solubility of lactide in noncoordinating solvents can decrease control over the polymerization, producing broader molecular weight distribution polymers (*vide supra*).

Table 1 Polymerization of *rac*-lactide or L-lactide by mononuclear rare earth pincer complexes

Entry	Complex	M	Solv.	T (°C)	Time (min)	[LA ₀]/[I ₀]	Conv. (%)	M_n^{calc} ($\times 10^3$) ^a	M_n^{obs} ($\times 10^3$)	M_w/M_n	P_r	References
1	110	Y	THF	20	2	300	100	21.6 ^b	30.8	1.65	–	[106]
2	110	Y	THF	20	30	500	100	36.0 ^b	45.7	1.72	0.69	[107]
3	111	Y	THF	20	60	300	100	43.2	46.4	1.46		[106]
4	112	Y	THF	20	2	300	100	21.6 ^b	33.0	1.58		[106]
5	113	Y	THF	20	60	300	100	43.2	61.2	1.31		[106]
6	114-Y	Y	THF	20	60	500	100	72.1	76.4	1.29	0.62 ^c	[108]
7	114-Y	Y	Tol	20	60	500	67	48.3	49.5	1.23	0.56 ^c	[108]
8	114-Yb	Yb	THF	20	60	500	88	63.4	64.6	1.25	0.58 ^c	[108]
9	114-Yb	Yb	Tol	20	60	500	76	54.8	56.3	1.27	0.54 ^c	[108]
10	119	Y	Tol	20	240	500	100	72.1	72.3	1.23	0.70	[112]
11	119	Y	THF	20	240	500	65	46.8	46.2	1.28	0.71	[112]
12	120-Y	Y	Tol	20	240	500	100	72.1	72.3	1.21	0.74	[112]
13	120-Y	Y	THF	20	240	500	75	54.0	54.6	1.26	0.72	[112]
14	120-Sm	Sm	Tol	20	240	500	100	72.1	71.6	1.23	0.67	[112]
15	120-Yb	Yb	Tol	20	240	500	100	72.1	71.8	1.25	0.71	[112]
16	123-Sc	Sc	THF	20	700	100	100	14.4	16.2	1.55	0.65	[113]
17	123-Y	Y	THF	20	60	100	71	10.2	8.9	1.32	0.90	[113]
18	123-Y	Y	Tol	20	3	100	100	14.4	10.0	1.52	0.50	[113]
19	123-La	La	THF	20	40	100	87	12.5	12.7	1.43	–	[113]
20	124-Sc	Sc	THF	20	700	100	100	14.4	17.1	1.61	0.93	[113]
21	124-Y	Y	THF	20	700	100	100	14.4	17.3	1.52	0.84	[113]
22	124-La	La	THF	20	360	100	81	11.7	14.1	1.43	0.50	[113]
23	125-Sc	Sc	THF	20	700	100	100	14.4	13.1	1.42	0.66	[113]
24	125-Y	Y	THF	20	700	100	100	14.4	14.0	1.82	0.68	[113]
25	125-La	La	THF	20	700	100	100	14.4	11.6	1.51	0.75	[113]

(continued)

Table 1 (continued)

Entry	Complex	M	Solv.	T (°C)	Time (min)	[LA ₀]/[I ₀]	Conv. (%)	M_n^{calc} ($\times 10^3$) ^a	M_n^{obs} ($\times 10^3$)	M_w/M_n	P_r	References
26	126-Sc-ⁱPr	Sc	THF	RT	1,200	200	38	11.0	8.1	1.20	–	[114]
27	126-Sc-ⁱPr	Sc	Tol	RT	1,200	200	27	7.8	8.3	1.22	–	[114]
28	126-Sc-Ph	Sc	Tol	RT	1,200	200	23	6.6	6.4	1.50	–	[114]
29	126-Sc-ⁱPr	Sc	–	130	60	200	49	14.4	3.1	1.20	–	[114]
30	126-Y-ⁱPr	Y	THF	RT	15	200	65	18.7	15.9	1.25	–	[114]
31	126-Y-ⁱPr	Y	Tol	RT	15	200	82	23.6	20.4	1.47	–	[114]
32	126-Y-Ph	Y	THF	RT	15	200	79	22.8	21.5	1.25	–	[114]
33 ^d	126-Sc-Ph	Sc	THF	RT	1,200	500	44	5.3 ^e	4.0	1.06	–	[115]
34 ^d	126-Y-Ph	Y	THF	RT	60	500	78	56.2 ^e	47.0	1.26	–	[115]
35 ^d	126-Y-Ph	Y	THF	RT	60	500	85	20.4 ^e	23.7	1.13	–	[115]
36 ^d	126-Y-Ph	Y	THF	RT	60	500	85	10.2 ^e	10.0	1.07	–	[115]
37	127-Sc	Sc	THF	20	180	200	21	6.1	9.5	1.58	0.72	[116]
38	127-Y	Y	THF	20	5	200	89	25.7	25.4	2.23	0.77	[116]
39	127-Y	Y	Tol	20	5	200	88	25.4	14.9	2.23	0.57	[116]
40	127-Y	Y	DCM	20	2	200	100	28.8	25.2	1.54	0.64	[116]
41	127Y	Y	–	130	10	200	87	25.1	29.7	2.02	0.59	[116]
42	128	Y	THF	20	15	200	67	19.3	21.9	1.94	0.74	[116]
43	129-Me	Y	DCM	25	30	50	91	6.6	9.8	1.21	–	[117]
44	129-ⁱBu	Y	DCM	25	30	50	88	6.3	10.7	1.19	–	[117]
45	129-ⁱBu	Y	Tol	25	30	50	87	6.3	12.0	1.22	–	[117]
46	129-ⁱBu	Y	DCM	25	30	100	86	12.4	28.0	1.28	–	[117]
47	130-Y	Y	THF	20	1,440	100	0	–	–	–	–	[118]
48	130-Nd	Nd	THF	20	360	100	99	14.3	3.9	1.46	–	[118]
49	132-Y	Y	THF	25	0.5	100	95	13.8	32.0	1.18	0.72	[119]
50	132-Y	Y	THF	25	1.5	100	99	14.4	30.1	1.24	0.73	[119]
51	133-Y	Y	THF	25	1.5	100	95	13.9	35.5	1.38	0.76	[119]

52	134-Y	Y	THF	25	1.5	100	95	13.5	31.1	1.23	0.69	[119]
53	135-Y	Y	THF	25	300	100	88	12.8	17.9	1.55	0.70	[119]
54	135-Sm	Sm	THF	25	300	100	90	13.2	13.2	1.92	0.66	[119]
55	135-La	La	THF	25	10	100	88	12.8	22.8	2.15	0.68	[119]

^a $M_n^{\text{calc}} = (144.13 \times [L\text{-}A_0]/[I_0] \times \% \text{conv.})$

^b $M_n^{\text{calc}} = (144.13 \times [L\text{-}A_0]/2[I_0] \times \% \text{conv.})$

^c P_{m} = probability of *meso* linkages between monomers

^d polymerization performed in the presence of ^tPrOH (5, 0, 2, and 5 equiv. compared to initiator for entries 33–36, respectively)

^e $M_n^{\text{calc}} = (144.13 \times [L\text{-}A_0]/[I_0 + \text{^tPrOH}] \times \% \text{conv.})$

Table 2 Polymerization of *rac*-lactide or L-lactide by dinuclear rare earth pincer complexes

Entry	Complex	M	Solv.	T (°C)	Time (min)	[L-A ₀]/[I ₀]	Conv. (%)	$M_n^{\text{calc}} (\times 10^3)^a$	$M_n^{\text{obs}} (\times 10^3)$	M_w/M_n	P_r	References
1	109	Y	THF	20	60	300	93	40.2	24.4	1.49	–	[105]
2	115	Sm	THF	20	60	1,000	87	62.7	54.2	1.23	0.54	[109]
3	115	Sm	Tol	20	60	1,000	90	64.9	66.2	1.28	0.58	[109]
4	116	Y	THF	20	60	500	88	63.4	59.3	1.26	0.59	[109]
5	116	Y	Tol	20	60	500	100	72.1	72.9	1.21	0.68	[109]
6	117-Y	Y	Tol	70	240	400	35	20.2	70.8	1.35	–	[110]
7	117-Nd	Nd	Tol	70	240	400	96	55.3	84.7	1.73	–	[110]
8	117-Sm	Sm	Tol	70	240	400	97	55.9	13.1	1.61	–	[110]
9	117-Yb	Yb	Tol	70	240	100	40	5.8	19.7	2.37	–	[110]
10	118-Y	Y	Tol	70	240	100	52	7.5	12.6	2.03	–	[111]
11	118-Nd	Nd	Tol	70	240	200	95	27.4	80.8	2.02	–	[111]
12	118-Sm	Sm	Tol	70	240	200	64	18.4	32.2	1.68	–	[111]
13	118-Yb	Yb	Tol	70	240	100	20	2.9	7.5	2.44	–	[111]
14	121-Sm	Sm	Tol	20	240	500	93	67.0	66.5	1.24	0.68	[112]
15	121-Yb	Yb	Tol	20	240	500	90	64.9	64.4	1.22	0.66	[112]
16	122-Y	Y	Tol	20	240	500	78	56.2	56.8	1.21	0.69	[112]
17	122-Y	Y	THF	20	240	500	56	40.4	40.6	1.32	0.67	[112]
18	122-Yb-H	Yb	Tol	20	240	500	84	60.5	60.2	1.24	0.72	[112]
19	122-Yb-^tBu	Yb	Tol	20	240	500	80	57.7	57.2	1.21	0.69	[112]

$$^a M_n^{\text{calc}} = (144.13 \times [\text{L-A}_0]/[\text{I}_0] \times \% \text{conv.})$$

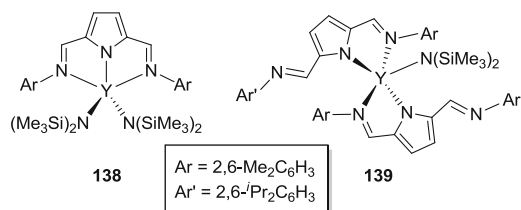


Chart 10 Mono- and bis(pyrrolyl) yttrium ϵ -caprolactone polymerization catalysts

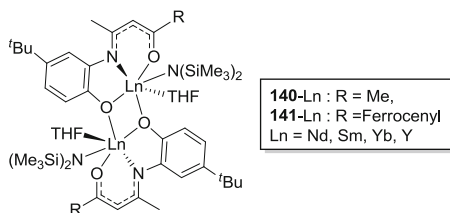


Chart 11 Dinuclear monoamido compounds **140-Ln** and **141-Ln**

4.1.2 Polymerization of ϵ -Caprolactone

Poly(ϵ -caprolactone) (PCL) is a highly attractive target for new plastics and commodity polymers owing to its properties as a biodegradable polymer. Supplementary to their popularity in the polymerization of PLA, rare earth metal complexes have garnered significant attention as catalysts for PCL production. As a result, many novel species which exhibit high or even exceptional catalytic activity have been reported [120]. The performance of pincer-supported rare earth complexes (with anionic initiating groups) as catalysts for the ROP of ϵ -caprolactone (ϵ -CL) is detailed below.

At the turn of the millennium, Mashima and co-workers prepared the heteroleptic diamido mono(pyrrolyl) complex (Xyl₂-pyr)Y(N(SiMe₃)₂)₂, **138** (Xyl₂-pyr = 2,5-bis[*N*-(2,6-Me₂C₆H₃)iminomethyl]pyrrolyl). Although not a bona fide pincer complex, a bis(pyrrolyl) monoamido species (Dipp₂-pyr)₂YN(SiMe₃)₂, **139**, Dipp₂-pyr = 2,5-bis[*N*-(2,6-^{*i*}Pr₂C₆H₃)iminomethyl]pyrrolyl was also obtained when Dipp₂-pyr was used as the ancillary ligand (Chart 10). Catalytic studies indicated that complexes **138** and **139** initiated the ROP of ϵ -CL and also demonstrated that the monoamido complex **139** acted as a single-site initiator to give PCL with narrow molecular weight distribution (PDI = 1.2). It should also be noted that the homoleptic Y(Xyl₂-pyr)₃ complex was shown to be virtually inactive [12].

In addition to their studies on the ROP of lactide (vide supra), Arnold et al. have also investigated mononuclear yttrium diamido complexes **129-R** in the ring-opening polymerization of ϵ -CL. Specifically, complex **129-^{*t*}Bu** produced PCL with low PDIs under mild experimental conditions. However, an undesirable

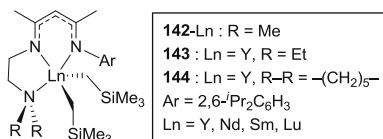


Chart 12 Mononuclear rare earth dialkyl complexes **142–144**

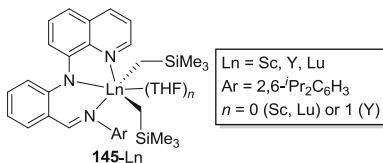


Chart 13 Sc, Y, and Lu dialkyl complexes **145-Ln**

range of chain lengths was observed when longer reaction times were employed, implying that **129-R** can also facilitate undesirable transesterifications [117].

Dinuclear monoamido complexes [LLnN(SiMe₃)₂(THF)]₂, **140-Ln**, (Ln = Nd, Sm, Yb, Y; L = MeCOCHC(Me)N(2-O-5-*t*Bu-C₆H₃)) were prepared by Yao et al. (Chart 11) [121]. All **140-Ln** compounds initiated the ROP of ϵ -CL with modest activity, producing polymers with high molecular weight and relatively broad polydispersities. The size of the metal center clearly had an effect on polymerization as substantial loss in activity occurred with decreasing ionic radius. In an intriguing structural modification, the introduction of a ferrocenyl moiety into the ancillary ligand framework produced complexes **141-Ln**. Unfortunately, no increase in catalytic activity was observed, as **141-Ln** produced polycaprolactone in a similar fashion to its methyl-substituted brethren **140-Ln** [122].

In 2008, Chen and co-workers reported Y-, Lu-, Sm-, and Nd-dialkyl complexes that exhibit high ϵ -CL polymerization activities and relatively narrow PDIs, ranging from 1.34 to 1.39 (Chart 12) [123]. Interestingly, exchanging the metal in complexes **142-Ln** (Ln = Y, Lu, Sm, Nd) had little effect on catalytic activity, whereas modification of the ligand substituents had a pronounced impact. For example, replacement of the NMe₂ group in **142-Ln** for an NEt₂, **143**, or a piperidine moiety, **144**, resulted in improved catalytic activities and molecular weights without a noticeable increase in polydispersity.

Cui et al. reported the mononuclear dialkyl complexes LLn(CH₂SiMe₃)₂(THF)_n (Ln = Sc, Y, Lu, n = 0; Ln = Y, n = 0; L = *N*-(2-(((2,6-*i*-Pr₂C₆H₃)imino)methyl)-phenyl)quinolin-8-amine) **145-Ln** (Chart 13) [124]. Notably, the scandium and lutetium species **145-Sc** and **145-Lu** were THF-free with ancillaries arranged in a square-pyramidal geometry. Meanwhile, the geometry about the larger yttrium center in complex **145-Y** is best described as distorted octahedral with one coordinated THF molecule. All of the complexes were highly active living catalysts for the ROP of ϵ -caprolactone, but the Y and Lu species were the most active. The rigid and bulky nature of the ancillary ligand in **145-Ln** appears to suppress the

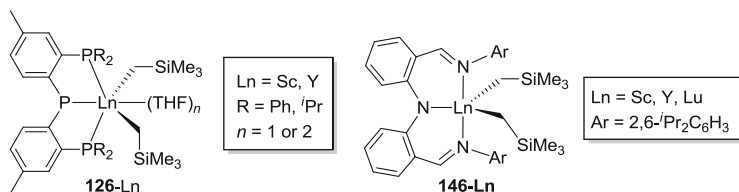


Chart 14 Rare earth dialkyl complexes bearing PPP, **126-Ln**, or NNN, **146-Ln**, pincer ligands

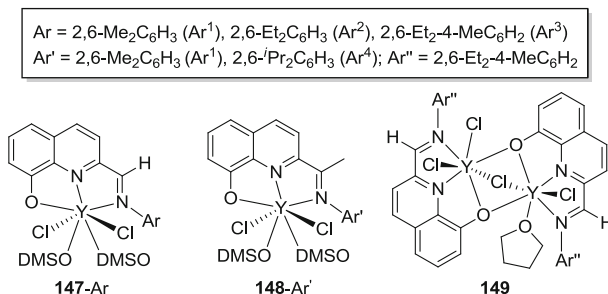


Chart 15 Mono- and dinuclear yttrium imino(methyl) quinolate complexes

backbiting and chain-transfer processes frequently observed in ϵ -CL polymerization catalyzed by dialkyl lanthanide complexes.

In addition to being active in lactide polymerization catalysis (vide supra), scandium and yttrium dialkyl complexes $LLn(CH_2SiMe_3)_2(THF)_n$ ($Ln = Sc, Y$; $L = (4\text{-methyl-6-}PR_2\text{-}C_6H_3)_2P$; $R = ^iPr, Ph$, $n = 1$ or 2) **126-Ln-R**, which possess PPP donor ligands (Chart 14, left), catalyze ϵ -CL polymerization with very high TOFs [115]. The yttrium species **126-Y-R** were found to be more active than the scandium derivatives, which is not particularly surprising given the previous correlations noted between catalytic activity and ionic radius. Upon examining the substituents, the higher activity observed for **126-Ln-Ph** most likely originates from the weaker electron-donating ability of the phenyl groups attached to the phosphorus donors, thus increasing the Lewis acidity of the metal. Interestingly, living ROP of ϵ -CL was observed when complexes **126-Ln-R** were combined with 5 equiv. of isopropanol. Samples of PCL with close to predicted molecular weights and narrow PDIs were produced when appropriate ⁱPrOH/initiator ratios were used.

Dialkyl complexes $LLn(CH_2SiMe_3)_2$ **146-Ln** ($Ln = Sc, Lu, Y$; $L = (2,6\text{-}^iPr_2C_6H_3\text{-}N=CH\text{-}C_6H_4)_2N$) involving modified NNN ancillary frameworks (Chart 14, right), reported by Li et al., also proved to be highly active initiators for the polymerization of ϵ -CL polymerization [125]. Again, the yttrium derivative **146-Y** was the most active system, as it polymerized ϵ -CL in a rapid and living manner. In addition to the polymerization of ϵ -CL, **146-Y** was also active in the random copolymerization of ϵ -CL and γ -butyrolactone (γ -BL) (vide infra).

As a new contribution to the field, Sun, Glaser, and colleagues prepared a series of yttrium dihalide complexes of the form $LYCl_2(DMSO)_2$ ($L = 2\text{-}((\text{arylimino})$

alkyl)quinolin-8-ol), **147**-Ar and **148**-Ar' (Chart 15) [126]. Moreover, the stoichiometric reaction of potassium 2-((2,6-dimethylphenylimino)methyl)quinolin-8-olate with $\text{YCl}_3(\text{THF})_3$ in the absence of DMSO resulted in the formation of dimeric yttrium species **149**. Subsequent in situ metathesis with $\text{LiCH}_2\text{SiMe}_3$ or $\text{LiCH}_2\text{SiMe}_3$ and benzyl alcohol (BzOH) produced catalytically active complexes that could facilitate polymerization of ϵ -CL with high efficiency. In the presence of BzOH, PCL possessing narrow molecular weight distribution was produced in a living manner. However, polymerization in the absence of alcohol resulted in higher than expected molecular weights, as well as broadened PDI values indicative of a more poorly controlled polymerization process. Differently substituted ancillaries (Ar = 2,6-Me₂C₆H₃ (Ar¹), 2,6-Et₂C₆H₃ (Ar²), 2,6-Et₂-4-MeC₆H₂ (Ar³); Ar' = 2,6-Me₂C₆H₃ (Ar¹), 2,6-ⁱPr₂C₆H₃ (Ar⁴); Ar'' = 2,6-Et₂-4-MeC₆H₂) did not bring about major differences in catalytic behavior, and similar activities and polymer features were observed by both the aforementioned dinuclear species and their mononuclear analogues, thus suggesting that both precatalysts lead to the same catalytically active species.

In 2005, Huang et al. prepared the chloride-bridged dinuclear ate complex **150**, $\text{LYCl}_2(\mu\text{-Cl}_2)\cdot\text{Li}(\text{OEt})_2$ (L = 2,5-(CH₂NMe₂)₂C₄H₂N). Unfortunately, this complex was not an active catalyst for the ROP of ϵ -caprolactone. Such inertness is not surprising, given the lack of precedent for chloride ligands to initiate ROP [127].

Although slow in the initiation of ROP of L-LA (vide supra) [118], complexes **130**-Ln were found to promote ROP of ϵ -CL under moderate experimental conditions (e.g., 90% conversion of 200 equiv. of monomer over 24 h at 70°C). Furthermore, the sodium cation in the ate complexes was shown to play a key role in the polymerization. As a result, studies on the effect of encapsulating the cation, to separate it from the lanthanide metal, were investigated by the addition of crown ether (18-crown-6) to a solution of **130**-Ln, generating new, discrete, ion pairs $[\text{L}_2\text{Ln}][(\text{18-crown-6})\text{Na}(\text{THF})_2]$ (Ln = Y, Yb) **131**-Ln. When compared to the aforementioned complexes, the catalytic activity of these “separated” ate complexes decreased considerably, indicating a bimetallic mechanism is most likely operative in polymerization mediated by these ate complexes.

Since most of the rare earth elements are relatively immune to reduction or oxidation, the +3 oxidation state dominates much of rare earth chemistry. However, divalent lanthanides, namely, samarium, europium, thulium, and ytterbium, are reasonably common. Accordingly, divalent Eu(II) and Yb(II) complexes were recently probed by Roesky and co-workers for their ability to polymerize ϵ -CL [128]. Heteroleptic complexes (Dipp₂-pyr)Ln(BH₄)(THF)₃ (Ln = Eu, Yb; Dipp₂-pyr = 2,5-bis[N-(2,6-ⁱPr₂C₆H₃)iminomethyl]pyrrolyl), **151**-Ln, were successfully prepared by a salt metathesis reaction between deprotonated ancillary Dipp₂-pyr and $[\text{Ln}(\text{BH}_4)_2(\text{THF})_2]$. Out of the two complexes, **151**-Eu proved to be an active initiator, producing PCL with high molecular weight and good control over polymer features.

Similar to the ROP of lactide, polymerization of ϵ -caprolactone has been performed under various reaction conditions (temperatures, reaction times, etc.), using distinct monomer to initiator ratios. In general, the complexes noted above

Table 3 Polymerization of ϵ -caprolactone by mononuclear rare earth pincer complexes

Entry	Complex	M	Solv.	T (°C)	Time (min)	[CL ₀]/[I ₀]	Conv. (%)	M_n^{calc} ($\times 10^3$) ^a	M_n^{obs} ($\times 10^3$)	M_w/M_n	References
1	129 -Bu	Y	Tol	25	30	500	99	56.5	43.5	1.19	[117]
2	129 -Bu	Y	Tol	25	60	500	99	56.5	64.5	1.29	[117]
3	129 -Bu	Y	Tol	25	240	500	97	55.4	94.8	1.55	[117]
4	130 -Y	Y	Tol	70	1,440	100	91	5.2	7.2	1.49	[118]
5	130 -Nd	Nd	Tol	70	1,440	100	>99	5.6	8.9	1.39	[118]
6	130 -Er	Er	Tol	70	1,440	100	66	3.8	3.9	1.44	[118]
7	130 -Yb	Yb	Tol	70	1,440	100	95	5.4	6.2	1.56	[118]
8	131 -Y	Y	Tol	70	1,440	100	40	2.3	2.7	1.17	[118]
9	131 -Yb	Yb	Tol	70	1,440	100	39	2.2	2.4	1.13	[118]
10	138	Y	Tol	0	5	100	71	8.1	66.0	1.60	[12]
11	139	Y	Tol	0	5	100	99	11.3	61.3	1.20	[12]
12	142 -Y	Y	Tol	26	20	2,000	89	203.2	23.7	1.37	[123]
13	142 -Nd	Nd	Tol	26	20	2,000	89	203.2	29.4	1.35	[123]
14	142 -Sm	Sm	Tol	26	20	2,000	85	194.0	28.7	1.35	[123]
15	142 -Lu	Lu	Tol	26	20	2,000	95	216.9	46.9	1.35	[123]
16	143	Y	Tol	26	20	2,000	97	221.4	62.5	1.39	[123]
17	144	Y	Tol	26	20	2,000	98	223.7	67.8	1.34	[123]
18	110	Y	Tol	25	5	945	100	107.9	91.0	1.87	[124]
19	145 -Sc	Sc	Tol	25	30	945	99	106.8	94.5	1.18	[124]
20	145 -Y	Y	Tol	26	5	945	100	107.9	99.1	1.41	[124]
21	145 -Lu	Lu	Tol	27	2	945	100	107.9	112.0	1.41	[124]
22	126 -Sc-Ph	Sc	Tol	RT	5	1,000	80	91.3	69.5	1.34	[115]
23	126 -Sc- ⁱ Pr	Sc	Tol	RT	5	1,000	67	76.5	63.7	1.45	[115]
24	126 -Y-Ph	Y	Tol	RT	1	1,000	73	83.3	86.4	1.40	[115]
25	126 -Y-Ph	Y	Tol	RT	30	1,000	100	114.1	132.8	1.71	[115]

(continued)

Table 3 (continued)

Entry	Complex	M	Solv.	T (°C)	Time (min)	[CL ₀]/[I ₀]	Conv. (%)	M_n^{calc} ($\times 10^3$) ^a	M_n^{obs} ($\times 10^3$)	M_w/M_n	References
26 ^b	126-Y-Ph	Y	Tol	RT	30	1,000	100	38.0 ^c	30.0	1.29	[115]
27 ^b	126-Y-Ph	Y	Tol	RT	30	1,000	100	12.7 ^c	13.7	1.16	[115]
28 ^b	126-Y-Ph	Y	Tol	RT	30	1,000	85	2.4 ^c	2.6	1.13	[115]
29	126-Y-Pr	Y	Tol	RT	5	1,000	91	103.9	61.4	1.46	[115]
30	146-Sc	Sc	Tol	25	120	2,000	100	228.3	170.0	1.26	[125]
31	146-Y	Y	Tol	25	5	2,000	100	228.3	240.0	1.25	[125]
32 ^d	146-Y	Y	Tol	25	5	2,000	100	228.3	250.0	1.22	[125]
33	146-Lu	Lu	Tol	25	15	2,000	100	228.3	170.0	1.35	[125]
34 ^e	147-Ar¹	Y	Tol	20	30	500	89.7	51.2	65.7	1.68	[126]
35 ^{e,f}	147-Ar¹	Y	Tol	20	30	500	95.3	54.4	57.9	1.21	[126]
36 ^{e,f}	147-Ar²	Y	Tol	20	30	500	98.4	56.2	58.4	1.14	[126]
37 ^{e,f}	147-Ar³	Y	Tol	20	30	500	97.6	55.7	56.6	1.19	[126]
38 ^{e,f}	148-Ar¹	Y	Tol	20	30	500	94.4	53.9	52.0	1.09	[126]
39 ^{e,f}	148-Ar⁴	Y	Tol	20	30	500	96.9	55.3	63.6	1.28	[126]
40	151-Eu	Eu	Tol	20	30	200	100	22.8	15.4	1.11	[128]

^a $M_n^{\text{calc}} = (114.14 \times [\text{CL}_0]/[\text{I}_0]) \times \% \text{conv.}$

^bPolymerization performed in the presence of ^tPrOH (2, 8, and 40 equiv. to initiator for entries 20–22, respectively)

^c $M_n^{\text{calc}} = (144.13 \times [\text{L-A}_0]/[\text{I}_0 + \text{PrOH}]) \times \% \text{conv.}$

^dPolymerization of 1,000 equiv. of CL for 2 min followed by the addition of another 1,000 equiv. for 3 min

^eDihalides **147–148** were activated with 2 equiv. of LiCH₂SiMe₃

^fPolymerization was performed in the presence of 1 equiv. of benzyl alcohol

Table 4 Polymerization of ϵ -caprolactone by dinuclear rare earth pincer complexes

Entry	Complex	M	Solv.	T (°C)	Time (min)	[CL ₀]/[I ₀]	Conv. (%)	M_n^{calc} ($\times 10^3$) ^a	M_n^{obs} ($\times 10^3$)	M_w/M_n	References
1	140-Y	Y	Tol	50	120	200	62	14.2	65.9	2.46	[121]
2	140-Nd	Nd	Tol	50	120	400	95	43.4	150.4	2.62	[121]
3	140-Sm	Sm	Tol	50	60	200	100	22.8	15.2	1.99	[121]
4	140-Sm	Sm	Tol	50	120	300	100	34.2	57.8	1.64	[121]
5	140-Sm	Sm	THF	50	120	300	52	17.8	67.1	1.56	[121]
6	140-Yb	Yb	Tol	50	120	200	17	3.9	10.9	1.66	[121]
7	141-Y	Y	Tol	50	120	300	70	24.0	82.3	1.85	[122]
8	141-Nd	Nd	Tol	50	120	200	98	22.4	78.5	1.73	[122]
9	141-Nd	Nd	Tol	50	120	400	90	41.1	167.7	1.69	[122]
10	141-Nd	Nd	THF	50	120	400	53	24.2	86.2	1.33	[122]
11	141-Nd	Nd	DCM	50	120	400	25	11.4	18.6	1.45	[122]
12	141-Sm	Sm	Tol	50	120	300	100	34.2	136.3	1.44	[122]
13	141-Yb	Yb	Tol	50	120	200	76	17.3	46.3	1.76	[122]
14 ^{b,c}	149	Y	Tol	20	30	500	94.8	54.1	51.4	1.21	[126]
15	150	Y	Tol	RT	1,440	100	0	0.0	–	–	[127]

^a $M_n^{\text{calc}} = (114.14 \times [\text{CL}_0]/[\text{I}_0] \times \% \text{conv.})$ ^bDihalide **132** was activated with 2 equiv. of LiCH₂SiMe₃^cPolymerization was performed in the presence of 1 equiv. of benzyl alcohol

are very active catalysts for the production of PCL in a relatively controlled manner with good, or occasionally even excellent, polymer properties. Alkyl variants appear to serve as better initiators compared to amido counterparts, whereas chloride species seem to be virtually inactive. Although examples of ϵ -CL polymerization in solvents other than toluene are few in number, the effect of solvent is similar to that observed in the ROP of lactide. Representative results from each reference are tabulated in Tables 3 and 4, which can be utilized to draw certain conclusions in regard to the performance of each individual rare earth pincer complex.

4.1.3 Polymerization of Other Cyclic Esters

Aside from recently popularized ROP of lactide and ϵ -caprolactone, only a few studies have been undertaken with other cyclic esters. The dialkyl complex **126-Y** (Chart 14) was shown to polymerize δ -valerolactone with comparable activity and a similar rate constant (pseudo first order) to that observed for the ROP of lactide. Consequently, it was surmised that the reactivity of cyclic esters toward ROP is dependent on the Lewis basicity of the carbonyl groups, which is inherently affected by the size of the ring [115]. Complexes **126-Ln** were also active in the ROP of *rac*- β -butyrolactone (BBL) at elevated temperatures, but the process was considerably slower when either ϵ -CL or LA was used as the monomer. The addition of isopropanol did not change the polymer features, whereas elongated reaction time and/or altering the quantity of monomer resulted in lower molecular weight polymers and broader molecular weight distributions [115].

Monoamido complexes **123-Ln** and **125-Ln** were also active in the ROP of BBL, whereas SiMe_2^tBu -substituted **124-Ln** did not exhibit any polymerization activity (Chart 5). The lack of activity of this series is clearly related to the nature of the silyl substituents (SiMe_2^tBu vs. SiPh_3), although the exact cause for inactivity remains unknown. However, **123-Ln** and **125-Ln** were able to facilitate polymerization of *rac*-BBL at ambient temperature. Also, the addition of isopropanol to presumably generate the Sc-isopropoxide species in situ led to faster rates of reaction, suggesting a slow initiation step when amido ligands are employed. Lanthanum complexes **123-La** and **125-La** demonstrated the highest polymerization activity, while the detrimental influence of THF solvent, compared to toluene, was identical

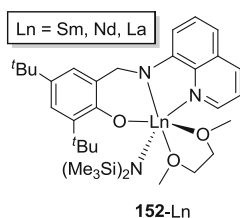


Chart 16 Monoamido lanthanide catalysts for the ROP of 1,4-dioxan-2-one

to that observed in LA catalysis. Relatively low PDI values indicated a good level of polymerization control. Finally, high stereoselectivities were observed in all cases, especially with **123-Y** and **123-La** [113].

Further contributions to the ROP of cyclic monomers were reported by Yao, Wang, and co-workers who investigated polymerization of 1,4-dioxan-2-one using monoamido complexes $\text{LLnN}(\text{SiMe}_3)_2(\text{DME})$ ($\text{Ln} = \text{Sm}, \text{Nd}, \text{La}$; $\text{L} = (3,5\text{-tBu}_2\text{-2-O-C}_6\text{H}_2\text{CH}_2\text{N-C}_9\text{H}_6\text{N})$), **152-Ln** (Chart 16) [129]. All complexes produced high molecular weight polymers, but the neodymium species **152-Nd** was found to be the most active. Polymerization in the presence of a stoichiometric quantity of benzyl alcohol was also investigated, wherein higher activities than the corresponding amido complexes by themselves were observed, presumably because the initiating group had been converted to an alkoxide. Significantly, when reaction temperatures were higher than 60°C, lower conversion was observed and the isolated polymers had lower molecular weights.

4.1.4 Copolymerization Studies

Although more prevalent in the catalyses noted above, rare earth pincer complexes have also been tested as catalysts for the preparation of copolymers, exploiting ROP activity of two different cyclic esters. For example, complex **126-Y**, equipped with a phenyl substituted PPP donor ligand, produced PCL–PLA block copolymers via the addition of $\epsilon\text{-CL}$ followed by LA. Interestingly, when the order of monomer addition was reversed, no copolymer was observed whatsoever, and only the homopolymer PLA was formed. This seems somewhat contradictory since, as noted above, **126-Y** was more active for $\epsilon\text{-CL}$ homopolymerization than the ROP of lactide. Therefore, the reactivity order appears to be reversed for copolymerization of the two monomers. The origin of this reversal of monomer reactivity during copolymerization is not completely understood, but it may be rationalized by the combination of the stronger coordinative ability of lactide, combined with the electrophilic initiator **126-Y** [115].

Copolymerization experiments were also conducted with **146-Y** and **146-Lu** which bear NNN pincer ligands [125]. Although the lutetium derivative **146-Lu** exhibited higher activity than **146-Y**, both complexes initiated copolymerization of $\epsilon\text{-CL}$ and $\gamma\text{-BL}$, despite the fact that neither complex exhibited activity for the homopolymerization of $\gamma\text{-BL}$. The $\gamma\text{-BL}$ content in poly($\epsilon\text{-CL-co-}\gamma\text{-BL}$) was determined to be less than 20 mol% even when a 1:3 $\epsilon\text{-CL}:\gamma\text{-BL}$ monomer ratio was used.

4.2 Polymerization of Dienes

Synthetic polymers play an extremely important role in our everyday life as they are used virtually everywhere, from food packaging to the automotive industry.

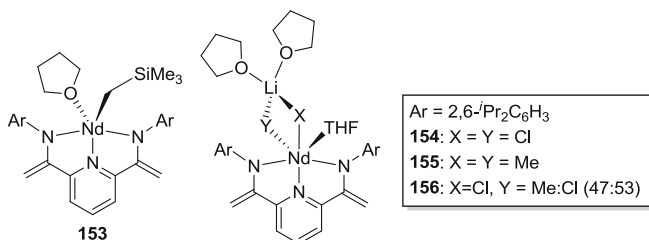


Chart 17 Yttrium pincer species **153–156** which are active catalysts for the polymerization of butadiene

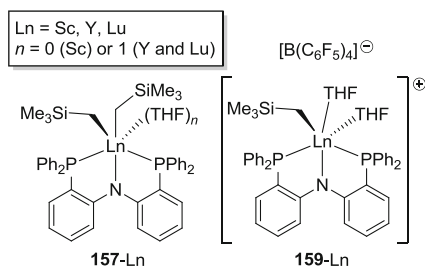


Chart 18 Neutral and cationic rare earth alkyl complexes **157-Ln** and **159-Ln**

Preparation of polymers with desired properties requires precise control over polymer microstructure. In the preparation of these desirable materials, the polymerization of 1,3-conjugated dienes serves as an excellent tool to convert simple monomers into materials with versatile properties. For example, *cis*-1,4-polybutadiene can be used as a component in the preparation of tires, and polyisoprene with high *cis*-1,4-regularity can be utilized as an alternative to natural rubber [130].

Wilson, Gambarotta, and colleagues were one of the first to study rare earth pincer complexes as diene polymerization catalysts [131]. Neodymium compounds $\text{LNd}(\text{CH}_2\text{SiMe}_3)(\text{THF})$, **153**, $\text{LNd}(\mu\text{-X})_2[\text{Li}(\text{THF})_2]$ X = Cl, **154**, and Me, **155**, $\text{Nd}(\mu\text{-Cl})(\mu\text{-X})[\text{Li}(\text{THF})_2](\text{THF})$, X = Me:Cl in a 47:53 occupation ratio, **156**, (L = [2,6-(2,6-*i*-Pr₂C₆H₃)-N-C=(CH₂)₂C₅H₃N]) (Chart 17) were prepared, and their butadiene polymerization behavior was investigated. All ate complexes, **154–156**, were found to be highly active precatalysts for stereoselective *cis*-butadiene polymerization at 50°C, though they first needed to be activated with modified methylaluminoxane (MMAO). Meanwhile, the monoalkyl species **153** displayed negligible activity. Catalysts **154–156** were able to generate polybutadiene possessing a high *cis* content (95–97%), and polymer yields generally greater than 70%, except for the methyl-bridged complex **155**, which afforded a polymer yield less than 20%. The ancillary ligand was shown to be advantageous: complexes **154–156** were more active than $\text{NdCl}_3(\text{THF})_2$. It should also be noted that complex **156** was found to be much more active in cyclohexane than in toluene.

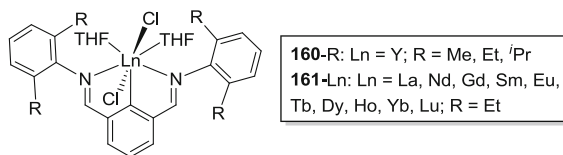


Chart 19 NCN-pincer-supported rare earth complexes **160-R** and **161-Ln**

The pincer-ligated Sc, Y, and Lu dialkyl complexes (PNP)Ln-(CH₂SiMe₃)₂(THF)_n (Ln = Sc, Y, Lu; PNP = (2-Ph₂P-C₆H₄)₂N; Ln = Sc, *n* = 0; Ln = Y, Lu, *n* = 1), **157-Ln** (Chart 18), were prepared using straightforward alkane elimination protocols, while the subsequent cationic monoalkyl species **158-Ln** were generated from the neutral species by the addition of 1 equiv. of [PhMe₂NH][B(C₆F₅)₄]. Although these cationic complexes decompose rapidly in C₆D₅Cl solution, the corresponding bis(THF) adducts **159-Ln** [(PNP)Ln(CH₂SiMe₃)(THF)₂][B(C₆F₅)₄] can be isolated when the reaction is carried out in THF solvent. All **158-Ln** compounds, generated in situ in C₆D₅Cl solution, showed excellent activity in the living polymerization of isoprene at ambient temperature. The polymer contained high *cis*-1,4 content (96.5–99.3%) with **158-Y** giving the most impressive values, coupled with narrow molecular weight distribution (PDIs < 1.11). These properties, selectivity and living character, can even be sustained at elevated temperatures (up to 80°C). In attempts to improve catalysis, Hou and co-workers discovered that the addition of [PhMe₂NH][B(C₆F₅)₄] to a solution of neutral **157-Ln** and isoprene improves catalyst activity by nearly twofold compared to polymerization results obtained from pregenerated **158-Ln**. Interestingly, the use of alternate activators (e.g., [Ph₃C][B(C₆F₅)₄] or B(C₆F₅)₃) resulted in substantially lower polymer yields and catalytically inactive complexes, respectively. Furthermore, the corresponding neutral **157-Ln** was not active under the same polymerization conditions. Finally, precatalysts **158-Ln** can also be utilized in the living *cis*-1,4 polymerization of butadiene and living *cis*-1,4-copolymerization of butadiene and isoprene to yield polymers with 99% *cis*-1,4 content and PDI values less than 1.13 [132].

Rare earth metal dichlorides possessing an aryldiimine NCN-pincer ligand LLnCl₂(THF)₂ (Ln = Y, **160-R**, La, Nd, Gd, Sm, Eu, Tb, Dy, Ho, Yb, Lu, **161-Ln**; L = 2,6-(2,6-R₂C₆H₃N=CH)₂-C₆H₃, R = Me, Et, ⁱPr) (Chart 19) were synthesized via transmetalation between the lithiated ligand and [LnCl₃(THF)_n] [133]. Upon the addition of Al^{*i*}Bu₃ and [Ph₃C][B(C₆F₅)₄] activators, high activities and excellent *cis*-1,4 selectivities in the polymerization of butadiene and isoprene were observed. The yttrium species **160-R** were used to study the influence of the ligand *N*-aryl *ortho* substituent on catalytic activity. Significantly, **160-Et** was found to warrant the best activity, topping both methyl- and isopropyl-substituted compounds. Furthermore, the steric bulk of the alkylaluminum compounds was found to be critical to the catalytic behavior of the complexes. As seen in other studies, the high *cis*-1,4 selectivity endured at polymerization temperatures up to 80°C and did not vary with different lanthanide metals. In-depth mechanistic

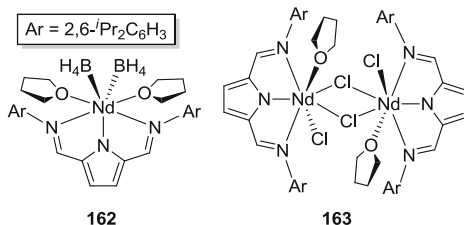


Chart 20 Mono- and dinuclear neodymium complexes **162** and **163**

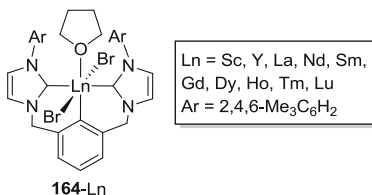


Chart 21 Xylenyl dicarbene rare earth metal dibromide complexes **164-Ln**

studies implied that alkyl-bridged Ln–Al bimetallic cations were the catalytically active species. It is important to note that **161-Sm**, **161-Yb**, and **161-Eu** did not initiate the polymerization reaction, likely because of the reducible nature of these elements.

Later on, Cui and colleagues studied the diene polymerization capabilities of **161-Nd** without the addition of $[\text{Ph}_3\text{C}][\text{B}(\text{C}_6\text{F}_5)_4]$ activator [134]. Once again, this system exhibited high activity and high *cis*-1,4 selectivity for the polymerization of isoprene. Catalytic performance persisted over a wide range of temperatures, and monomer/catalyst ratios of 500 to 8,000 permitted the isolation of high molecular weight polymers with relatively narrow molecular weight distributions ($\text{PDI} \geq 1.68$). Although the neodymium species appeared to be relatively robust, the catalytic activity does appear to be impacted by the steric bulk of the aluminum co-catalysts. Dynamic investigation of the reaction showed that the molecular weight of the resultant polymer had a near linear correlation with conversion.

Roesky, Eickerling, and co-workers prepared an intriguing neodymium bis(borohydride) $\text{LNd}(\text{BH}_4)_2(\text{THF})_2$ complex, **162**, and its dinuclear chloride-bridged counterpart $[\text{LNdCl}(\mu\text{-Cl})(\text{THF})_2]_2$ ($\text{L} = 2,5\text{-bis}[N\text{-}(2,6\text{-}i\text{Pr}_2\text{C}_6\text{H}_3)\text{-iminomethyl}]\text{pyrrole}$), **163** (Chart 20), which they used as catalysts for the polymerization of 1,3-butadiene [135]. In the presence of various co-catalysts (MMAO, $\text{AlEt}_3/\text{B}(\text{C}_6\text{F}_5)_3$ or $\text{AlEt}_3/[\text{PhMe}_2\text{NH}][\text{B}(\text{C}_6\text{F}_5)_4]$), high activities and good *cis*-selectivities were observed, even when very low catalyst loadings were used (1:20,000–22,600).

In 2010, Cui et al. prepared a series of 2,6-xylenyl dicarbene-ligated rare earth metal dibromides $\text{L}_n\text{Br}_2(\text{THF})$ ($\text{L}_n = \text{Sc}, \text{Y}, \text{La}, \text{Nd}, \text{Sm}, \text{Gd}, \text{Dy}, \text{Ho}, \text{Tm}, \text{Lu}$; $\text{L} = (2,6\text{-}(2,4,6\text{-Me}_3\text{C}_6\text{H}_2\text{-NCHCHNCCH}_2)_2\text{-C}_6\text{H}_3)$), **164-Ln** (Chart 21). Using AlR_3 ($\text{R} = \text{Me}, \text{Et}, i\text{Bu}$) or $[\text{Ph}_3\text{C}][\text{B}(\text{C}_6\text{F}_5)_4]$ as co-catalysts, a variety of complexes,

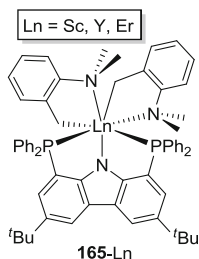


Chart 22 Rare earth bis(alkylamine) complexes **165-Ln**

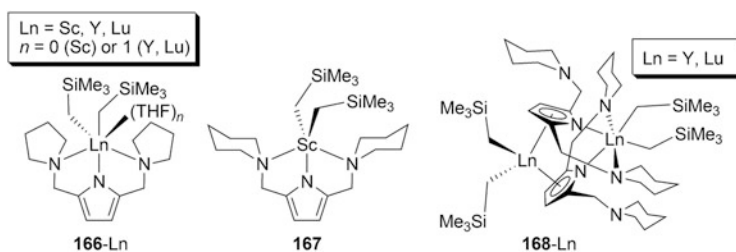


Chart 23 Dialkyl complexes **166-Ln**, **167**, and **168-Ln**

notably **164-Y**, **164-Nd**, and **164-Dy**, found success as catalysts for the polymerization of isoprene, wherein high activity and *cis*-1,4 selectivity (99.6%, 25°C) were noted. Selectivity remained unaffected by the identity of the metal itself and was only slightly influenced by the AlR_3 , when temperatures were kept at 80°C (97.6%). In order to gain deeper mechanistic insight, a series of stoichiometric reactions were conducted which ultimately identified an yttrium hydrido aluminate cation $[\text{LY}(\mu\text{-H})_2\text{Al}^t\text{Bu}_2]^+$ as the catalytically active species [136].

The ligands in tris(aminobenzyl) rare earth complexes $[\text{Ln}(\text{CH}_2\text{C}_6\text{H}_4\text{-2-NMe}_2)_3]$ can be replaced by diphosphinocarbazole ligands to afford the first bis(alkylamine) species $\text{LLn}(\text{CH}_2\text{C}_6\text{H}_4\text{-2-NMe}_2)_2$ ($\text{Ln} = \text{Sc, Y, Er}$; $\text{L} = 3,6\text{-}^t\text{Bu}_2\text{-1,8-(PPh}_2\text{)}_2\text{-carbazole}$), **165-Ln** (Chart 22). In the presence of $[\text{Ph}_3\text{C}][\text{B}(\text{C}_6\text{F}_5)_4]$, **165-Ln** was transformed into a cationic variant that initiated the polymerization of isoprene and butadiene with high activities. In particular, the yttrium species **165-Y** displayed excellent *cis*-1,4-selectivity (>99%), as well as living polymerization character. This behavior was made evident by the linear relationship between polymer molecular weight and monomer/initiator ratio, which persisted over a wide range of temperatures (0–80°C). Notably, the active catalyst, presumably some form of yttrium diene complex, can further initiate the ROP of ϵ -caprolactone to selectively produce low PDI (1.15–1.47) poly(*cis*-1,4-diene)-*b*-polycaprolactone block copolymers with predetermined molecular weight ($M_n = 10\text{--}70 \times 10^4$) [137].

Mononuclear dialkyl complexes $\text{L}^1\text{Ln}(\text{CH}_2\text{SiMe}_3)_2(\text{THF})_n$ ($\text{Ln} = \text{Sc}$, $n = 0$; $\text{Ln} = \text{Y, Lu}$, $n = 1$; $\text{L}^1 = 2,5\text{-bis}(\text{pyrrolidin-1-yl})\text{methylene-1H-pyrrole}$), **166-Ln**,

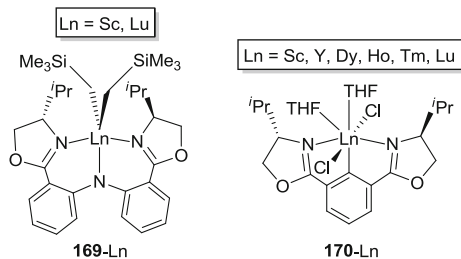


Chart 24 Chiral dialkyl **169-Ln** and dihalide **170-Ln** complexes

and $L^2\text{Sc}(\text{CH}_2\text{SiMe}_3)_2$ ($L^2 = 2,5\text{-bis}((\text{piperidino})\text{methylene})\text{-}1H\text{-pyrrole}$), **167**, or dinuclear tetra-alkyl $L^2_2\text{Ln}_2(\text{CH}_2\text{SiMe}_3)_4$, **168-Ln** (Chart 23), can be prepared in moderate to high yields by straightforward alkane elimination between the requisite proteo ligand and trialkyl rare earth complexes. Upon activation with the Lewis acid $[\text{Ph}_3\text{C}][\text{B}(\text{C}_6\text{F}_5)_4]$, all complexes demonstrated controlled polymerization of isoprene, with complexes **167** and **168-Ln** exhibiting higher activity than **166-Ln**, in general. Complex **168-Y** (although not a bona fide pincer compound) gave high *cis*-1,4-selectivity (94.1%) and the highest activity for the polymerization of isoprene. Conversely, scandium species **166-Sc** and **167** gave high 3,4-selectivity (up to 87%) irrespective of the ancillary ligand, and **166-Lu** and **168-Lu** initiated atactic isoprene polymerization [138].

Zhang, Li, and colleagues utilized a chiral pincer ligand to generate the scandium and lutetium dialkyl complexes $\text{LLn}(\text{CH}_2\text{SiMe}_3)_2$ ($\text{Ln} = \text{Sc}, \text{Lu}$; $L = (S,S)\text{-bis}(\text{oxazolinylphenyl})\text{amido}$), **169-Ln** (Chart 24). When combined with Lewis or Brønsted acid activators, complexes **169-Ln** afforded activities up to $6.8 \times 10^5 \text{ g mol Ln}^{-1} \text{ h}^{-1}$ and atypical *trans*-1,4-selectivity (up to 100%) in the “quasi-living” polymerization of isoprene. The isolated polyisoprene had molecular weights of $M_n = 2\text{--}10 \times 10^4 \text{ g/mol}$ and molecular weight distributions of $M_w/M_n = 1.02\text{--}2.66$ [139].

Finally, NCN-pincer-ligated rare earth dichlorides $\text{LLnCl}_2(\text{THF})_2$ ($\text{Ln} = \text{Sc}, \text{Y}, \text{Dy}, \text{Ho}, \text{Tm}, \text{Lu}$; $L = (S,S)\text{-}2,6\text{-bis}(4'\text{-}i\text{Pr}\text{-}2'\text{-oxazolinyl})\text{phenyl}$), **170-Ln**, were generated by Xu, et al. via standard salt metathesis routes (Chart 24, right). Upon activation by $[\text{PhNHMe}_2][\text{B}(\text{C}_6\text{F}_5)_4]$, together with Al^iBu_3 , Y, Dy, Ho, and Tm complexes exhibited impressive isoprene polymerization activity and noteworthy *cis*-1,4-selectivity (>98%). Interestingly, complexes involving Sc and Lu were virtually inactive in this process, while yttrium proved to be the most active. Polymers generated by this system were up to 99.5% *cis*-1,4, which seemed consistent regardless of reaction temperature (up to 80°C) [140].

Selected results from the aforementioned diene polymerization studies are gathered in Tables 5 and 6. In brief summary, neutral rare earth pincer species were not active for diene polymerization. Instead, complexes required activation by the addition of a Lewis or Brønsted acid. Once activated, rare earth pincer compounds showed excellent activities and high selectivities in the polymerization of both 1,3-butadiene and isoprene.

Table 5 Polymerization of 1,3-butadiene catalyzed by rare earth pincer complexes

Entry	Complex	Metal	T (°C)	Time (min)	Co-cat.	[BU]/[Al]/[X]/[Ln]	Conv. (%)	M_n ($\times 10^4$)	M_w/M_n	cis-1,4	trans-1,4	1,2	References
1	153	Nd	50	30	MMAO	998:303:0:1	75.0	4.40	2.18	61.8	36.4	1.8	[131]
2	154	Nd	50	10	MMAO	998:303:0:1	78.6	26.2	2.80	97.0	2.3	0.7	[131]
3	155	Nd	50	10	MMAO	998:303:0:1	17.2	15.5	4.90	95.9	3.3	0.8	[131]
4	156	Nd	50	15	MMAO	998:303:0:1	77.3	26.3	2.50	97.0	2.5	0.5	[131]
5	156	Nd	50	15	MMAO	998:303:0:1	67.5	16.4	2.31	95.0	4.5	0.5	[131]
6 ^a	156	Nd	50	15	MMAO	998:303:0:1	84.8	16.4	2.34	96.1	4.5	3.4	[131]
7	160-Me	Y	25	60	Al ^t Bu ₃ / B	500:20:1:1	80.0	4.0	1.47	98.5	1.3	0.2	[133]
8	160-Et	Y	25	60	Al ^t Bu ₃ / B	500:20:1:1	100	8.6	2.23	99.7	0.3	0.0	[133]
9	160-Pr	Y	25	60	Al ^t Bu ₃ / B	500:20:1:1	68.0	2.6	1.31	95.3	4.2	0.5	[133]
10	161-La	La ^a	25	60	Al ^t Bu ₃ / B	500:20:1:1	87.0	7.0	1.59	99.3	0.5	0.2	[133]
11	161-Nd	Nd	25	15	Al ^t Bu ₃ / B	500:20:1:1	100	18.0	2.08	99.5	0.4	0.1	[133]
12	161-Gd	Gd	25	10	Al ^t Bu ₃ / B	500:20:1:1	100	32.2	2.18	99.7	0.3	0.0	[133]
13	161-Sm	Sm	25	120	Al ^t Bu ₃ / B	500:20:1:1	0.0	–	–	–	–	–	[133]
14	161-Eu	Eu	25	120	Al ^t Bu ₃ / B	500:20:1:1	0.0	–	–	–	–	–	[133]
15	161-Tb	Tb	25	10	Al ^t Bu ₃ / B	500:20:1:1	100	21.0	2.43	99.7	0.3	0.0	[133]
16	161-Dy	Dy	25	10	Al ^t Bu ₃ / B	500:20:1:1	100	26.0	2.24	99.4	0.6	0.0	[133]

(continued)

Table 5 (continued)

Entry	Complex	Metal	T (°C)	Time (min)	Co-cat.	[BU]/[Al]/[X]/[Ln]	Conv. (%)	M_n ($\times 10^4$)	M_w/M_n	cis-1,4	trans-1,4	1,2	References
17	161 -Ho	Ho	25	15	Al ⁱ Bu ₃ / B	500:20:1:1	100	14.2	2.44	99.4	0.6	0.0	[133]
18	161 -Yb	Yb	25	120	Al ⁱ Bu ₃ / B	500:20:1:1	0.0	–	–	–	–	–	[133]
19	161 -Lu	Lu	25	60	Al ⁱ Bu ₃ / B	500:20:1:1	90.0	9.8	2.48	99.3	0.6	0.1	[133]
20 ^b	162	Nd	65	60	MMAO	20,963:291:0:1	10.8	5.0	10.00	–	–	–	[135]
21 ^c	162	Nd	65	60	AlEt ₃	20,958:144:2:1	44.9	7.8	5.37	83.9	13.1	3.0	[135]
22 ^c	162	Nd	65	60	AlEt ₃	22,065:146:2:1	85.7	11.2	2.88	75.2	23.3	1.5	[135]
23 ^b	163	Nd	65	60	MMAO	22,623:291:1	84.9	24.7	2.30	84.9	13.3	1.8	[135]
24 ^c	163	Nd	65	60	AlEt ₃	21,825:143:2:1	94.9	24.6	2.74	76.1	23.1	0.8	[135]
25 ^c	163	Nd	65	60	AlEt ₃	20,404:145:2:1	19.4	–	–	85.3	13.7	1.0	[135]
26	165 -Y	Y	25	150	B	1,000:0:1:1	71.0	8.2	1.06	>99	–	–	[137]

A = [PhMe₂NH][B(C₆F₅)₄]; B = [Ph₃C][B(C₆F₅)₄]; C = B(C₆F₅)₃^aOrder of the addition of MMAO and Nd was inverted^bFeatures based on polymer after 15 min reaction^cFeatures based on polymer after 10 min reaction

Table 6 Polymerization of isoprene catalyzed by rare earth pincer complexes

Entry	Complex	Metal	T (°C)	Time (min)	Co-cat.	[IP]/[Al]/[X]/[Ln]	Conv. (%)	M_n ($\times 10^4$)	M_w/M_n	cis-1,4	trans-1,4	1,2	References
1	157-Sc	Sc	RT	60	A	600:0:1:1	100	16.0	1.10	96.5	0.0	1.2	[132]
2	157-Y	Y	RT	60	A	600:0:1:1	100	23.0	1.10	99.3	0.0	0.7	[132]
3	157-Lu	Lu	RT	60	A	600:0:1:1	100	19.0	1.09	97.1	0.0	2.9	[132]
4	157-Y	Y	RT	60	B	600:0:1:1	79	32.0	1.11	99.3	0.0	0.7	[132]
5	157-Y	Y	RT	60	C	600:0:1:1	0	–	–	–	–	–	[132]
6 ^a	157-Y	Y	RT	60	C	600:0:1:1	200	23.0	1.08	99.3	0.0	0.7	[132]
7	160-Me	Y	25	120	Al ⁱ Bu ₃ /B	500:20:1:1	40	13.5	2.47	98.3	0.0	1.7	[133]
8	160-Et	Y	25	120	Al ⁱ Bu ₃ /B	500:20:1:1	100	7.8	1.76	98.8	0.0	1.2	[133]
9	160-Pr	Y	25	120	Al ⁱ Bu ₃ /B	500:20:1:1	28	14.3	3.63	91.0	0.0	9.0	[133]
10	161-La	La	25	120	Al ⁱ Bu ₃ /B	500:20:1:1	54	7.0	2.06	98.6	0.0	1.4	[133]
11	161-Nd	Nd	25	15	Al ⁱ Bu ₃ /B	500:20:1:1	100	4.3	1.70	97.6	0.0	2.4	[133]
12	161-Gd	Gd	25	10	Al ⁱ Bu ₃ /B	500:20:1:1	100	5.7	2.49	98.3	0.0	1.7	[133]
13	161-Sm	Sm	25	120	Al ⁱ Bu ₃ /B	500:20:1:1	0	–	–	–	–	–	[133]
14	161-Eu	Eu	25	120	Al ⁱ Bu ₃ /B	500:20:1:1	0	–	–	–	–	–	[133]
15	161-Tb	Tb	25	60	Al ⁱ Bu ₃ /B	500:20:1:1	100	8.9	2.44	92.9	0.0	7.1	[133]
16	161-Dy	Dy	25	15	Al ⁱ Bu ₃ /B	500:20:1:1	100	5.3	2.64	98.4	0.0	1.6	[133]

(continued)

Table 6 (continued)

Entry	Complex	Metal	T (°C)	Time (min)	Co-cat.	[IP]/[Al]/[X]/[Ln]	Conv. (%)	M_n ($\times 10^4$)	M_w/M_n	cis- 1,4	trans- 1,4	1,2	References
17	161 -Ho	Ho	25	15	Al ⁱ Bu ₃ / B	500:20:1:1	90	5.1	2.59	98.5	0.0	1.5	[133]
18	161 -Yb	Yb	25	15	Al ⁱ Bu ₃ / B	500:20:1:1	0	–	–	–	–	–	[133]
19	161 -Lu	Lu	25	60	Al ⁱ Bu ₃ / B	500:20:1:1	80	6.2	2.43	98.6	0.0	1.4	[133]
20	161 -Nd	Nd	20	240	Al ⁱ Bu ₃	1,000:2:0:1	0	–	–	–	–	–	[134]
21	161 -Nd	Nd	20	240	Al ⁱ Bu ₃	1,000:3:0:1	35	71.7	2.09	97.6	0.0	2.4	[134]
22	161 -Nd	Nd	20	240	Al ⁱ Bu ₃	1,000:4:0:1	93	75.6	2.00	97.8	0.0	2.2	[134]
23	161 -Nd	Nd	20	240	Al ⁱ Bu ₃	1,000:10:0:1	100	28.8	2.41	98.1	0.0	1.8	[134]
24	161 -Nd	Nd	20	240	AlEt ₃	1,000:10:0:1	100	11.6	1.87	81.1	17.6	1.3	[134]
25	161 -Nd	Nd	20	240	AlMe ₃	1,000:10:0:1	94	36.7	4.67	97.2	1.0	1.8	[134]
26	164 -Y	Y	25	300	Al ⁱ Bu ₃ / B	500:20:1:1	50	14.4	3.81	99.6	0.0	0.4	[136]
27	164 -Nd	Nd	25	90	Al ⁱ Bu ₃ / B	500:20:1:1	100	28.0	3.09	97.3	0.0	2.7	[136]
28	164 -Nd	Nd	25	15	AlEt ₃ /B	500:20:1:1	100	19.0	1.77	96.3	0.0	3.7	[136]
29	164 -Nd	Nd	25	30	AlMe ₃ / B	500:20:1:1	100	62.2	1.70	96.7	0.0	3.3	[136]
30	164 -Gd	Gd	25	180	Al ⁱ Bu ₃ / B	500:20:1:1	100	23.7	3.87	98.6	0.0	1.4	[136]
31	164 -Dy	Dy	25	200	Al ⁱ Bu ₃ / B	500:20:1:1	100	15.1	2.61	99.3	0.0	0.7	[136]
32	165 -Sc	Sc	25	5	B	1,000:0:1:1	100	11.6	1.49	98.3	–	–	[137]
33	165 -Y	Y	25	10	B	1,000:0:1:1	100	11.7	1.07	>99	–	–	[137]
34	165 -Y	Y	25	45	AlMe ₃ / B	1,000:10:1:1	100	7.6	1.11	98.8	–	–	[137]

35	165-Y	Y	25	45	AlEt ₃ /B	1,000:10:1:1	100	8.3	1.12	99.0	–	–	[137]
36	165-Y	Y	25	45	Al ⁱ Bu ₃ / B	1,000:10:1:1	100	7.5	1.11	98.6	–	–	[137]
37	165-Er	Er	25	30	B	1,000:0:1:1	100	10.3	1.08	97.6	–	–	[137]
38	166-Sc	Sc	RT	360	B	1,000:0:1:1	100	17.4	1.14	–	–	85.5	[138]
39	166-Y	Y	RT	720	B	1,000:0:1:1	52	18.0	1.05	80.9	1.4	–	[138]
40	166-Lu	Lu	RT	360	B	1,000:0:1:1	100	47.0	1.31	–	–	42.2	[138]
41	167	Sc	RT	150	B	1,000:0:1:1	57	10.4	1.25	–	–	81.3	[138]
42	168-Y	Y	RT	150	B	1,000:0:1:1	100	10.3	1.22	94.1	0.9	–	[138]
43	168-Lu	Lu	RT	150	B	1,000:0:1:1	100	19.2	1.15	–	–	53.1	[138]
44	169-Sc	Sc	25	360	A	500:0:1:1	73	4.8	1.23	–	–	>99.5	[139]
45	169-Sc	Sc	25	360	B	500:0:1:1	80	3.3	1.25	–	–	>99.5	[139]
46	169-Sc	Sc	25	1,440	C	500:0:1:1	38	4.6	1.29	–	–	>99.5	[139]
47	169-Sc	Sc	25	360	Al ⁱ Bu ₃ / B	1,000:2:1:1	100	3.1	1.47	–	–	99.0	[139]
48	169-Sc	Sc	25	360	Al ⁱ Bu ₃ / A	1,200:2:1:1	50	2.5	1.59	–	–	99.0	[139]
49	169-Sc	Sc	25	360	Al ⁱ Bu ₃ / B	1,200:2:1:1	77	3.0	1.70	–	–	99.0	[139]
50	169-Sc	Sc	25	360	Al ⁱ Bu ₃ / C	1,200:2:1:1	21	2.0	1.31	–	–	99.0	[139]
51	169-Lu	Lu	25	180	Al ⁱ Bu ₃ / B	500:0:1:1	100	6.4	1.38	–	–	99.5	[139]
52	169-Lu	Lu	25	360	Al ⁱ Bu ₃ / B	1,000:2:1:1	100	3.7	1.45	–	–	99.0	[139]
53	170-Sc	Sc	30	60	Al ⁱ Bu ₃ / A	500:10:1:1	0	–	–	–	–	–	[140]
54	170-Y	Y	30	30	Al ⁱ Bu ₃ / A	500:10:1:1	100	11.6	2.12	98.6	0.8	0.6	[140]

(continued)

Table 6 (continued)

Entry	Complex	Metal	T (°C)	Time (min)	Co-cat.	[IP]/[Al]/[X]/[Ln]	Conv. (%)	M_n ($\times 10^4$)	M_w/M_n	cis-1,4	trans-1,4	References
55	170-Y	Y	30	30	AlMe ₃ / A	500:10:1:1	100	23.6	1.75	94.8	4.6	1,2 0.6 [140]
56	170-Y	Y	30	8	AlEt ₃ /A	500:10:1:1	100	12.9	1.74	90.7	8.4	[140]
57	170-Y	Y	30	30	Al ⁱ Bu ₃ / B	500:10:1:1	100	7.4	4.13	97.1	1.6	[140]
58	170-Y	Y	30	90	Al ⁱ Bu ₃ / C	500:10:1:1	91	8.2	3.14	98.9	0.3	[140]
59	170-Dy	Dy	30	15	Al ⁱ Bu ₃ / A	500:10:1:1	100	11.0	2.34	98.9	0.6	[140]
60	170-Ho	Ho	30	30	Al ⁱ Bu ₃ / A	500:10:1:1	100	13.9	3.21	99.2	0.4	[140]
61	170-Tm	Tb	30	60	Al ⁱ Bu ₃ / A	500:10:1:1	78	12.0	3.69	98.3	0.9	[140]
62	170-Lu	Lu	30	60	Al ⁱ Bu ₃ / A	500:10:1:1	7	–	–	–	–	[140]

A = [PhMe₂NH][B(C₆F₅)₄]; B = [Ph₃C][B(C₆F₅)₄]; C = B(C₆F₅)₃

^a600 equiv. of isoprene was polymerized for 30 min after which another 600 equiv. was added. The activator was added to a solution of **157-Y** and isoprene

4.2.1 Rare Earth Metal Oxazoline Complexes in Asymmetric Catalysis

In addition to various polymerization reactions, rare earth complexes with various substituted 2,6-bis(oxazolanyl)-pyridine (pybox) and other oxazoline derived pincer-type ligands have been exploited for several other catalytic applications. For example, complexes with the general formula $\text{Ln}(\text{pybox})(\text{A})_3$ (A = monodentate anionic ligand) have been shown to catalyze a broad selection of reactions, such as enantioselective Diels–Alder [141] and nitrono cycloadditions [142], Friedel–Craft alkylations [143], asymmetric Mannich-type reactions [144], as well as a variety of ene-reactions [145]. It is important to note that most of these processes are catalyzed by in situ prepared complexes, rather than well-defined species, and thus remain out of the scope of this review. In addition, studies concerning rare earth metals with diverse oxazoline-based ligands have been recently and comprehensively reviewed. Thus, the interested reader is encouraged to procure further insight from that source [146].

4.3 Other Polymerization Reactions

Polyethylene (PE), the world's most common plastic, is generally produced by the polymerization of ethylene using well-established transition metal species, such as Ziegler–Natta or Phillips catalysts. However, in recent years, interest in rare earth pincer ethylene polymerization catalysts has increased. Selected results from these studies are gathered in Table 7 and briefly discussed in the paragraphs below.

In 2008, Waymouth, Anwender, and co-workers examined the use of the lanthanide dialkyl complexes $\text{LLn}(\text{CH}_2\text{SiMe}_3)_2$ ($\text{Ln} = \text{Sc}, \text{Lu}$; $\text{L} = [2-(2,6\text{-}^i\text{Pr}_2\text{C}_6\text{H}_3)\text{-N}=\text{CMe}]-6-\{(2,6\text{-}^i\text{Pr}_2\text{C}_6\text{H}_3)\text{NCMe}_2\}\text{C}_5\text{H}_3\text{N}]$), **171**-Ln (Chart 25), in ethylene polymerization [147]. Although the neutral species **171**-Ln were inert toward ethylene, the cationic analogues, generated by reaction with $[\text{PhMe}_2\text{NH}][\text{B}(\text{C}_6\text{F}_5)_4]$ or $[\text{Ph}_3\text{C}][\text{B}(\text{C}_6\text{F}_5)_4]$, produced polyethylene in moderate yields. Meanwhile, the addition of the activator *N*-[tris(pentafluorophenyl)borane]-3*H*-indole to **171**-Ln led to species that were catalytically inactive. These binary catalytic systems were also tested in the polymerization of styrene and the copolymerization of styrene and ethylene, but no polymeric material was obtained.

Evans, Reid, and Tromp used a neutral SNS pincer ligand to create the scandium complex LScCl_3 ($\text{L} = \text{HN}(\text{CH}_2\text{CH}_2\text{SC}_{10}\text{H}_{21})_2$), **172** (Chart 25). The ability of this complex to catalyze ethylene polymerization was studied using two different modified methylaluminumoxanes as co-catalysts [148].

In 2010 Trifonov, Giambastiani, and co-workers reported the ability of mono-nuclear cyclometalated yttrium amidopyridinate complexes $\text{LY}(\text{CH}_2\text{SiMe}_3)(\text{THF})_2$ ($\text{L} = [2-(\text{C}_6\text{H}_4)-6-\{(2,6\text{-}^i\text{Pr}_2\text{C}_6\text{H}_3)\text{NCMe}_2\}\text{C}_5\text{H}_3\text{N}]$), **173**, $[2-(2\text{-Me-6-CH}_2\text{-C}_6\text{H}_3)-6-\{(2,6\text{-}^i\text{Pr}_2\text{C}_6\text{H}_3)\text{NCMe}_2\}\text{C}_5\text{H}_3\text{N}]$, **174**, or $[2-(\text{C}_4\text{HR}'\text{S})-6-\{(2,6\text{-}^i\text{Pr}_2\text{C}_6\text{H}_3)\text{-NCMe}_2\}\text{C}_5\text{H}_3\text{N}]$, **175-R'** (Chart 25), as well as dinuclear hydride-bridged species

Table 7 Selected results from ethylene polymerization experiments

Entry	Complex	Metal	T (°C)	Time (min)	Co-catalyst	[Al]/[X]/[Ln]	Pressure (bar)	Solvent	Activity ^a	References
1	I71-Sc	Sc	25	60	A	0:1:1	10	Tol	33.0	[147]
2	I71-Sc	Sc	25	60	B	0:1:1	10	Tol	25.0	[147]
3	I71-Sc	Sc	25	60	D	0:1:1	10	Tol	–	[147]
4	I71-Lu	Lu	25	60	A	0:1:1	10	Tol	13.0	[147]
5	I71-Lu	Lu	25	60	B	0:1:1	10	Tol	15.0	[147]
6	I71-Lu	Lu	25	60	D	0:1:1	10	Tol	–	[147]
7	I72	Sc	60	17	MMAO-3A	500:0:1	40	C ₆ H ₅ Cl	18.1	[148]
8	I72	Sc	60	10	PMAO-IP	500:0:1	40	C ₆ H ₅ Cl	0.6	[148]
9	I73	Y	22	30	MAO	300:0:1	10	Tol	2.4	[29]
10	I73	Y	50	30	MAO	300:0:1	10	Tol	1.6	[29]
11	I73	Y	65	30	Al ⁱ Bu ₃ /A	200:1.2:1	10	Tol	0.8	[29]
12	I73	Y	22	30	MAO	300:0:1	10	Tol	0.3	[29]
13	I75-H	Y	22	30	MAO	300:0:1	10	Tol	2.2	[29]
14	I75-Et	Y	22	30	MAO	300:0:1	10	Tol	3.1	[29]
15	I75-Et	Y	50	30	MAO	300:0:1	10	Tol	2.7	[29]
16	I75-Et	Y	65	30	Al ⁱ Bu ₃ /A	200:1.2:1	10	Tol	0.4	[29]
17	30	Y	22	30	MAO	300:0:1	10	Tol	traces	[29]
18	30	Y	65	30	Al ⁱ Bu ₃ /A	200:1.2:1	10	Tol	traces	[29]
19	31	Y	22	30	MAO	300:0:1	10	Tol	traces	[29]
20	I76	Y	65	30	Al ⁱ Bu ₃ /A	200:1.2:1	10	Tol	traces	[29]

A = [PhMe₂NH][B(C₆F₅)₄]; B = [Ph₃C][B(C₆F₅)₄]; D = *N*-[tris(pentafluorophenyl)borane]-3*H*-indole

^aActivity = [kg PE / (mol Ln bar h)⁻¹]

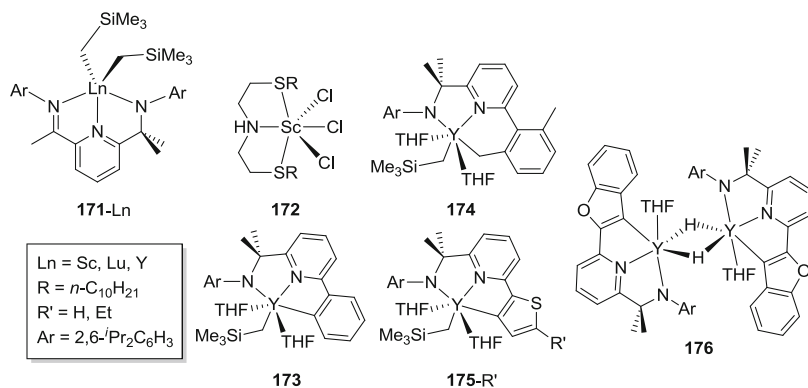


Chart 25 Chloride, alkyl, and hydride ethylene polymerization catalysts

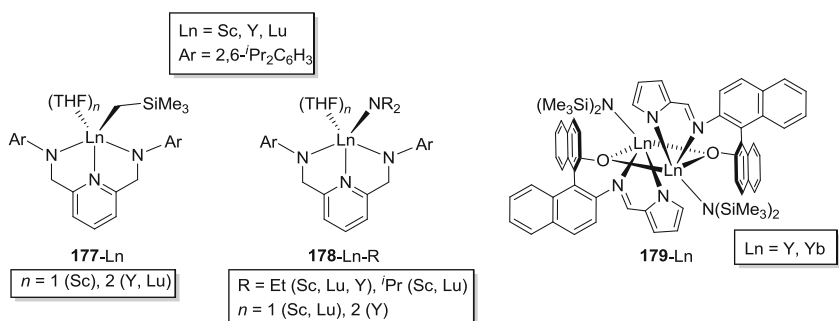


Chart 26 Alkyl and amido MMA polymerization catalysts

29 and **30** (see Sect. 3.1.2) and $[\text{LY}(\mu\text{-H})(\text{THF})_2]$ ($\text{L} = [2\text{-C}_8\text{H}_4\text{O-6-}\{(2,6\text{-}^i\text{Pr}_2\text{C}_6\text{H}_3)\text{-NCMe}_2\}\text{C}_5\text{H}_3\text{N}]$, **176**, to polymerize ethylene when activated with MAO or $[\text{PhMe}_2\text{NH}][\text{B}(\text{C}_6\text{F}_5)_4]$. More specifically, complexes **173** and **175**-Et were capable of producing up to 2.4 and 3.1 kg of PE $[(\text{mol of Y}) \text{ bar h}]^{-1}$, respectively, at ambient temperature. A notable reduction in catalytic activity was observed when the metalated sp^2 carbon of the aryl substituent was replaced by an sp^3 hybridized carbon, **174**. Under all conditions tested, the dinuclear hydride complexes **29**, **30**, and **176** were completely inactive [29].

In addition to ethylene polymerization catalysis, rare earth pincer complexes have also been used to polymerize methyl methacrylate (MMA) to poly(methylmethacrylate) (PMMA), which is also known as acrylic glass. This exceedingly useful polymer is a transparent thermoplastic that is commonly used as an alternative for glass when more lightweight and durable material is required.

In 2003, Anwander published a series of alkyl complexes, $\text{LLn}(\text{CH}_2\text{SiMe}_3)(\text{THF})_n$ ($\text{Ln} = \text{Sc}$, $n = 1$; Y , Lu , $n = 2$; $\text{L} = 2,6\text{-bis}(\{(2,6\text{-}^i\text{Pr}_2\text{C}_6\text{H}_3)\text{amino}\}\text{methyl})\text{-pyridine}$), **177**-Ln, and amido $\text{LLn}(\text{NR}_2)(\text{THF})_n$, **178**-Ln, that were used to polymerize MMA (Chart 26). The scandium complexes produced MMA that

featured narrow polydispersities ($M_w/M_n < 1.5$) and predominantly syndio- and heterotactic microstructures. Interestingly, the heavier yttrium and lutetium analogues gave only negligible conversions (Table 8) [14]. Likewise, even upon the addition of MAO, **171**-Ln gave only traces of PMMA, a fact which highlights the capacity of even seemingly subtle steric or electronic ligand modifications to dramatically impact catalyst performance [147].

A few years later, Zi et al. investigated dinuclear yttrium and ytterbium complexes of the formula $[\text{LLnN}(\text{SiMe}_3)_2]_2$ (Ln = Y, Yb; L = (*S*)-2-(pyrrol-2-ylmethyleneamino)-2'-hydroxy-1,1'-binaphthyl), **179**-Ln (Chart 26), as catalysts for the preparation of PMMA [149]. Both **179**-Y and **179**-Yb initiated MMA polymerization, affording syndiotactic-rich PMMA, although conversions were quite low (Table 8). As observed with heavier lanthanide metals, catalyst deactivation tends to kill MMA polymerization after several hours.

4.4 Hydroamination Reactions

Hydroamination, the formal addition of N–H across an unsaturated C–C fragment, offers an atom economical route to commercially important amines from relatively common alkenes or alkynes. Rare earth metals have consistently proven to be particularly useful in catalyzing this transformation [150]. A variety of examples of intramolecular hydroamination catalyzed by rare earth pincer complexes are presented both in the paragraphs below and in Table 9.

Hultsch et al. [151, 156] reported the use of early rare earth pincer catalysts for hydroamination reactions in 2004. Yttrium complexes $\text{LYN}(\text{SiHMe}_2)_2(\text{THF})$ (L = (2,4,6-Me₃C₆H₂NCH₂CH₂)₂NMe), **180**, $\text{LYN}(\text{SiMe}_3)_2$, **181–183**, and $\text{LY}(\text{2-NMe}_2\text{CH}_2\text{C}_6\text{H}_4)$, **184–186**, (L = (ArNCH₂CH₂)₂NMe with Ar = 2,4,6-Me₃C₆H₂, **181**, **184**, 2,6-Et₂C₆H₃, **182**, **185**, or 2,6-Cl₂C₆H₃, **183**, **186**) (Chart 27) were shown to efficiently catalyze the intramolecular hydroamination of aminoalkenes and aminoalkynes. The nature of the leaving group was found to have a significant influence on the catalytic activity of the complexes. For example, systems possessing a bis(trimethylsilyl)amido or bidentate aryl amine functionality, **181–186**, displayed similar activities and TOFs, while catalysts equipped with a bis(dimethylsilyl)amido moiety, **180**, were much less active. Furthermore, the mesityl-substituted complex **184** quickly decomposed in solution ($t_{1/2} = 6$ h), whereas the corresponding 2,6-diethylphenyl and 2,6-dichlorophenyl-substituted species **185** and **186** were considerably more stable. The chloride substituents on the phenyl ring also appear to increase catalyst stability toward protonolysis, although the hydroamination activity of **183** and **186** suffered compared to their alkyl substituted counterparts (Table 9).

A few years later, Zi et al. [108, 109, 152] studied an extended series of rare earth complexes **114**-Ln (Ln = Y, Yb), **115–116**, **179**-Ln (Ln = Y, Yb), and L_3Ln ((Ln = Y, Yb; L = (*S*)-2-(pyrrol-2-ylmethyleneamino)-2'-hydroxy-1,1'-binaphthyl, **187**-Y and **187**-Yb, or Ln = Sm; L = (*S*)-5,5',6,6',7,7',8,8'-octahydro-2-(pyrrol-2-

Table 8 Selected results from MMA polymerization studies

Entry	Complex	M	T (°C)	Time (h)	[MMA]/[Ln]	Conv. (%)	Mn ($\times 10^3$)	Mw/Mn	Tacticity ^a			References
									mr	mm	rr	
1	177-Sc	Sc	40	48	500	95.0	81.0	1.60	44.0	6.5	49.5	[14]
2	177-Y	Y	40	48	500	12.0	58.0	29.90	25.0	37.0	38.0	[14]
3	177-Lu	Lu	40	48	500	11.0	60.0	86.50	27.0	20.0	53.0	[14]
4	178-Sc-Et	Sc	40	48	500	87.0	65.0	1.28	49.5	9.0	41.5	[14]
5	178-Sc- ⁱ Pr	Sc	40	48	500	>99	67.0	1.56	47.5	8.0	44.5	[14]
6	178-Lu- ⁱ Pr	Y	40	48	500	Trace	105.0	17.50	21.0	19.5	59.5	[14]
7	179-Y	Y	20	3	500	3.5	27.0	1.82	24.0	18.0 ^b	58.0	[149]
8	179-Y	Y	0	3	500	5.0	42.3	1.87	26.0	15.0 ^b	59.0	[149]
9	179-Y	Y	-20	3	500	7.0	47.8	1.99	25.0	21.0 ^b	54.0	[149]
10	179-Yb	Yb	20	3	500	3.2	32.6	2.28	28.0	27.0 ^b	45.0	[149]
11	179-Yb	Yb	0	3	500	3.7	34.8	2.32	25.0	18.0 ^b	57.0	[149]
12	179-Yb	Yb	-20	3	500	5.5	33.2	2.19	23.0	22.0 ^b	55.0	[149]

^amr, mm, and rr are hetero-, iso-, and syndiotactic triads, respectively^bCalculated as $mm = 100 - (mr + rr)$

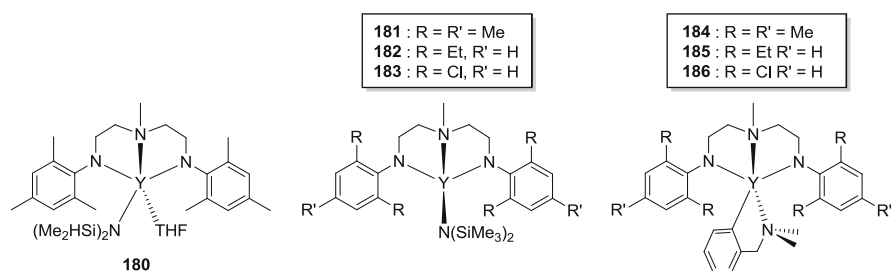
Table 9 Selected results from the intramolecular hydroamination/cyclization of 2,2-dimethylpent-4-enylamine to 2,4,4-trimethylpyrrolidine

Entry	Complex	Metal	T (°C)	Time (h)	[AA]/[Ln]	Conv. (%)	TOF ^a	<i>ee</i>	References
1	180	Y	40	13	25.0	41.0	0.8	–	[151]
2	181	Y	25	3.5	33.3	96.0	9.1	–	[151]
3	182	Y	25	4	33.3	98.0	8.2	–	[151]
4	183	Y	25	41	50.0	92.0	1.1	–	[151]
5	184	Y	25	3.65	95.0	95.0	24.7	–	[151]
6	185	Y	25	5	97.0	97.0	18.8	–	[151]
7	186	Y	25	25	96.0	96.0	3.7	–	[151]
8	114-Y	Y	20	48	20.0	93.0	0.4	39	[108]
9	114-Yb	Yb	60	48	20.0	65.0	0.3	44	[108]
10	187-Y	Y	120	160	20.0	–	–	–	[108]
11	187'	Sm	120	160	20.0	–	–	–	[108]
12	187-Yb	Yb	120	160	20.0	–	–	–	[108]
13	115	Sm	20	16	40.0	98.0	2.5	55	[109]
14	116	Y	20	16	40.0	95.0	2.4	54	[109]
15	179-Y	Y	23	48	20.0	81.0	0.3	5	[152]
16	179-Yb	Yb	120	160	20.0	–	–	–	[152]
17	188-Sm	Sm	23	48	20.0	100.0	0.4	37	[152]
18	188-Yb	Yb	23	48	20.0	55.0	0.2	43	[152]
19	189-Y	Y	60	48	20.0	46.0	0.2	11	[152]
20	189-Yb	Yb	120	60	20.0	31.0	0.1	61	[152]
21	190-Y	Y	40	4 ^b	50.0	95.0	11.9	18	[153]
22	190-Lu	Lu	40	4 ^b	50.0	95.0	11.9	52	[153]
23	191-Y	Y	40	5 ^b	50.0	95.0	9.5	5	[153]
24	192-Sc	Sc	40	96 ^b	25.0	95.0	0.2	18	[153]
25	192-Y	Y	40	3 ^b	50.0	95.0	15.8	35	[153]
26	192-Lu	Lu	40	7 ^b	71.4	95.0	9.7	62	[153]
27	193-Y	Y	40	12 ^b	50.0	95.0	4.0	6	[153]
28	193-Lu	Lu	40	12 ^b	50.0	95.0	4.0	10	[153]
29	194-Y	Y	40	7 ^b	50.0	95.0	6.8	47	[153]
30	194-Lu	Lu	40	3 ^b	50.0	95.0	15.8	63	[153]
31	195-Sc	Sc	60	24	100.0	<5	0.2	–	[154]
32	195-Y	Y	60	4	100.0	98.0	24.5	–	[154]
33	195-Lu	Lu	60	12	100.0	96.0	8.0	–	[154]
34	196-Y	Y	60	2	100.0	97.0	48.5	–	[154]
35	196-Nd	Nd	60	0.5	100.0	98.0	196.0	–	[154]
36	196-Nd	Nd	60	1	200.0	98.0	196.0	–	[154]
37	196-Gd	Gd	60	1	100.0	98.0	98.0	–	[154]
38	196-Dy	Dy	60	1	100.0	97.0	97.0	–	[154]
39	197	Y	60	1	40.0	96.0	38.4	–	[155]
40	198	Y	60	0.6	40.0	97.0	66.5	–	[155]
41	199	Y	60	2	40.0	97.0	19.4	–	[155]

(continued)

Table 9 (continued)

Entry	Complex	Metal	T (°C)	Time (h)	[AA]/[Ln]	Conv. (%)	TOF ^a	<i>ee</i>	References
42	200	Y	60	1.17	40.0	98.0	33.6	–	[155]
43	132	Y	50	168	10.0	0.0	0.0	–	[119]
44	135-La	La	30	72	10.0	99.0	0.6	7	[119]
45	135-Pr	Pr	22	12	10.0	99.0	0.8	14	[119]
46	136-Pr	Pr	22	12	10.0	99.0	0.8	16	[119]
47	137-Pr	Pr	22	12	10.0	99.0	0.8	10	[119]
48	135-Nd	Nd	22	168	10.0	0.0	0.0	–	[119]
49	135-Sm	Sm	22	12	10.0	99.0	0.8	14	[119]

^aTOF = [%conv. × [AA]/[Ln] / time (in h)]^bTime to >95% conversion**Chart 27** Amido and alkylamino hydroamination catalysts **180–186**

ylmethyleneamino)-2'-methoxy-1,1'-binaphthyl, **187'**, [LLnN(SiMe₃)₂]₂ (Ln = Sm, Yb; L = (*S*)-2-(pyrrol-2-ylmethyleneamino)-2'-hydroxy-6,6'-dimethyl-1,1'-biphenyl, **188**-Ln, and (L₂Ln)₂LnN(SiMe₃)₂ (Ln = Ym Yb; L = (*S*)-5,5',6,6',7,7',8,8'-octahydro-2-(pyrrol-2-ylmethyleneamino)-2'-methoxy-1,1'-binaphthyl, **189**-Ln (Chart 28), supported by 2-amino-2'-hydroxy-1,1'-binaphthyl)-based (NOBIN) ligands, as catalysts for the asymmetric hydroamination/cyclization of aminoalkenes. These complexes were capable of producing cyclic amines in good yield with moderate *ee* values. Notably, homoleptic complexes **187**-Ln and **187'** did not display any catalytic activity, even after heating at 120°C for 1 week.

More recently, Hultsch and co-workers prepared a series of related rare earth complexes ligated by various substituted NOBIN-derived aminodiols, LLn(NMe₂CH₂C₆H₄) (Ln = Sc, Y, Lu, L = 2-[(3,5-di-*tert*-butyl-2-hydroxybenzyl)-methylamino]-3-(triphenylsilyl)-1,1-binaphthalen-2-ol), **190–194**-Ln (Chart 29). These complexes achieved excellent catalytic activity in intramolecular hydroamination reactions and also boasted *ee* values up to 92%. However, when bound to scandium, the smallest rare earth metal, the steric bulk of these systems necessitated considerably longer reaction times to reach conversions comparable to that achieved by yttrium and lutetium derivatives. Significantly these complexes also catalyze asymmetric intermolecular hydroaminations with similarly impressive activities, although only moderate enantioselectivities were observed (up to

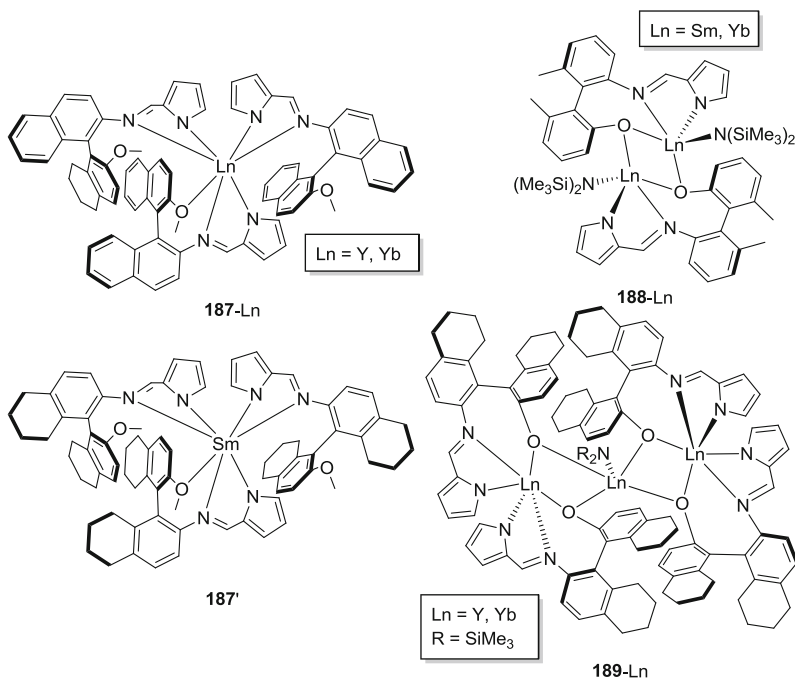


Chart 28 NOBIN supported rare earth complexes **187–189-Ln**

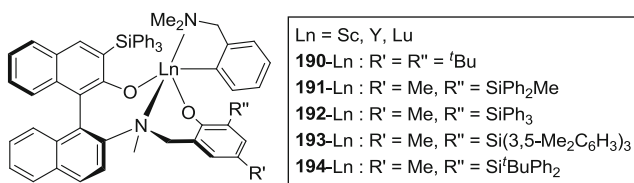


Chart 29 Selected examples of rare earth aminodiolate complexes

40% *ee*). As with the intramolecular catalysis, substituent effects played a major role. Specifically, the sterically demanding ligands that helped procure high enantioselectivities in intramolecular reactions completely shut down all activity in the intermolecular systems. Hence, less bulky ancillaries were required. Finally, it should be noted that these catalysts were less active than previously reported bidentate binaphtholate complexes [153].

Monoalkyl and monoamido rare earth complexes $\text{LLn}(\text{CH}_2\text{SiMe}_3)(\text{THF})$ (Ln = Sc, Y, Lu; L = MeC(2,6-*i*Pr₂C₆H₃N)CHCMe(NCH₂CH₂NR), R = 2,6-Me₂C₆H₃, **195-Ln**, or 2,6-*i*Pr₂C₆H₃, **196-Ln**) and $\text{LY}(\text{R})(\text{THF})$ (L = 2-SiMe₂CH₂-6-CHC(Me)(2,6-*i*Pr₂C₆H₃N)C₅H₃N, R = CH₂SiMe₃, **197**, or R = NH-(2,6-*i*Pr₂C₆H₃), **198**, or L = 2-C₆H₄-6-CHC(Me)(2,6-*i*Pr₂C₆H₃N)C₅H₃N, R = CH₂SiMe₃, **199**, or R = NH(2,6-*i*Pr₂C₆H₃), **200**) (Chart 30) were also studied

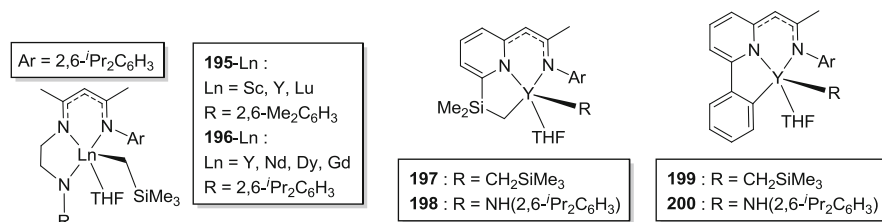


Chart 30 Monoalkyl complexes bearing β -diketiminato derived ancillary pincer ligands

by Chen and colleagues as catalysts for intramolecular hydroamination. All of the studied complexes were able to promote hydroamination catalysis with varying activity. In this work, the property with the most significant influence on catalytic behavior was the ionic radius of metal. For example, complex **196-Nd**, which contained the largest lanthanide examined, was found to convert 200 equiv. of 2,2-dimethylpent-4-enylamine into 2,4,4-trimethylpyrrolidine in 1 h at 60°C, while the yttrium analogue required twice as long for only 100 equiv. of starting material. Additionally, the yttrium alkyl species **197** and **199** were found to be slightly more active than their amido counterparts **198** and **200** [154, 155].

One of the most recent reports of rare earth hydroamination catalysis was that of Ward and Mountford in 2014, wherein metals bearing alkyl, **132–134**, and amido **135–137-Ln**, functionalities were found to catalyze both hydroamination and the ROP of LA [119]. The yttrium derivatives were inactive for the hydroamination of 2,2-dimethylpent-4-enylamine, even after being converted into the corresponding alkyl cations [LY(CH₂SiMe₂Ph)][B(C₆F₅)₄] (L = substituted bis(oxazolinylphenyl) amide). However, the yttrium species **132–134** were highly active when phenyl substituted 2,2-diphenylpent-4-enylamines were used as the hydroamination substrate. Complexes of larger metals (La, Pr, Nd, and Sm) catalyzed the hydroamination of 2,2-dimethylpent-4-enylamine more readily, although long reaction times (12 h or more) were still needed to reach complete conversion. Slightly better *ee* values were acquired when the phenyl-substituted **136-Ln** were used.

4.5 Other Catalytic Reactions

Rare earth pincer complexes have also proven useful in a number of other catalytic transformations. For example, Arnold reported dinuclear samarium species [LSmOAr]₂ (L = 1,1'-S(2-OC₆H₂-3-*t*-Bu-5-Me)₂, **201**, or 1,1'-S(2-OC₁₀H₄-3,6-*t*-Bu)₂, **202**), which were successfully proven to initiate the acylation of 1,2-diols, selectively converting 50% of substrate into the monoacyl product in 24 h at ambient temperature (Fig. 2) [13, 157].

Samarium has also been employed to catalyze other non-conventional chemical transformations, such as reports by Evans et al. in the early 1990s, wherein the

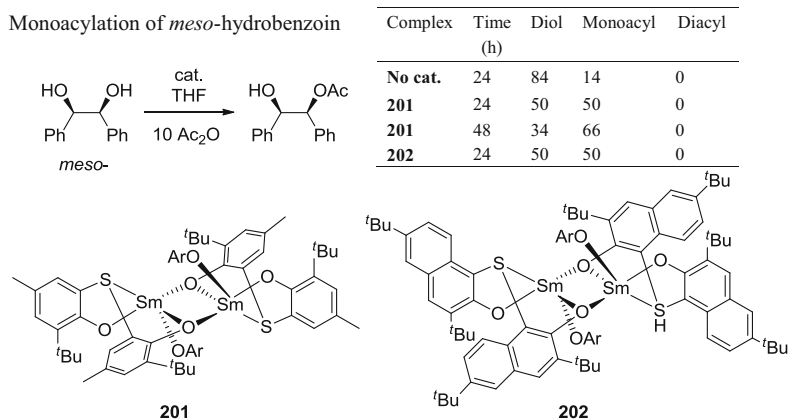


Fig. 2 Monoacylation of *meso*-hydrobenzoin catalyzed by dinuclear complexes **201** and **202**

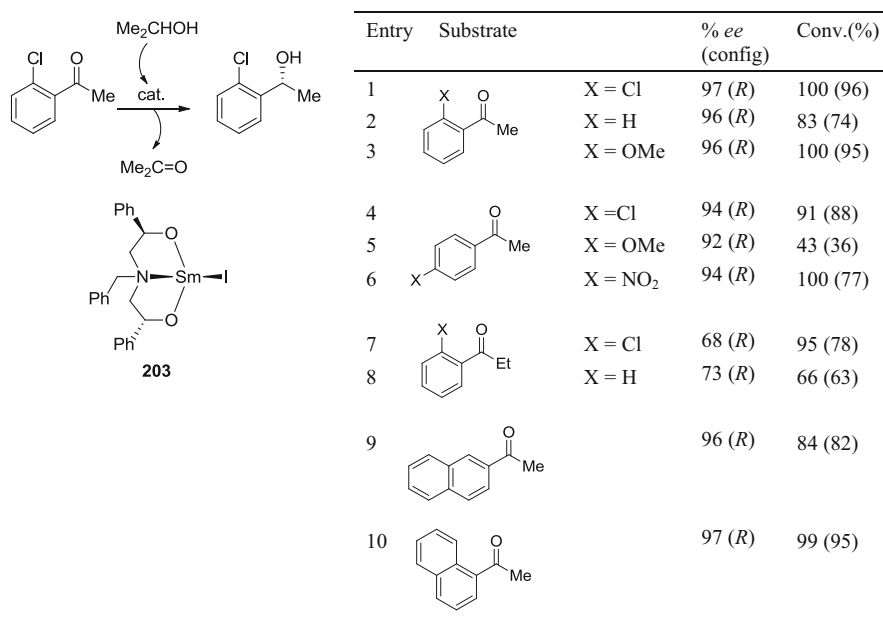


Fig. 3 Meerwein–Ponndorf–Verley reduction catalyzed by complex **203**

samarium iodo complex LSmI (L = PhCH(O)CH₂N(CH₂Ph)CH₂CH(O)Ph), **203**, catalyzed the Meerwein–Ponndorf–Verley reduction of various ketones (Fig. 3). Other lanthanide derivatives of **203** were also studied, with results suggesting that large metals (Y, Nd, Sm, Tb) were the most active, as well as the most enantioselective (*ee* >90%) [10].

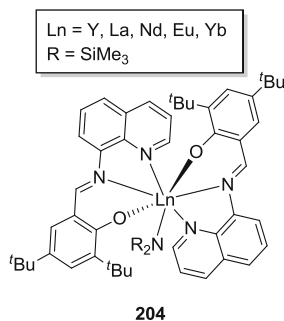


Chart 31 Monoamido catalysts, **204-Ln**, for the addition of amines to carbodiimides

Finally, at a loading of 1%, monoamido rare earth complexes $L_2LnN(SiMe_3)_2$ ($Ln = Y, La, Nd, Eu, Yb$; $L = 3,5\text{-}tBu_2\text{-}2\text{-}O\text{-}C_6H_2CH=N\text{-}8\text{-}C_9H_6N$), **204-Ln** (Chart 31), efficiently catalyzed the transformation of amines into carbodiimides. The activity of **204-Ln** was dominated by the ionic radius of the metal. Detailed studies of different substrates demonstrated that the **204-Nd** complex was able to convert various substituted anilines into the corresponding guanidines in 1 h. Reaction times were not influenced by either electron-donating or electron-withdrawing substrates, although 2- and/or 6-substituted amine moieties required up to 24 h for complete conversion [158].

5 Conclusion

In this chapter, the chemistry of pincer-supported rare earth metal complexes has been thoroughly reviewed, with an emphasis upon small molecule reactivity and catalysis. Pincer complexes can be prepared by various well-known synthetic procedures including alkane, amine, or alcohol elimination, as well as by distinct salt metathesis (transmetalation) reactions. A wide array of pincer ligands has been reported, and many of these compounds can be easily fine-tuned, thus providing a broad spectrum of ligands that vary widely in their steric and electronic properties. As most of these ligands are either neutral or monoanionic, rare earth complexes bearing such scaffolds are typically equipped with one or more reactive groups that can be used for subsequent stoichiometric reactions or catalytic applications.

The reaction chemistry of these compounds is rich, originating from the intrinsic reactivity of lanthanide metals which can be effectively governed by sterically demanding pincer ligands that serve to generate well-behaved metal complexes. For example, a limited number of structurally characterized rare earth complexes that feature terminal multiply bonded ligands have all been supported by pincer, or closely related, ancillary ligands. Accordingly, pincer-ligated rare earth complexes have demonstrated application as catalysts in numerous industrially relevant

reactions, including the ring-opening polymerization of cyclic esters, the polymerization of dienes, and the hydroamination of alkenes and alkynes.

As novel pincer ligand designs continue to be applied to rare earth metals, we can realistically expect that unprecedented complexes with remarkable properties and reaction chemistry will be realized at an ever accelerating pace. As numerous examples of such complexes have demonstrated outstanding catalytic properties, such compounds are expected to play prominent roles in key areas of catalysis in the future.

Acknowledgments Thanks are extended to the Natural Sciences and Engineering Research Council (NSERC) of Canada for financial support as well as to Prof. Dr. Jun Okuda and RWTH Aachen University for hosting PGH during the preparation of this manuscript.

References

1. Morales-Morales D, Jensen CM (2007) The chemistry of pincer compounds. Elsevier, Amsterdam
2. Albrecht M, van Koten G (2001) *Angew Chem Int Ed* 40:3750
3. Hogerheide MP, Grove DM, Boersma J, Jastrzebski JTBH, Kooijman H, Spek AL, van Koten G (1995) *Chem Eur J* 1:343
4. Hogerheide MP, Boersma J, Spek AL, van Koten G (1996) *Organometallics* 15:1505
5. Hogerheide MP, Boersma J, van Koten G (1996) *Coord Chem Rev* 155:87
6. Singleton JT (2003) *Tetrahedron* 59:1837
7. Boom ME, Milstein D (2003) *Chem Rev* 103:1759
8. Piers WE, Emslie DJH (2002) *Coord Chem Rev* 233:131
9. Fryzuk MD, Haddad TS (1988) *J Am Chem Soc* 110:8263
10. Evans DA, Nelson SG, Gagne MR, Muci AR (1993) *J Am Chem Soc* 115:9800
11. Meyer N, Jenter J, Roesky PW, Eickerling G, Scherer W (2009) *Chem Commun* 4693
12. Matsuo Y, Mashima K, Tani K (2001) *Organometallics* 20:3510
13. Arnold PL, Natrajan LS, Hall JJ, Bird SJ, Wilson C (2002) *J Organomet Chem* 647:205
14. Estler F, Eickerling G, Herdtweck E, Anwender R (2003) *Organometallics* 22:1212
15. Zimmermann M, Anwender R (2010) *Chem Rev* 110:6194
16. Zimmermann M, Tornroos KW, Anwender R (2006) *Organometallics* 25:3593
17. Bourget-Merle L, Lappert MF, Severn JR (2002) *Chem Rev* 102:3031
18. Tsai Y-C (2012) *Coord Chem Rev* 256:722
19. Crabtree RH (2005) The organometallic chemistry of the transition metals. Wiley, Hoboken
20. Johnson KR, Hayes PG (2013) *Chem Soc Rev* 42:1947
21. Hayes PG, Piers WE, Lee LWM, Knight LK, Parvez M, Elsegood MRJ, Clegg W (2001) *Organometallics* 20:2533
22. Knight LK, Piers WE, Fleurat-Lessard P, Parvez M, McDonald R (2004) *Organometallics* 23:2087
23. Chu T, Piers WE, Dutton JL, Parvez M (2013) *Organometallics* 32:1159
24. Knight LK, Piers WE, McDonald R (2006) *Organometallics* 25:3289
25. Hitchcock PB, Lappert MF, Protchenko AV (2005) *Chem Commun* 951
26. Li D, Li S, Cui D, Zhang X (2010) *J Organomet Chem* 695:2781
27. Conroy KD, Piers WE, Parvez M (2008) *J Organomet Chem* 693:834
28. Skvortsov GG, Fukin GK, Trifonov AA, Noor A, Döring C, Kempe R (2007) *Organometallics* 26:5770

29. Luconi L, Lyubov DM, Bianchini C, Rossin A, Faggi C, Fukin GK, Cherkasov AV, Shavyrin AS, Trifonov AA, Giambastiani G (2010) *Eur J Inorg Chem* 2010:608
30. Liu B, Yang Y, Cui D, Tang T, Chen X, Jing X (2007) *Dalton Trans* 4252
31. Izod K, Liddle ST, McFarlane W, Clegg W (2004) *Organometallics* 23:2734
32. Roering AJ, Davidson JJ, MacMillan SN, Tanski JM, Waterman R (2008) *Dalton Trans* 4488
33. Wicker BF, Scott J, Fout AR, Pink M, Mindiola DJ (2011) *Organometallics* 30:2453
34. Johnson KRD, Hayes PG (2009) *Organometallics* 28:6352
35. Johnson KRD, Hayes PG (2011) *Organometallics* 30:58
36. Jie S, Diaconescu PL (2010) *Organometallics* 29:1222
37. Han F, Li B, Zhang Y, Wang Y, Shen Q (2010) *Organometallics* 29:3467
38. Xu X, Chen Y, Zou G, Sun J (2010) *Dalton Trans* 39:3952
39. Parshall GW, Ittel SD (1993) *Homogeneous catalysis*. Wiley, New York
40. van Leeuwen WNMP (2004) *Homogeneous catalysis: understanding the art*. Kluwer, Dordrecht
41. Konkol M, Okuda J (2008) *Coord Chem Rev* 252:1577
42. Fegler W, Venugopal A, Kramer M, Okuda J (2015) *Angew Chem Int Ed* 54:1724
43. Nishiura M, Hou Z (2010) *Nat Chem* 2:257
44. Cheng J, Saliu K, Ferguson MJ, McDonald R, Takats J (2010) *J Organomet Chem* 695:2696
45. Konkol M, Spaniol TP, Kondracka M, Okuda J (2007) *Dalton Trans* 4095
46. Konkol M, Kondracka M, Voth P, Spaniol TP, Okuda J (2008) *Organometallics* 27:3774
47. Lyubov DM, Fukin GK, Cherkasov AV, Shavyrin AS, Trifonov AA, Luconi L, Bianchini C, Meli A, Giambastiani G (2009) *Organometallics* 28:1227
48. Liu B, Liu X, Cui D, Liu L (2009) *Organometallics* 28:1453
49. Lu E, Chen Y, Leng X (2011) *Organometallics* 30:5433
50. Lu E, Chen Y, Zhou J, Leng X (2012) *Organometallics* 31:4574
51. Cheng J, Shima T, Hou Z (2011) *Angew Chem Int Ed* 50:1857
52. Johnson KRD, Kamenz BL, Hayes PG (2014) *Organometallics* 33:3005
53. Chauvin Y (2006) *Angew Chem Int Ed* 45:3740
54. Schrock RR (2006) *Angew Chem Int Ed* 45:3748
55. Grubbs RH (2006) *Angew Chem Int Ed* 45:3760
56. Summerscales OT, Gordon JC (2013) *RSC Adv* 3:6682
57. Rong W, Cheng J, Mou Z, Xie H, Cui D (2013) *Organometallics* 32:5523
58. Scott J, Basuli F, Fout AR, Huffman JC, Mindiola DJ (2008) *Angew Chem Int Ed* 47:8502
59. Lu E, Li Y, Chen Y (2010) *Chem Commun* 46:4469
60. Lu E, Chu J, Chen Y, Borzov MV, Li G (2011) *Chem Commun* 47:743
61. Lu E, Zhou Q, Li Y, Chu J, Chen Y, Leng X, Sun J (2012) *Chem Commun* 48:3403
62. Chu J, Lu E, Liu Z, Chen Y, Leng X, Song H (2011) *Angew Chem Int Ed* 50:7677
63. Chu J, Lu E, Chen Y, Leng X (2013) *Organometallics* 32:1137
64. Chu J, Kefalidis CE, Maron L, Leng X, Chen Y (2013) *J Am Chem Soc* 135:8165
65. Scott J, Fan H, Wicker BF, Fout AR, Baik MH, Mindiola DJ (2008) *J Am Chem Soc* 130:14438
66. Cameron TM, Gordon JC, Michalczyk R, Scott BL (2003) *Chem Commun* 2282
67. Zou J, Berg DJ, Stuart D, McDonald R, Twamley B (2011) *Organometallics* 30:4958
68. Izod K, Liddle ST, Clegg W (2004) *Chem Commun* 1748
69. Johnson KRD, Hannon MA, Ritch JS, Hayes PG (2012) *Dalton Trans* 41:7873
70. Jantunen KC, Scott BL, Hay PJ, Gordon JC, Kiplinger JL (2006) *J Am Chem Soc* 128:6322
71. Masuda JD, Jantunen KC, Scott BL, Kiplinger JL (2008) *Organometallics* 27:803
72. Zimmermann M, Tornroos KW, Anwender R (2007) *Angew Chem Int Ed* 46:3126
73. Zimmermann M, Estler F, Herdtweck E, Törnroos KW, Anwender R (2007) *Organometallics* 26:6029
74. Paolucci G, Bortoluzzi M, Bertolasi V (2008) *Eur J Inorg Chem* 2008:4126
75. Yang Y, Cui D, Chen X (2010) *Dalton Trans* 39:3959
76. Johnson KRD, Hayes PG (2013) *Organometallics* 32:4046

77. Karpov AA, Cherkasov AV, Fukin GK, Shavyrin AS, Luconi L, Giambastiani G, Trifonov AA (2013) *Organometallics* 32:2379
78. Johnson KRD, Hayes PG (2014) *Dalton Trans* 43:2448
79. Wicker BF, Pink M, Mindiola DJ (2011) *Dalton Trans* 40:9020
80. Fryzuk MD, Haddad TS (1990) *J Chem Soc Chem Commun* 1088
81. Fryzuk MD, Haddad TS, Berg DJ, Rettig SJ (1991) *Pure Appl Chem* 63:845
82. Fryzuk MD, Haddad TS, Rettig SJ (1991) *Organometallics* 10:2026
83. Fryzuk MD, Haddad TS, Rettig SJ (1992) *Organometallics* 11:2967
84. Fryzuk MD, Giesbrecht GR, Rettig SJ (1996) *Organometallics* 15:3329
85. Fryzuk MD, Giesbrecht GR, Rettig SJ (2000) *Can J Chem* 78:1003
86. Evans LTJ, Coles MP, Cloke FGN, Hitchcock PB (2010) *Inorg Chim Acta* 363:1114
87. Fryzuk MD, Yu P, Patrick BO (2001) *Can J Chem* 79:1194
88. Meyer N, Kuzdrowska M, Roesky PW (2008) *Eur J Inorg Chem* 2008:1475
89. Jenter J, Gamer MT, Roesky PW (2010) *Organometallics* 29:4410
90. Roesky PW, Jenter J, Koppe R (2010) *C R Chim* 13:603
91. Peruzzini M, Gonsalvi L (2011) *Phosphorus compounds – advanced tools in catalysis and material sciences*. Springer, Berlin
92. Nief F (1998) *Coord Chem Rev* 178–180, Part 1:13
93. Li T, Kaercher S, Roesky PW (2014) *Chem Soc Rev* 43:42
94. Masuda JD, Jantunen KC, Ozerov OV, Noonan KJ, Gates DP, Scott BL, Kiplinger JL (2008) *J Am Chem Soc* 130:2408
95. Wicker BF, Scott J, Andino JG, Gao X, Park H, Pink M, Mindiola DJ (2010) *J Am Chem Soc* 132:3691
96. Li T, Wiecko J, Pushkarevsky NA, Gamer MT, Köppe R, Konchenko SN, Scheer M, Roesky PW (2011) *Angew Chem Int Ed* 50:9491
97. Zou J, Berg DJ, Oliver A, Twamley B (2013) *Organometallics* 32:6532
98. Edworthy I, Blake A, Wilson C, Arnold P (2007) *Organometallics* 26:3684
99. Painter PC, Coleman MM (2009) *Essentials of polymer science and engineering*, 1st edn. DEStech Publications Inc., Lancaster, p 1
100. “The Nobel in Chemistry 1963” Nobelprize.org. Nobel Media AB 2014. http://www.nobelprize.org/nobel_prizes/chemistry/laureates/1963/. Accessed 29 Aug 2014
101. “The Nobel in Chemistry 2005” Nobelprize.org. Nobel Media AB 2014. http://www.nobelprize.org/nobel_prizes/chemistry/laureates/2005/. Accessed 29 Aug 2014
102. Dijkstra PJ, Du H, Feijen J (2011) *Polym Chem* 2:520
103. Amgoune A, Thomas CM, Carpentier JF (2007) *Pure Appl Chem* 79:2013
104. Dechy-Cabaret O, Martin-Vaca B, Bourissou D (2004) *Chem Rev* 104:6147
105. Yang Y, Li S, Cui D, Chen X, Jing X (2007) *Organometallics* 26:671
106. Shang X, Liu X, Cui D (2007) *J Polym Sci A Polym Chem* 45:5662
107. Liu X, Shang X, Tang T, Hu N, Pei F, Cui D, Chen X, Jing X (2007) *Organometallics* 26:2747
108. Zi G, Wang Q, Xiang L, Song H (2008) *Dalton Trans* 5930
109. Wang Q, Xiang L, Song H, Zi G (2009) *J Organomet Chem* 694:691
110. Peng H, Zhang Z, Qi R, Yao Y, Zhang Y, Shen Q, Cheng Y (2008) *Inorg Chem* 47:9828
111. Xu B, Han X, Yao Y, Zhang Y (2010) *Chin J Chem* 28:1013
112. Ren W, Chen L, Zhao N, Wang Q, Hou G, Zi G (2014) *J Organomet Chem* 758:65
113. Grunova E, Kirillov E, Roisnel T, Carpentier J (2010) *Dalton Trans* 39:6739
114. Mazzeo M, Lamberti M, D’Auria I, Milione S, Peters JC, Pellicchia C (2010) *J Polym Sci A Polym Chem* 48:1374
115. D’Auria I, Mazzeo M, Pappalardo D, Lamberti M, Pellicchia C (2011) *J Polym Sci A Polym Chem* 49:403
116. Li G, Lamberti M, Mazzeo M, Pappalardo D, Roviello G, Pellicchia C (2012) *Organometallics* 31:1180
117. Westmoreland I, Arnold J (2006) *Dalton Trans* 4155
118. Liang Z, Ni X, Li X, Shen Z (2012) *Dalton Trans* 41:2812

119. Bennett SD, Core BA, Blake MP, Pope SJA, Mountford P, Ward BD (2014) *Dalton Trans* 43:5871
120. Arbaoui A, Redshaw C (2010) *Polym Chem* 1:801
121. Han X, Wu L, Yao Y, Zhang Y, Shen Q (2009) *Chin Sci Bull* 54:3795
122. Huang L-L, Han X-Z, Yao Y-M, Zhang Y, Shen Q (2011) *Appl Organomet Chem* 25:464
123. Xu X, Xu X, Chen Y, Sun J (2008) *Organometallics* 27:758
124. Gao W, Cui D, Liu X, Zhang Y, Mu Y (2008) *Organometallics* 27:5889
125. Du G, Wei Y, Zhang W, Dong Y, Lin Z, He H, Zhang S, Li X (2013) *Dalton Trans* 42:1278
126. Zhang W, Liu S, Yang W, Hao X, Glaser R, Sun W-H (2012) *Organometallics* 31:8178
127. Kuo P, Chang J, Lee W, Lee HM, Huang J (2005) *J Organomet Chem* 690:4168
128. Schmid M, Guillaume SM, Roesky PW (2013) *J Organomet Chem* 744:68
129. Zhou H, Jiang Y, Chen M, Wang Y, Yao Y, Wu B, Cui D (2014) *J Organomet Chem* 763–764:52
130. Zhang Z, Cui D, Wang B, Liu B, Yang Y (2010) Men in blue. In: Roesky PW (ed) *Molecular catalysis of rare-earth elements*. Springer, Berlin, p 49
131. Sugiyama H, Gambarotta S, Yap GPA, Wilson DR, Thiele SKH (2004) *Organometallics* 23:5054
132. Zhang L, Suzuki T, Luo Y, Nishiura M, Hou Z (2007) *Angew Chem Int Ed* 46:1909
133. Gao W, Cui D (2008) *J Am Chem Soc* 130:4984
134. Liu D, Cui D, Gao W (2010) *Sci Chin Chem* 53:1641
135. Jenter J, Meyer N, Roesky PW, Thiele SK, Eickerling G, Scherer W (2010) *Chem Eur J* 16:5472
136. Lv K, Cui D (2010) *Organometallics* 29:2987
137. Wang L, Cui D, Hou Z, Li W, Li Y (2011) *Organometallics* 30:760
138. Wang L, Liu D, Cui D (2012) *Organometallics* 31:6014
139. Liu H, He J, Liu Z, Lin Z, Du G, Zhang S, Li X (2013) *Macromolecules* 46:3257
140. Pan Y, Xu T, Yang G-W, Jin K, Lu XB (2013) *Inorg Chem* 52:2802
141. Desimoni G, Faita G, Guala M, Pratelli C (2003) *J Org Chem* 68:7862
142. Evans DA, Song HJ, Fandrick KR (2006) *Org Lett* 8:3351
143. Evans DA, Fandrick KR, Song HJ (2005) *J Am Chem Soc* 127:8942
144. Morimoto H, Lu G, Aoyama N, Matsunaga S, Shibasaki M (2007) *J Am Chem Soc* 129:9588
145. Qian C, Wang L (2000) *Tetrahedron Asymmetry* 11:2347
146. Ward BD, Gade LH (2012) *Chem Commun* 48:10587
147. Zimmermann M, Törnroos KW, Waymouth RM, Anwander R (2008) *Organometallics* 27:4310
148. Bartlett SA, Cibin G, Dent AJ, Evans J, Hanton MJ, Reid G, Toozee RP, Tromp M (2013) *Dalton Trans* 42:2213
149. Wang Q, Xiang L, Zi G (2008) *J Organomet Chem* 693:68
150. Müller TE, Hultzsich KC, Yus M, Foubelo F, Tada M (2008) *Chem Rev* 108:3795
151. Hultzsich KC, Hampel F, Wagner T (2004) *Organometallics* 23:2601
152. Wang Q, Xiang L, Song H, Zi G (2008) *Inorg Chem* 47:4319
153. Reznichenko AL, Hultzsich KC (2013) *Organometallics* 32:1394
154. Lu E, Gan W, Chen Y (2009) *Organometallics* 28:2318
155. Lu E, Gan W, Chen Y (2011) *Dalton Trans* 40:2366
156. Hultzsich KC, Gribkov DV, Hampel F (2005) *J Organomet Chem* 690:4441
157. Natrajan LS, Hall JJ, Blake AJ, Wilson C, Arnold PL (2003) *J Solid State Chem* 171:90
158. Han F, Teng Q, Zhang Y, Wang Y, Shen Q (2011) *Inorg Chem* 50:2634